

1-1-2007

Nonlinear suboptimal and adaptive pectoral fin control of autonomous underwater vehicle

Mugdha S Naik
University of Nevada, Las Vegas

Follow this and additional works at: <https://digitalscholarship.unlv.edu/rtds>

Repository Citation

Naik, Mugdha S, "Nonlinear suboptimal and adaptive pectoral fin control of autonomous underwater vehicle" (2007). *UNLV Retrospective Theses & Dissertations*. 2179.
<http://dx.doi.org/10.25669/b8qv-dfn6>

This Thesis is protected by copyright and/or related rights. It has been brought to you by Digital Scholarship@UNLV with permission from the rights-holder(s). You are free to use this Thesis in any way that is permitted by the copyright and related rights legislation that applies to your use. For other uses you need to obtain permission from the rights-holder(s) directly, unless additional rights are indicated by a Creative Commons license in the record and/or on the work itself.

This Thesis has been accepted for inclusion in UNLV Retrospective Theses & Dissertations by an authorized administrator of Digital Scholarship@UNLV. For more information, please contact digitalscholarship@unlv.edu.

NONLINEAR SUBOPTIMAL AND ADAPTIVE PECTORAL FIN CONTROL OF
AUTONOMOUS UNDERWATER VEHICLE

by

Mugdha S. Naik

Bachelor of Engineering
University of Pune, Maharashtra, India
2004

A thesis submitted in partial fulfillment
of the requirements for the

Master of Science Degree in Electrical Engineering
Department of Electrical and Computer Engineering
Howard R. Hughes College of Engineering

Graduate College
University of Nevada, Las Vegas
August 2007

UMI Number: 1448411

INFORMATION TO USERS

The quality of this reproduction is dependent upon the quality of the copy submitted. Broken or indistinct print, colored or poor quality illustrations and photographs, print bleed-through, substandard margins, and improper alignment can adversely affect reproduction.

In the unlikely event that the author did not send a complete manuscript and there are missing pages, these will be noted. Also, if unauthorized copyright material had to be removed, a note will indicate the deletion.

UMI[®]

UMI Microform 1448411

Copyright 2007 by ProQuest Information and Learning Company.

All rights reserved. This microform edition is protected against unauthorized copying under Title 17, United States Code.

ProQuest Information and Learning Company
300 North Zeeb Road
P.O. Box 1346
Ann Arbor, MI 48106-1346



Thesis Approval
The Graduate College
University of Nevada, Las Vegas

July 30, 2007

The Thesis prepared by

Mugdha Naik

Entitled

Nonlinear Suboptimal and Adaptive Pectoral Fin Control
of Autonomous Underwater Vehicle

is approved in partial fulfillment of the requirements for the degree of

Master of Science in Electrical Engineering

Examination Committee Chair

Dean of the Graduate College

Examination Committee Member

Examination Committee Member

Graduate College Faculty Representative

ABSTRACT

Nonlinear Suboptimal and Adaptive Pectoral Fin Control of Autonomous Underwater Vehicle

by

Mugdha S. Naik

Dr. Sahjendra N. Singh, Examination Committee Chair
Professor of Electrical and Computer Engineering Department
University of Nevada, Las Vegas

Autonomous underwater vehicles (AUVs) are used for numerous applications in the deep sea; such as hydrographic survey, sea bed mining and oceanographic mapping, etc. Presently, significant amount of effort is being made in developing biorobotic AUVs (BAUVs) with biologically-inspired control surfaces. However, the dynamics of AUVs and BAUVs are highly nonlinear and the hydrodynamic coefficients are not precisely known. As such the development of nonlinear and adaptive control systems is of considerable importance.

We consider the suboptimal dive plane control of AUVs using the state-dependent Riccati equation (SDRE) technique. This method provides effective means of designing nonlinear control systems for minimum as well as nonminimum phase AUV models. Moreover, hard control constraints are included in the design process.

We also attempt to design adaptive control systems for BAUVs using biologically-inspired pectoral-like fins. The fins are assumed to be oscillating harmonically with a combined linear

(sway) and angular (yaw) motion. The bias (mean) angle of the angular motion of the fin is used as a control input. Using discrete-time state variable representation of the BAUV, adaptive sampled-data control systems for the trajectory control are derived using state feedback as well as output feedback. We develop direct as well as indirect adaptive control systems for BAUVs. The advantage of the indirect adaptive law lies in its applicability to minimum as well as nonminimum phase systems. Simulation results are presented to evaluate the performance of each control system.

TABLE OF CONTENTS

ABSTRACT	iii
LIST OF FIGURES	vii
ACKNOWLEDGMENTS	ix
CHAPTER 1 INTRODUCTION	1
Biological Classification	1
Literature Review	2
Thesis Outline	5
CHAPTER 2 MATHEMATICAL AUV MODEL AND CONTROL PROBLEM	9
Fin Force And Moment	9
Yaw Plane Dynamics	10
CHAPTER 3 STATE-DEPENDENT RICCATI EQUATION-BASED ROBUST DIVE PLANE CONTROL	14
Nonlinear AUV Model And Control Problem	15
Robust Suboptimal Control Law: Unconstrained Fin Angle	18
Robust Control Law: Control Fin Constrained	23
Simulation Results For Dive Plane Maneuvers	26
CHAPTER 4 STATE FEEDBACK ADAPTIVE PECTORAL-LIKE FIN CONTROL SYSTEM	37
BAUV Control Problem	38
Adaptive Controller	40
Simulation Results For Yaw Plane Maneuvers	44
CHAPTER 5 OUTPUT FEEDBACK ADAPTIVE PECTORAL-LIKE FIN CONTROL SYSTEM	51
Problem Formulation	52
Control Law	53
Simulation Results For Yaw Plane Maneuvers	57
CHAPTER 6 INDIRECT ADAPTIVE OUTPUT FEEDBACK SERVOREGULATION	70
Problem Statement	71
Parameter Identifier	72
Adaptive Control Law	75
Simulation Results For Yaw Plane Maneuvers	80
CHAPTER 7 CONCLUSION	89

APPENDIX I	92
APPENDIX II	93
REFERENCES	95
VITA	102

LIST OF FIGURES

Figure 1.1 A diagram of a fish showing its different fins	8
Figure 2.1 The AUV model with pectoral fins	13
Figure 3.1 The AUV model	30
Figure 3.2 Nominal REMUS control with unconstrained input: $U = 2$ m/s, $z_r = 0.65$ m	31
Figure 3.3 Nominal REMUS control with saturating fin: $U = 2$ m/s, $z_r = 1.5$ m . .	32
Figure 3.4 Off-nominal ($p = +25p^*$) REMUS control with saturating fin: $U = 2$ m/s, $z_r = 1.5$ m	33
Figure 3.5 Off-nominal ($p = -.25p^*$) REMUS control with saturating fin: $U = 2$ m/s, $z_r = 1.5$ m	34
Figure 3.6 Off-nominal ($p = -.25p^*$) REMUS control with saturating: $U = 1.54$ m/s, $z_r = 1$ m	35
Figure 3.7 Off-nominal ($p = -0.25p^*$) REMUS control with saturating control: $U =$ 2 m/s, $z_r = 1.5$ m, $W = B_o$	36
Figure 4.1 The Complete Closed-loop system with State feedback and Parameter Adap- tation	47
Figure 4.2 Adaptive set point control: Frequency of flapping 8Hz for $\psi^* = -5$ (deg) and parameter uncertainty 50%	48
Figure 4.3 Adaptive sinusoidal trajectory control: Frequency of flapping 8Hz for $y_m =$ $3.5 \sin 2\pi fkT$ (deg) and parameter uncertainty 50%	49
Figure 4.4 Adaptive turning maneuver: Frequency of flapping 8Hz for 360 (deg) turn with turning rate of 4 (deg / sec) and parameter uncertainty 50%	50
Figure 5.1 The Complete Closed-loop system with Output feedback and Parameter Adaptation	62
Figure 5.2 Adaptive set point control: Frequency of flapping 8Hz for $\psi^* = 10$ (deg) and parameter uncertainty 25%	63
Figure 5.3 Adaptive set point control: Frequency of flapping 8Hz for $\psi^* = 10$ (deg) and parameter uncertainty 50%	64
Figure 5.4 Adaptive set point control: Frequency of flapping 8Hz for $\psi^* = 10$ (deg) and parameter uncertainty 50% but the command is faster	65
Figure 5.5 Adaptive sinusoidal trajectory control: Frequency of flapping 8Hz for $y_m =$ $10 \sin 2\pi fkT$ (deg) and parameter uncertainty 25%	66
Figure 5.6 Adaptive sinusoidal trajectory control: Frequency of flapping 8Hz for $y_m =$ $10 \sin 2\pi fkT$ (deg) and parameter uncertainty 50%	67
Figure 5.7 Adaptive sinusoidal trajectory control: Frequency of flapping 8Hz for $y_m =$ $10 \sin 2\pi fkT$ (deg) and parameter uncertainty 50% but for faster command . .	68
Figure 5.8 Adaptive turning maneuver: Turn rate of 2 deg/sec and parameter uncer- tainty 50%	69

Figure 6.1	The Closed-loop system including the internal model	84
Figure 6.2	The Closed-loop system including the identifier and stabilizer	85
Figure 6.3	Adaptive set point control: Frequency of flapping 8Hz for $\psi^* = 10$ (deg) and parameter uncertainty 20%	86
Figure 6.4	Adaptive set point control: Frequency of flapping 8Hz for $\psi^* = 50$ (deg) and parameter uncertainty 20%	87
Figure 6.5	Adaptive turning maneuver: Frequency of flapping 8Hz for 180 (deg) turn with turning rate of 1.3 (deg / sec) and parameter uncertainty 20%	88

ACKNOWLEDGMENTS

I would like to express my deep and sincere gratitude to my advisor Dr. Sahjendra N. Singh, whose help, encouragement and wonderful guidance helped me throughout this work.

I wish to express my warm thanks to Dr. Venkatesan Muthukumar, Dr. Emma Regentova and Dr. Woosoon Yim for monitoring my research work and taking effort in reading my thesis and providing me with valuable comments.

I am grateful to the Department of Electrical and Computer Engineering at the University of Nevada, Las Vegas for providing me an excellent work environment and the staff for their cheerful assistance.

I would also like to thank several of my peers for their valuable help at several critical junctions of this thesis.

Finally a special thanks to my family and friends whose continuous support and encouragement enabled me to complete this work.

CHAPTER 1

INTRODUCTION

Aquatic animals are magnificent swimmers and present diverse maneuvering behaviors and hydrodynamic mechanism for their locomotion. They propel themselves through rhythmic unsteady motions of their body, tails and use of variety of fins (dorsal, caudal, pectoral, etc. as shown in Figure. 1.1). Their outstanding agility underwater provides us with new concept and technology to significantly enhance the maneuvering ability of the man-made vehicles. This has inspired researchers to investigate the basic swimming mechanisms of fish, to incorporate resembling control surface into man-made vehicles.

1.1 Biological Classification

Fish are designed to be unstable and are continuously using their control surfaces to generate opposing and balancing forces in addition to thrust. They are classified into body and/or caudal fin (BCF) mode, and median and/or paired fin (MPF) mode, based on how they utilize the parts of their bodies for locomotion.

Body/Caudal Fin Propulsion (BCF propulsion)

In BCF mode the propulsion is achieved by the overall movement of the body and the caudal fin. This type of swimming provides great thrust and acceleration. They are further classified into undulatory BCF motion involving passage of a wave along the propulsive structure and BCF oscillation involving fin movement.

Median/Paired Fin Propulsion (MPF propulsion)

This propulsion mode makes use of the median and pectoral fins for maneuvering and stabilization at slow speeds. They are further classified into undulatory MPF modes and MPF oscillation modes. The undulatory MPF modes undulate the fins to generate the propulsive forces. In MPF oscillation modes the dorsal, anal or the pectoral fins oscillate to provide propulsion.

The MPF oscillation mode identifies two main oscillatory movement types for the pectoral fins: (i) rowing action and (ii) flapping action. The agility achieved by the use of pectoral fins is very striking and intriguing to the researcher. This form is thus an ideal choice to be modeled.

Now the challenge is to make a propulsive system mimicking the motion of the median and paired fins and to enhance the propulsive and maneuvering performance of man-made vehicles at low speeds.

1.2 Literature Review

Aquatic animals have splendid ability to move smoothly through water using a variety of control surfaces for propulsion and maneuvering [1 - 4, 8]. Presently there exists considerable interest in designing flapping foils for propulsion and control of BAUVs [5, 6, 11, 15, 34]. These biologically-inspired control surfaces can provide AUVs with greater maneuverability as well as efficient propulsion. Several studies have been conducted on fish morphology, locomotion, and application of biologically inspired control surfaces for the control of AUVs [5, 8, 18, 26, 39]. Researchers are developing variety of biomimetic fish robots which utilize oscillating fins for propulsion and control [9 - 14]. A robot weever (Blackbass) has been developed in [9], which uses pectoral-like fins. A two-joint robotic dolphin has also been designed in [13]. The special issue of IEEE Journal of Oceanic Engineering includes several interesting articles on biologically-inspired science and technology for autonomous underwater vehicles (AUVs) [4, 5, 7, 8]. Readers may

refer to an excellent article [15] which provides recent advances in biorobotic research on biology-inspired high lift unsteady hydrodynamics, artificial muscle technology [16] and neuroscience [17] based control of BAUVs. Mechanical fins with multiple degree-of-freedom can produce variety of control forces. But the fin movements such as lead-lag, feathering, and flapping, can be identified as the basic oscillating patterns, which produce large lift and thrust. Laboratory experiments have been performed to measure forces and moments produced by oscillating foils [18, 19, 26, 34, 39]. Attempts have also been made to characterize the forces and moments produced by oscillating fins using computational methods [20 - 22]. An analytical representation of unsteady hydrodynamics of flapping foils has been obtained using Theodorsen theory [35]. These results show that oscillating foils produce periodic forces and their profile can be changed for the purpose of the control by altering the oscillation parameters (such as bias (mean) angle, frequency, relative phase angle, rotation angle at the end of stroke, etc.) of the fins. Thus one can develop biorobotic AUVs (BAUVs) equipped with biologically inspired control surfaces. However, the dynamics of AUVs and BAUVs are highly nonlinear and the hydrodynamic coefficient are not precisely known. As such the development of nonlinear control systems for AUVs with uncertain dynamics is of considerable importance.

Recently developed state-dependent Riccati equation (SDRE) techniques provide a systematic and effective means for the design of control systems for nonlinear dynamical systems [42, 52, 53]. For simplicity, control laws for AUVs are designed using linearized models [24, 36, 50, 55]. Recent designs of dorsal and pectoral fin control systems for BAUVs have also ignored model nonlinearities [27, 28, 34]. For nonlinear models of AUVs with known dynamics, control laws have been designed using the Lyapunov stability theory, and the backstepping design technique [24, 45]. For the control of AUV models in the presence of uncertainties, sliding mode control has been considered [36, 40, 43]. Sliding mode control approach requires high-gain feedback for

the compensation of uncertainties. Adaptive control laws have been also designed for the control of AUVs [24, 38, 44, 51, 54]. For adaptive control, dynamic feedback loop is used for generating the estimates of unknown controller parameters for compensation. A sliding mode fuzzy control law has been proposed by Guo [46]. A digital control system has been also designed in which the unknown parameters are estimated using a discrete time parameter identifier [56]. A neural network based control system has been developed for AUVs by Ishii [48]. Considerable research has been done for controlling AUVs using traditional control surfaces [24]. But the control of AUVs using oscillating fins poses considerable difficulty due to the time-varying nature of oscillatory control forces. For simplicity in design, averaging technique has been suggested for the control of robotic insects using flapping wings and AUVs [25]. Using this approach, the time-varying models are approximated by averaged time-invariant systems for the control law design. An oscillating fin propulsion control system using neural network has been developed and tests have been performed [26]. The guidance and control of a fish robot equipped with mechanical pectoral fins has been considered and rule-based fuzzy control system has been tested in laboratory experiments [9, 23, 37]. An adaptive control law for the control of undersea vehicles using dorsal fins have been considered, in which the control force is generated by cambering the fin [54]. The optimal and inverse control laws for the dive and yaw plane maneuvering of BAUVs using pectoral fins have been designed [27, 28]. For the derivation of these control laws, a parameterization of periodic fin forces using the CFD analysis has been obtained and bias angle of fin rotation has been used for the purpose of control. But the pectoral fin control laws of [27] and [28] have been derived on the assumption that the model parameters are completely known. This is rather a stringent requirement since, in a real case, the vehicle parameters and the hydrodynamic coefficients are not precisely known. Especially the precise knowledge of the forces and moments of unsteadily moving foils is not realistic. Furthermore, the parameterization

of the fin forces using the Fourier series of [27] and [28] depends on the order of truncation of the Fourier expansion, and as such different input matrices are obtained as the additional harmonic functions are included in the series representation. Apparently, it is important to design control systems for the control of AUVs using oscillating foils in the presence of parametric uncertainties.

1.3 Thesis Outline

Biomimetic studies and observations from fish have provided a wealth of information on the kinematics, i.e. how these animals employ their flapping tails and several fins to produce propulsive and maneuvering forces. It seems highly desirable to use these principles from fish to derive man-made underwater vehicles that are capable of emulating the performance of the aquatic animals. Such autonomous underwater vehicles (AUVs) are in great demand for variety of undersea applications. However, the dynamics of AUVs and BAUVs are highly nonlinear and the hydrodynamic coefficient are not precisely known. Thus the development of nonlinear control systems for AUVs with uncertain dynamics is extremely important.

The contribution of this thesis lies in the design of control systems for the dive plane and yaw plane maneuvering of AUVs and biorobotic AUVs. Chapter 2 provides the model of an AUV. In chapter 3, the thesis deals with the design of a robust suboptimal control system for the control of AUVs in the dive plane using the state-dependent Riccati equation method using traditional control surfaces. The model of the AUV is nonlinear and the state-dependent Riccati equation (SDRE) techniques provide a systematic and effective means for the design of control systems for nonlinear dynamical systems, which may be minimum or nonminimum phase. For a realistic design, a hard constraint on the control surface (control fin) deflection is imposed. It is also assumed that the hydrodynamic parameters are not known precisely. Simulation results for the dive plane control in presence of parameter uncertainty and constraints on the control fin

deflection is obtained.

The remaining parts of the thesis considers control of AUVs using biologically inspired control surfaces. First we consider the design of a state feedback adaptive control system for the yaw plane maneuvering of a biorobotic AUV using biomimetic mechanism resembling the pectoral fin of fish, in chapter 4. The pair of fins attached to the AUV are assumed to undergo combined oscillatory linear (sway) and angular (yaw) motion, and consequently generate periodic forces and moments. The model of the AUV considered here is similar to that of [27] and [28], in which the fin forces and moments are parameterized using computation fluid dynamics (CFD) analysis. For the purpose of design, it is assumed that the vehicle's physical parameters, the hydrodynamics coefficients, and the fin forces and moments are not known. It may be pointed out that the control laws of [27] and [28] have been developed by assuming that the systems parameters are completely known. A discrete-time model of the vehicle is obtained and a sampled-data adaptive control law is derived for the trajectory control of the yaw angle. Unlike the derivation of [27] and [28], the control law is independent of the number of harmonics retained in the truncated Fourier expansion of the fin force and moment. Here the bias (mean) angle of the yaw motion of the fin is treated as a control variable. For the purpose of control, the bias angle is switched to new values at the chosen sampling instants which are integer multiple of the fundamental time period of the fin force and moment. In this controller it is essential to measure all the state variables for the synthesis of the control law. From the practical point of view, the synthesis using state feedback is not attractive, because one must use sensors to measure each state variable. Thus an output feedback adaptive control system for the control of BAUVs using pectoral fins is preferred.

The control of BAUV using only yaw angle feedback is considered in chapter 5. Simulation results for set point, sinusoidal trajectory tracking and turning maneuver are presented and show that the adaptive control system accomplishes precise yaw angle trajectory control in spite of

the parameter uncertainties. These two direct adaptive control design approaches are applicable only to minimum phase systems. However, the vehicle model is nonminimum phase (the transfer function relating the output and input has unstable zeros) for the choice of most of the location of the fins on the vehicle and the oscillation parameters. Therefore one cannot design a direct adaptive control system for tracking of the output trajectory. In chapter 6 of the thesis deals with the problem of designing a control system for control of BAUVs, which are not necessarily minimum phase. It considers the design of a servoregulator for yaw plane maneuvering of BAUVs using pectoral fins. Here the mean (bias) of the angular motion of the fin is treated as the control input and the yaw angle is the controlled output variable. An indirect sampled-data output feedback adaptive control system for the tracking of the constant and ramp yaw angle reference trajectories and rejecting constant disturbance inputs is derived. For the derivation of the control law, a second-order internal model of the exosignals (reference signals and disturbance inputs) is introduced in the control loop. The adaptive control system has a modular structure, which includes a gradient-based identifier and a stabilizer, designed using pole placement technique. Simulation results are presented which show that in the closed-loop system, output regulation of the yaw angle is accomplished in spite of the uncertainties in the system parameters.

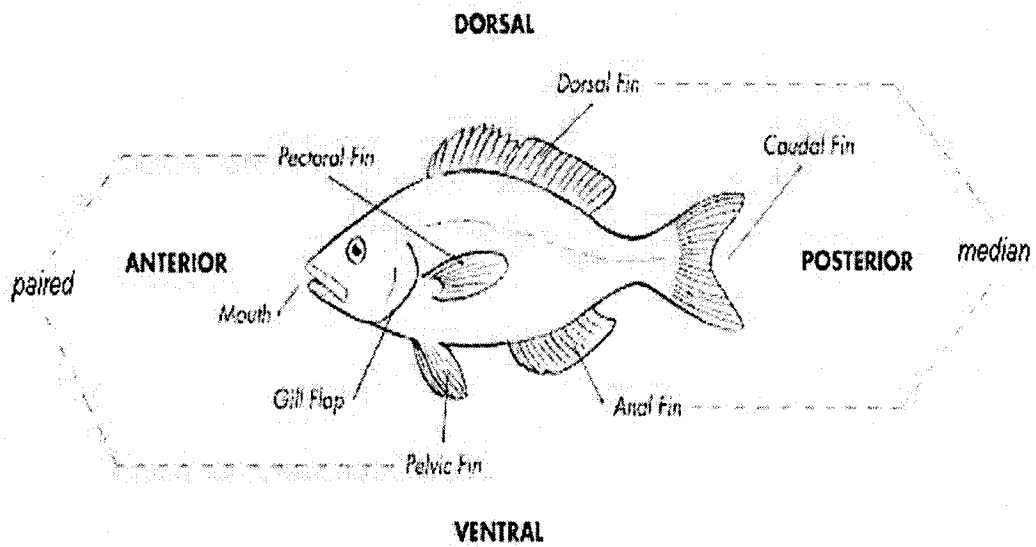


Figure 1.1: A diagram of a fish showing its different fins

CHAPTER 2

MATHEMATICAL AUV MODEL AND CONTROL PROBLEM

The mathematical model of BAUV used in chapters 4, 5 and 6 is presented in this chapter, while the model of the AUV considered in chapter 3 is presented in that chapter itself.

Let the vehicle be moving in the yaw plane ($X_I - Y_I$ plane), where $O_I X_I Y_I$ is an inertial coordinate system. $O_B X_B Y_B$ is body-fixed coordinate system with its origin at the center of buoyancy. X_B is in the forward direction. Figure. 2.1 shows the schematic of a typical AUV. Two fins resembling the pectoral fins of fish are symmetrically attached to the vehicle. Each fin has two degrees of freedom (sway and yaw) and oscillates harmonically.

2.1 Fin Force And Moment

We assume that the combined sway-yaw motion of the fin is described as follows:

$$\delta(t) = \delta_m \sin(2\pi f t)$$

$$\theta_y(t) = \beta + \theta_{ym} \sin(2\pi f t + \nu) \quad (2.1)$$

where δ and θ_y correspond to sway and yaw angle of the fin, δ_m and θ_{ym} are the amplitudes of linear and angular oscillations, β is the bias (mean) angle, f (Hz) is the frequency of oscillations, and ν is the phase difference between the sway and yaw motion. Based on the CFD analysis, it has been shown in [27] and [28] that the periodic lateral force (f_y) and yawing moment (m_y)

generated by the oscillating fin can be described by the Fourier series given by

$$\begin{aligned}
f_y(t) &= \sum_{n=0}^N [f_n^s(\beta) \sin(n\omega_f t) + f_n^c(\beta) \cos(n\omega_f t)] \\
m_y(t) &= \sum_{n=0}^N [m_n^s(\beta) \sin(n\omega_f t) + m_n^c(\beta) \cos(n\omega_f t)]
\end{aligned} \tag{2.2}$$

where f_n^a and m_n^a , $a \in \{s, c\}$ are the Fourier coefficients, and N is an arbitrarily large integer such that the neglected harmonics have insignificant effect. (The control law designed does not depend on N .) The Fourier coefficients are nonlinear functions of the bias angle. Assuming that β is small, fin force and moment can be approximated as ($k = 1, 2, 3, \dots$).

$$\begin{aligned}
f_k^a(\beta) &= f_k^a(0) + \left(\frac{\partial f_k^a(0)}{\partial \beta}\right)\beta \\
m_k^a(\beta) &= m_k^a(0) + \left(\frac{\partial m_k^a(0)}{\partial \beta}\right)\beta
\end{aligned} \tag{2.3}$$

where $a \in \{s, c\}$. Defining a vector $\phi(t)$ of sinusoidal signals

$$\phi(t) = [1, \sin\omega_f(t), \cos\omega_f(t), \dots, \sin N\omega_f(t), \cos N\omega_f(t)]^T \in R^{2N+1} \tag{2.4}$$

and using (2.2) - (2.4), one obtains

$$\begin{aligned}
f_y(t) &= \phi^T(f_a + \beta f_b) \\
m_y(t) &= \phi^T(m_a + \beta m_b)
\end{aligned} \tag{2.5}$$

where f_a , f_b , m_a , and m_b are approximate vectors, which can be obtained from (2.2) and (2.3).

2.2 Yaw Plane Dynamics

We assume that vehicle's forward speed U is held constant by some control mechanism. The equations of motion of a neutrally buoyant vehicle is described by Fossen [24]

$$m(\dot{v} + Ur + X_G \dot{r} - Y_G r^2) = Y_r \dot{r} + (Y_v \dot{v} + Y_r Ur) + Y_v Uv + F_y$$

$$I_z \dot{r} + m(X_G \dot{v} + X_G U r + Y_G v r) = N_{\dot{r}} \dot{r} + (N_{\dot{v}} \dot{v} + N_r U r) + N_v U v + M_y$$

$$\dot{\psi} = r \quad (2.6)$$

where ψ is the heading angle, $r = \dot{\psi}$ is the yaw rate, v is the lateral velocity along the Y_B -axis, $(X_G, Y_G) = (X_G, 0)$ is the coordinate of the center of gravity with respect to O_B , m is the mass, and I_z is the moment of inertia of the vehicle. $Y_v, N_{\dot{r}}, Y_v$, etc are the hydrodynamic coefficients, and F_y and M_y are the net fin force and moment. The global position coordinates X and Y of the vehicle are described by the kinematic equations

$$\dot{X} = U \cos(\psi) - v \sin(\psi)$$

$$\dot{Y} = U \sin(\psi) + v \cos(\psi) \quad (2.7)$$

For small motion of the vehicle, linearizing (2.6) gives

$$\begin{bmatrix} m - Y_{\dot{v}} & mX_G - Y_{\dot{r}} & 0 \\ mX_G - N_{\dot{v}} & I_z - N_{\dot{r}} & 0 \\ 0 & 0 & 1 \end{bmatrix} \begin{bmatrix} \dot{v} \\ \dot{r} \\ \dot{\psi} \end{bmatrix} = \begin{bmatrix} Y_v U & Y_r U - mU & 0 \\ N_v U & N_r U - mX_G U & 0 \\ 0 & 1 & 0 \end{bmatrix} \begin{bmatrix} v \\ r \\ \psi \end{bmatrix} + \begin{bmatrix} F_y \\ M_y \\ 0 \end{bmatrix} \quad (2.8)$$

Defining the state vector $x = (v, r, \psi)^T \in R^3$ and using (2.8) gives the state variable form

$$\dot{x} = Ax + B_v \begin{bmatrix} F_y \\ M_y \end{bmatrix} \quad (2.9)$$

where A and B_v are appropriate matrices. The net lateral force and moment due to two fins is given by $F_y = 2f_y$ and $M_y = 2(d_{gf} \cdot f_y + m_y)$, respectively, where d_f is the moment arm due to the fin location. Then substituting the fin force and moment from (2.5) in (2.9), gives the state

variable representation

$$\begin{aligned}\dot{x} &= Ax + B\Phi(t)f_c + B\Phi(t)f_v\beta \\ y(t) &= \begin{bmatrix} 0 & 0 & 1 \end{bmatrix} x(t) = Cx(t)\end{aligned}\tag{2.10}$$

where $y=\psi$ is selected as the controlled output variable, B is an appropriate matrix satisfying $B[f_y, m_y]^T = B_v[F_y, M_y]^T$, $f_c = (f_a^T, m_a^T)^T \in R^{4N+2}$, $f_v = (f_b^T, m_b^T)^T \in R^{4N+2}$ and

$$\Phi(t) = \begin{bmatrix} \phi^T(t) & 0 \\ 0 & \phi^T(t) \end{bmatrix}\tag{2.11}$$

For the purpose of design, we assume that the system matrices A and B , and the parameter vectors f_c and f_v are not known. Let $y_m(t)$ be a given yaw angle reference trajectory. We are interested in designing an adaptive control law such that in the closed-loop system, all the signals are bounded, and the yaw angle ψ asymptotically tracks $y_m(t)$.

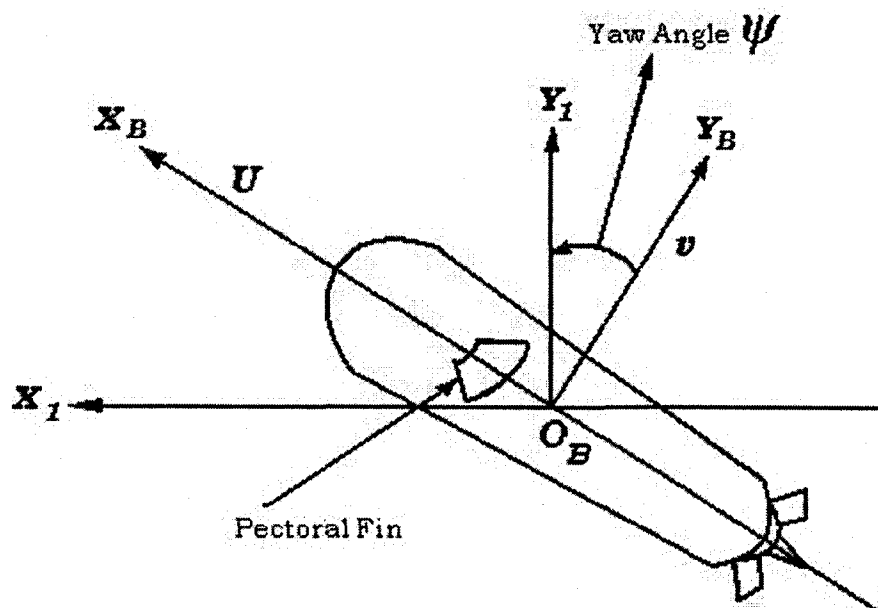


Figure 2.1: The AUV model with pectoral fins

CHAPTER 3

STATE-DEPENDENT RICCATI EQUATION-BASED ROBUST DIVE PLANE CONTROL

This chapter presents the design of robust suboptimal control system for the control of AUVs in the dive plane using the state-dependent Riccati equation method. The model of the AUV is nonlinear and, for a realistic design, a hard constraint on the control surface (control fin) deflection is imposed. Moreover, it is assumed that the hydrodynamic parameters are not known precisely. The problem of depth control is posed as a robust nonlinear output (depth) regulation problem in which the disturbance and reference output are constant exogenous signals. For this reason, a first order internal model fed by the output tracking error is constructed. A quadratic performance index is chosen for optimization and first a suboptimal control law for the model without control fin constraint is derived using the solution of an algebraic Riccati equation. This is followed by the design for the AUV with fin angle constraints. The design is accomplished by transforming the constrained problem into an unconstrained design problem by the introduction of a slack variable. Then a suboptimal control law is derived for the augmented system by the optimization of a modified performance index. Using the center manifold theorem [49] it is shown that in the closed-loop system, the control system designed using the SDRE method accomplishes robust regulation of the trajectories to a manifold (called output zeroing manifold) on which the depth tracking error vanishes and that the equilibrium state is asymptotically stable. Simulation results show that AUV can be effectively controlled in the dive plane in spite of the presence of parameter uncertainties and the constraints on the control fin deflection.

The organization of this chapter is as follows. Section 3.1 presents the AUV model and the output regulation problem. Suboptimal control laws for the constrained and unconstrained cases are derived in Section 3.2 and 3.3, respectively. Then simulation results are presented in Section 3.4.

3.1 Nonlinear AUV Model And Control Problem

A schematic of the AUV model with its body-fixed coordinate system is shown the Figure. 3.1. The earth-fixed frame is treated as an inertial frame. The motion of the AUV lies in a vertical plane. Let (X_B, Y_B, Z_B) be the coordinates of the center of buoyancy. The origin of the body fixed coordinate system is fixed at the center of buoyancy (i. e. $(X_B, Y_B, Z_B) = 0$). We denote the coordinates of the center of gravity of the vehicle with respect to the center of buoyancy by (X_G, Y_G, Z_G) .

The heave and pitch equations of motion of the vehicle with respect to the body fixed moving frame are described by a set of nonlinear differential equations. These equations of motion are given by Presterio [55]

$$\begin{aligned}
m[\dot{w} - Uq - X_G\dot{q} - Z_Gq^2] &= Z_{\dot{q}}\dot{q} + Z_{\dot{w}}\dot{w} + Z_{Uq}Uq + Z_{Uw}Uw + Z_{w|w}|w|w| + Z_{q|q}|q|q| + \\
&\quad (W - B_o) \cos \theta + U^2 Z_{UU} \delta_s \\
I_{yy}\dot{q} + m[X_G(Uq - \dot{w}) + Z_Gwq] &= M_{\dot{q}}\dot{q} + M_{\dot{w}}\dot{w} + M_{Uq}Uq + M_{Uw}Uw + M_{w|w}|w|w| + \\
&\quad M_{q|q}|q|q| - (X_GW - X_B B_o) \cos \theta - (Z_GW - Z_B B_o) \sin \theta + M_{UU}U^2 \delta_s \\
\dot{z} &= w \cos \theta - U \sin \theta \\
\dot{\theta} &= q
\end{aligned} \tag{3.1}$$

where θ is the pitch angle, w is the heave velocity, δ_s is the control fin angle, I_{yy} is the moment of inertia of the vehicle about the pitch axis, U is the forward velocity, W denotes the vehicle's

weight and B_o is the vehicle buoyancy. Although, here $(X_B, Y_B, Z_B) = 0$, we have retained these parameters in (3.1) for generality. $Z_{\dot{q}}, Z_{\dot{w}}, Z_{Uq}, M_{\dot{q}}$ and M_{Uw} , etc. are the hydrodynamics parameters. It is assumed that the forward velocity U is held constant by a control mechanism and the lateral velocity is zero.

Define the state vector $x = (w, q, z, \theta)^T \in R^4$ (T denotes matrix transposition). For the application of the SDRE method, the nonlinear dynamics (3.1) must be represented by a linear structure having state-dependent coefficients matrices. For this purpose, any nonlinear vector function of the form $f(x)$ must be factored as $f(x) = N(x)x$, where $N(x)$ is a state-dependent coefficient matrix. Now the representation of (3.1) in a linear-like form is considered.

The vehicle model (3.1) has $\sin\theta$ and $\cos\theta$ besides polynomial type nonlinearities. Since $\cos\theta = 1$ at $\theta = 0$, in order to express (3.1) in a linear form, we replace $\cos\theta$ and $\sin\theta$ by

$$\begin{aligned}\cos\theta &= \left(\frac{\cos\theta - 1}{\theta}\right)\theta + 1 \\ \sin\theta &= \left(\frac{\sin\theta}{\theta}\right)\theta\end{aligned}\quad (3.2)$$

Using (3.2) in (3.1), one can easily show that

$$\begin{aligned}\begin{pmatrix} \dot{w} \\ \dot{q} \end{pmatrix} &= M^{-1} \begin{bmatrix} Z_{Uw}U + Z_{w|w}|w| & Z_{Uq} + Z_{q|q}|q| + mZ_Gq + mU \\ M_{Uw}U + M_{w|w}|w| & M_{Uq}U + M_{q|q}|q| - m(X_GU + Z_Gw) \end{bmatrix} \begin{bmatrix} w \\ q \end{bmatrix} \\ &+ M^{-1} \begin{bmatrix} 0 & (W - B_o)(\cos\theta - 1)\theta^{-1} \\ 0 & (X_BB_o - X_GW)(\cos\theta - 1)\theta^{-1} - (Z_GW - Z_BB_o)\theta^{-1}\sin\theta \end{bmatrix} \begin{bmatrix} z \\ \theta \end{bmatrix} \\ &+ M^{-1} \begin{bmatrix} Z_{UU} \\ M_{UU} \end{bmatrix} U^2\delta_s + M^{-1} \begin{bmatrix} (W - B_o) \\ (X_BB_o - X_GW) \end{bmatrix} \\ &\triangleq A_1 \begin{pmatrix} w \\ q \end{pmatrix} + A_2 \begin{pmatrix} z \\ \theta \end{pmatrix} + B_1\delta_s + d_1\end{aligned}\quad (3.3)$$

$$\begin{aligned} \begin{pmatrix} \dot{z} \\ \dot{\theta} \end{pmatrix} &= \begin{bmatrix} \cos \theta & 0 \\ 0 & 1 \end{bmatrix} \begin{bmatrix} w \\ q \end{bmatrix} + \begin{bmatrix} 0 & -\theta^{-1}U \sin \theta \\ 0 & 0 \end{bmatrix} \begin{pmatrix} z \\ \theta \end{pmatrix} \\ &\triangleq A_3(x) \begin{pmatrix} w \\ q \end{pmatrix} + A_4(x) \begin{pmatrix} z \\ \theta \end{pmatrix} \end{aligned} \quad (3.4)$$

where A_i , $i = 1, \dots, 4$ are defined in Eqs. (3.3) and (3.4), and

$$\begin{aligned} M &= \begin{bmatrix} m - Z_{\dot{w}} & -mX_G - Z_{\dot{q}} \\ -mX_G - M_{\dot{w}} & I_{yy} - M_{\dot{q}} \end{bmatrix} \\ d_1 &= M^{-1}[(W - B_o), (X_B B_o - X_G W)]^T \\ B_1 &= M^{-1}[Z_{UU}, M_{UU}]^T U^2 \end{aligned} \quad (3.5)$$

It must be pointed out that the representation of the system (3.1) in linear-like form is not unique. Indeed one can obtain another representation by factoring the nonlinearity $mZ_G q$ as $[mZ_G q]w$ instead of the factorization $[mZ_G w]q$, which has been used in (3.3). Of course the control law will not be the same if one uses different form of the system.

It is assumed that the system parameters are not precisely known. Let $p_a \in R^p$ (p is the dimension of the unknown parameter vector) be the collection of all the unknown parameters in the matrices $A_i(x)$ and B_1 , and p^* and $p \in \Omega_p$ be the nominal value of p_a and the unknown part of p_a , respectively, where $\Omega_p \subset R^p$ is a compact set. That is

$$p_a = p^* + p \quad (3.6)$$

The nominal value of p_a is obtained if $p = 0$. Introducing the dependence of matrices A_i and B_1 on the perturbation vector p , one expresses these matrices as $A_i(x, p)$ and $B_1(p)$. In view of (3.3) and (3.4), one obtains a new representation of (3.1) in the desired form given as

$$\dot{x} = \begin{bmatrix} A_1(x, p) & A_2(x, p) \\ A_3(x) & A_4(x) \end{bmatrix} x + \begin{bmatrix} B_1(p) \\ 0 \end{bmatrix} \delta_s + \begin{bmatrix} d_1 \\ 0 \end{bmatrix}$$

$$\triangleq A(x, p)x + B(p)\delta_s + d \quad (3.7)$$

where 0 denote null matrices of appropriate dimensions, $B(p) = [B_1^T(p), 0^T]^T \in R^4$ and $d = \begin{bmatrix} d_1^T & 0 \end{bmatrix}^T \in R^4$. Here we treat d as a constant disturbance input since it is a function of the unknown parameters. The representation (3.7) has the desired linear-like structure with state-dependent coefficient matrices for the application of the SDRE method. Since we are interested in the dive plane control, consider a controlled output variable $y_c(t)$ as

$$y_c(t) = z(t) = Cx \quad (3.8)$$

where $C = [0, 0, 1, 0]$.

Suppose that it is desired to control the AUV to a prescribed depth z_r , a given constant. Then the output tracking error is

$$e = z - z_r = Cx - z_r \quad (3.9)$$

We are interested in deriving a control law such that in the closed-loop system, the tracking error tends to zero and the state vector x converges to an equilibrium state in spite of the uncertainties in the parameter vector p_a and the disturbance input d . Furthermore the control fin angle deflection is assumed to be limited.

3.2 Robust Suboptimal Control Law: Unconstrained Fin Angle

First, in this section, a control law is derived under the assumption that the control fin deflection is unconstrained. This is followed by the design of the control law with hard constraint on the control fin angle in the next section. The depth control problem for the system (3.7) is essentially a robust output regulation (servomechanism) problem. In the following, using the robust nonlinear output regulation (servomechanism) theory [47, 49] and the SDRE method a suboptimal nonlinear control law is derived.

We treat the signal v formed by the vector disturbance input d_1 and the command input z_r defined as

$$v = \begin{pmatrix} d_1 \\ z_r \end{pmatrix} \in \Omega_v \subset R^3 \quad (3.10)$$

as an exogenous signal, where Ω_v is a open neighborhood of $v = 0$. Of course, v can be generated by the exosystem

$$\dot{v} = 0, v(0) = v_0 \quad (3.11)$$

The exosystem (3.11) is capable of generating any constant disturbance d_1 and command input z_r . For the design of an output regulator, according to the nonlinear output regulation (servomechanism) theory, it is sufficient to introduce a dynamic system (internal model of the exosystem) of the form

$$\dot{x}_{s1} = e = z - z_r = Cx - z_r \quad (3.12)$$

The signal $x_{s1}(t)$ is the integral of the depth trajectory tracking error.

Define the augmented state vector as $x_{a1} = (x^T, x_{s1})^T \in \Omega_{a1} \subset R^5$, where Ω_{a1} is the open neighborhood of the origin. Then the composite system (3.7) and (3.12) can be written as

$$\begin{aligned} \dot{x}_{a1} &= \begin{bmatrix} A(x,p) & 0_{4 \times 1} \\ C & 0 \end{bmatrix} \begin{bmatrix} x \\ x_{s1} \end{bmatrix} + \begin{bmatrix} B(p) \\ 0 \end{bmatrix} \delta_s + \begin{bmatrix} d \\ -z_r \end{bmatrix} \\ &\triangleq A_{a1}(x,p)x_{a1} + B_{a1}(p)\delta_s + Ev \end{aligned} \quad (3.13)$$

where

$$E = \begin{bmatrix} 1 & 0 & 0 \\ 0 & 1 & 0 \\ 0 & 0 & 0 \\ 0 & 0 & 0 \\ 0 & 0 & -1 \end{bmatrix}$$

In the sequel, the regions Ω_{ai} , Ω_v , and Ω_p will be allowed to be sufficiently small so that various arguments in the derivation of the control laws remain valid.

We are interested in deriving a control law $\delta_s = \delta_s(x_{a1})$ such that the closed-loop system has the following properties:

- (i) For $v = 0$, the origin $x_{a1} = 0$ of the closed-loop system is exponentially stable.
- (ii) For $v \neq 0$, the tracking error e converges to zero as $t \rightarrow \infty$.

For the stabilization of the system (3.13) with $v = 0$, an optimal control problem is formulated.

Consider the optimal control problem for minimizing the performance index

$$J_1 = \frac{1}{2} \int_0^{\infty} [x_{a1}^T Q_1(x_{a1}) x_{a1} + R_1 \delta_s^2] dt \quad (3.14)$$

with respect to the state x_{a1} and input δ_s subject to the nominal nonlinear differential equation constraint:

$$\dot{x}_{a1} = A_{na1}(x) x_{a1} + B_{na1} \delta_s \quad (3.15)$$

where $A_{na1}(x) = A_{a1}(x, 0)$ and $B_{na1} = B_{a1}(0)$ are the matrices computed at the nominal value p^* (i.e. $p = 0$) of the parameter vector p_a , the matrix $Q_1(x_{a1})$ is a positive definite symmetric matrix (denoted as $Q_1(x_{a1}) > 0$) and R_1 is a positive real number. The weighting matrix $Q_1(x_{a1})$ and R_1 are properly selected to shape the response characteristics in the closed-loop system.

For deriving the optimal control law, one must solve the Hamilton-Jacobi-Bellman (HJB) equation which is a nonlinear partial differential equation. Since it is extremely difficult to solve this equation, instead, for simplicity, a suboptimal control law is designed using the SDRE method [41]. This control law is obtained by solving a simplified state-dependent Riccati equation given by

$$A_{na1}^T(x) P_1 + P_1 A_{na1}(x) - P_1 B_{na1} R_1^{-1} B_{na1}^T P_1 + Q_1(x_{a1}) = 0 \quad (3.16)$$

where $P_1(x_{a1}) > 0$. For the existence of solution for P_1 of (3.16), the pair $\{A_{na1}(x), B_{na1}\}$ has

to be pointwise stabilizable for all $x_{a1} \in \Omega_{a1} \subset R^5$, the domain of interest. For the AUV model, the rank of the controllability matrix

$$C_0 = [B_{na1}, A_{na1}(0)B_{na1}, \dots, A_{na1}^4(0)B_{na1}] \quad (3.17)$$

is 5, the dimension of x_{a1} . As such the system is pointwise controllable in a neighborhood of $x_{a1} = 0$ and the solution for $P_1(x_{a1})$ exists. The stabilizing control law is then given by

$$\delta_s = -R_1^{-1}B_{na1}^T P(x_{a1})x_{a1} \quad (3.18)$$

Readers may refer to [41] for the properties of the SDRE method. It is interesting to note that the suboptimal law satisfies

$$\frac{dH(x_{a1}, \lambda)}{d\delta_s} = 0 \quad (3.19)$$

where the Hamiltonian of the nonlinear optimal control problem is

$$H(x_{a1}, \lambda) = \frac{1}{2}[x_{a1}^T Q_1(x_{a1})x_{a1} + R_1 \delta_s^2] + \lambda^T [A_{na1}(x)x_{a1} + B_{na1}\delta_s] \quad (3.20)$$

and $\lambda \in R^5$ is the costate or the Lagrange multiplier.

Substituting the control law (3.18) in (3.13) with $v = 0$ gives

$$\dot{x}_{a1} = [A_{a1}(x, p) - B_{a1}R_1^{-1}B_{na1}^T P_1(x_{a1})]x_{a1} \triangleq A_{c1}(x_{a1}, p)x_{a1} \quad (3.21)$$

Let $A_{nc1}(x_{a1})$ be the nominal matrix $A_{c1}(x_{a1}, 0)$. Then the closed-loop matrix $A_{nc1}(x_{a1})$ is guaranteed to be Hurwitz in a neighborhood of the origin from the Riccati equation theory. Since the closed-loop matrix $A_{c1}(x_{a1}, p)$ is a continuous function of the parameter p , it remains Hurwitz for (x_{a1}, p) in a sufficiently small region $\Omega_{a1} \times \Omega_p$.

The composite closed-loop system ((3.13) and (3.18)) and the exosystem (3.11) can be written as

$$\dot{x}_{a1} = A_{c1}(x_{a1}, p)x_{a1} + Ev$$

$$\dot{v} = 0 \quad (3.22)$$

For the composite system, we state the following theorem.

Theorem 1. Consider the closed-loop system including the AUV model (3.7), the internal model (3.12) and the control law (3.18). Then there exists a region $D_1 = \Omega_{a1} \times \Omega_v \subset R^5 \times R^3$ and a compact set Ω_p such that for $(x_{a1}(0), v(0)) \in D_1$, and for $p \in \Omega_p$, the trajectory $x_{a1}(t, p)$ converges to an equilibrium point, and the depth tracking error $e(t)$ tends to zero as $t \rightarrow \infty$.

Proof: In view of the Riccati equation theory, $A_{cl}(x_{a1}, p)$ is Hurwitz in a domain $\Omega_{a1} \times \Omega_p$; and therefore, expanding A_{cl} about $x_{a1} = 0$ gives

$$\begin{aligned} \begin{bmatrix} \dot{x}_{a1} \\ \dot{v} \end{bmatrix} &= \begin{bmatrix} A_{cl}(0, p) & E \\ 0 & 0 \end{bmatrix} \begin{bmatrix} x_{a1} \\ v \end{bmatrix} + \begin{bmatrix} A_r(x_{a1}, p) \\ 0 \end{bmatrix} \\ &\triangleq A_{cc}(p) \begin{bmatrix} x_{a1} \\ v \end{bmatrix} + \begin{bmatrix} A_r(x_{a1}, p) \\ 0 \end{bmatrix} \end{aligned}$$

where $A_r(x_{a1}, p)$ denotes the second and higher order terms in x_{a1} . In the triangular matrix A_{cc} , $A_{cl}(0, p)$ is Hurwitz for $p \in \Omega_p$ and its remaining eigenvalues are zero. Therefore, according to the center manifold theorem [47, 49], there exists a vector function $X_{a1}(v, p)$ defined for (v, p) belonging to a sufficiently small region $\Omega_v \times \Omega_p$, with $X_{a1}(0, p) = 0$, that satisfies

$$\frac{\partial X_{a1}(v, p)}{\partial v} \dot{v} = 0 = A_{cl}(X_{a1}(v, p), p)X_{a1}(v, p) + Ev \quad (3.23)$$

Moreover

$$\|x_{a1}(t, p) - X_{a1}(v(t), p)\| \leq \alpha e^{-\beta t} \|x_{a1}(0) - X_{a1}(v(0), p)\| \quad (3.24)$$

where $x_{a1}(t, p)$ and $v(t)$ are the solutions of (3.22) and α and β are positive real numbers. It follows from (3.24) that $x_{a1}(t, p) = (w, q, z, \theta, x_{s1})^T$ converges to $X_{a1}(v(t), p)$ as $t \rightarrow \infty$. Note that one has $X_{a1}(v, p) = (X^T(v, p), X_{s1}(v, p))^T$, where on the center manifold $x = X(v, p)$ and

$x_{s1} = X_{s1}(v, p)$. Therefore, the last equation of (3.23) gives

$$\frac{\partial X_{s1}(v, p)}{\partial v} \dot{v} = 0 = X_3(v, p) - v_3 \quad (3.25)$$

where $v_3 = z_r$, on the center manifold $z = X_3$, and X_k denotes the k th component of X . Thus on the manifold $x_{a1} = X_{a1}$, in view of (3.25), the tracking error vanishes; and indeed it is an output zeroing manifold. The tracking error is

$$e = z - z_r = z - X_{a13} + X_{a13} - z_r \leq \|z - X_{a13}\| + \|X_{a13} - v_3\| \quad (3.26)$$

(For simplicity, the arguments of X_{a1} are suppressed here.) In view of (3.24)-(3.26), one has that $z(t) \rightarrow z_r$ as $t \rightarrow \infty$. Of course the convergence of $x_{a1}(t, p)$ to an equilibrium point on the center manifold follows from (3.24) since the exogenous signal v is some constant. This establishes Theorem 1.

The derivation of the control law (3.18) is based on the assumption that the control fin angle deflection is unlimited. However, this is not a valid assumption, and one must limit the control surface deflection to obtain a practical control law. The design of a constrained control law is considered in the following section.

3.3 Robust Control Law: Control Fin Constrained

For the design of a constrained control law, now we introduce a hard constraint on the fin angle given by

$$|\delta_s| \leq \delta_{sm} \quad (3.27)$$

where $\delta_{sm} > 0$ is the maximum permissible value of the fin angle. The SDRE methods provides means to include the control constraints (3.27) directly in the design process.

According to [41], the design is accomplished by transforming the bounded control problem

into an equivalent nonlinear regulator problem by introducing a slack variable x_{s2} that satisfies

$$\dot{x}_{s2} = u_n \quad (3.28)$$

where u_n is the new control input. The fin angle takes the form of a saturation sin function, given by

$$\delta_s = \text{satsin}(\delta_{sm}, x_{s2}) \quad (3.29)$$

where one defines

$$\text{satsin}(\delta_{sm}, x_{s2}) = \begin{cases} \delta_{sm} \text{sgn}(x_{s2}) & \text{for } |x_{s2}| > \frac{\pi}{2} \\ \delta_{sm} \sin(x_{s2}) & \text{for } |x_{s2}| \leq \frac{\pi}{2} \end{cases} \quad (3.30)$$

According to the definition (3.30) of the satsin function, fin angle is a function of the slack variable x_{s2} and does satisfy the control magnitude constraint for all $x_{s2} \in R$. But the new input u_n is unconstrained and now suboptimal regulator design is possible.

Define an augmented state vector $x_{a2} = (x_{a1}^T, x_{s2})^T \in \Omega_{a2} \subset R^6$ in an extended state space, where Ω_{a2} is an open set containing the origin. The composite system (3.13) and (3.28) can be written as

$$\begin{aligned} \dot{x}_{a2} &= \begin{bmatrix} A_{a1}(x, p) & x_{s2}^{-1} B_{a1}(p) \text{satsin}(\delta_{sm}, x_{s2}) \\ 0_{1 \times 5} & 0 \end{bmatrix} x_{a2} + \begin{bmatrix} 0_{5 \times 1} \\ 1 \end{bmatrix} u_n + \begin{bmatrix} E \\ 0 \end{bmatrix} v \\ &\triangleq A_{a2}(x_{a2}, p) x_{a2} + B_{a2} u_n + E_a v \end{aligned} \quad (3.31)$$

where A_{a2} , B_{a2} and E_a are defined in (3.31). Consider an optimal control problem, in which for the system (3.31), the performance index of the form

$$J_2 = \frac{1}{2} \int_0^\infty [x_{a2}^T Q_2(x_{a2}) x_{a2} + R_2 u_n^2] dt \quad (3.32)$$

is to be minimized, where $R_2 > 0$ is a design parameter, and the weighting matrix Q_2 is

$$Q_2 = \begin{bmatrix} Q_1(x_{a1}) & 0_{5 \times 1} \\ 0_{1 \times 5} & R_1 q_{s2}(x_{s2}) \end{bmatrix}$$

$$q_{s2}(x_{s2}) = \begin{cases} [\text{satsin}(\delta_{sm}, x_{s2})/x_{s2}]^2, & |x_{s2}| \leq \frac{\pi}{2} \\ (\delta_{sm}/x_s)^2, & |x_{s2}| > \frac{\pi}{2} \end{cases} \quad (3.33)$$

Note that the performance index (3.32) is obtained by substituting (3.29) for δ_s in the performance index J_1 of the unconstrained control problem. The matrix Q_2 is a positive definite symmetric matrix for all x_{a2} .

For the AUV model, the pair $\{A_{a2}(x_{a2}), B_{a2}\}$ is controllable in a suitably chosen domain Ω_{a2} , and similar to the derivation in the previous section, one obtains a suboptimal control law by solving the state-dependent algebraic Riccati equation

$$A_{na2}^T(x_{a2})P_2 + P_2A_{na2}(x_{a2}) - P_2B_{a2}R_2^{-1}B_{a2}^TP_2 + Q_2(x_{a2}) = 0 \quad (3.34)$$

where $A_{na2}(x_{a2}) = A_{a2}(x_{a2}, 0)$ is the nominal value evaluated at $p = 0$ and P_2 is the positive definite symmetric matrix. The new control law is given by

$$u_n = -R_2^{-1}B_{a2}^TP_2(x_{a2})x_{a2} \quad (3.35)$$

There exist a region $\Omega_{a2} \times \Omega_p$ such that the closed-loop matrix $A_{c2}(x_{a2}, p) = [A_{a2}(x_{a2}, p) - R_2^{-1}B_{a2}B_{a2}^TP_2(x_{a2})]$ is pointwise Hurwitz. Since $A_{c2}(0, p)$ is Hurwitz, according to the center manifold theorem, there exists a function $X_{a2}(v, p)$ defined in a sufficiently small region $\Omega_{a2} \times \Omega_v \times \Omega_p$ that satisfies

$$\frac{\partial X_{a2}(v, p)}{\partial v} \dot{v} = 0 = A_{c2}(X_{a2}(v, p), p)X_{a2}(v, p) + E_a v \quad (3.36)$$

Moreover

$$\|x_{a2}(t, p) - X_{a2}(v(t), p)\| \leq \alpha_2 e^{-\beta_2 t} \|x_{a2}(0) - X_{a2}(v(0), p)\| \quad (3.37)$$

where α_2 and β_2 are positive numbers, and $x_{a2}(t, p)$ and $v(t)$ are the solutions of (3.31) and (3.11).

Now in view of (3.36) and (3.37), using an argument similar to the unconstrained case, the following theorem is obtained.

Theorem 2. Consider the closed-loop system including the AUV model (3.7), the internal model (3.12), (3.28) for the slack variable, and the control law (3.35). Then there exists a region $D_2 = \Omega_{a2} \times \Omega_v \subset R^6 \times R^3$ and a compact set Ω_p such that for $(x_{a2}(0), v(0)) \in D_2$, and for $p \in \Omega_p$, the trajectory $x_{a2}(t)$ converges to an equilibrium point, and the depth tracking error $e(t)$ tends to zero as $t \rightarrow \infty$. Moreover the control fin constraint (3.27) is satisfied.

The regulation property of the control systems designed using the SDRE method has been established in a sufficiently small region $(x_{a2}, v, p) \in \Omega_{a2} \times \Omega_v \times \Omega_p$ surrounding the origin. However the results presented in the next section show that indeed the designed controller is capable of dive plane control for useful values of command inputs and large uncertainties in the system.

3.4 Simulation Results For Dive Plane Maneuvers

In this section, simulation results using *MATLAB* and *SIMULINK* for the depth control are presented. For the purpose of illustration, computer simulation is done for the REMUS (Remote Environmental Unit) AUV [55]. REMUS is a low-cost, modular vehicle with applications in autonomous docking, long-range oceanographic survey, and shallow-water mine reconnaissance. The parameters of the dive plane model of the REMUS are collected in the Appendix I. Here for the purpose of comparison, simulations are done using the controllers designed for the constrained as well as unconstrained fin angle. The performance of the optimal control systems depends on the choice of the weighting matrices in the performance index. Here the matrices Q_i and R_i have been selected by observing the simulated responses. The Initial conditions chosen are $x(0) = 0$. Responses are obtained for different values of U and the reference input z_r .

CASE A1. Nominal AUV control with unconstrained input: $U = 2$ m/s, $z_r = 0.65$ m

First the closed-loop system (3.13) with the unconstrained control law (3.18) is simulated. The vehicle's parameters are assumed to be nominal. The performance index has $Q_1 = 100I_{5 \times 5}$ and $R_1 = 1$. The vehicle's velocity is $U = 2$ (m/s) and it is desired to dive to a depth of $z_r = 0.65$ (m). The responses are shown in Figure. 3.2. We observe that for the chosen performance index, the desired depth is attained, but the control fin angle required for maneuver is extremely large (more than 50 (deg)). Simulation results for larger command z_r , show even larger fin deflections. This shows the limitation of unconstrained input design.

CASE A2. Control of AUV with nominal parameters and saturating fin angle: $U = 2$ m/s, $z_r = 1.5$ m

The AUV model (3.13) with the control law (3.28) is simulated. For an illustration, it is assumed that $|\delta_s(t)| \leq \delta_{sm} = 20$ deg. Noting that the performance index plays a key role in the design, for a meaningful comparison with the control system designed without any magnitude constraint on the fin angle, the weighting matrix Q_1 and the scalar parameter R_1 of the performance index J_1 of the unconstrained case A1 is retained in the performance index J_2 . The initial conditions are $x_{a2} = 0$ and $R_2 = 5$ and the command input is $z_r = 1.5$ (m). We have given a larger command ($z_r = 1.5$ instead of 0.65 (m) of Case A1) to show the advantage of the saturating control law design. It is assumed that the vehicle parameters are known (i.e. $p = 0$). The responses are shown in Figure. 3.3. It is observed that the depth trajectory converges to the target value in about 15 seconds. The fin angle saturates over a brief period in the transient phase, but it causes no problem in performing the desired maneuver. As expected the state vector remains bounded and converges to an equilibrium state. We observe the pitch angle and w converge to nonzero values in steady-state. This is because the weight of the vehicle and vehicle buoyancy B_o are not equal, and as such the equilibrium state is not at the origin. (Later for comparison, responses

for $W = B_o$ are presented.)

CASE A3. Control of AUV with perturbed parameters and saturating fin angle:

$$U = 2 \text{ m/s}, z_r = 1.5 \text{ m}$$

In order to examine the robustness of the control system, simulation is done using +25% perturbation in the hydrodynamics parameters (i.e. $p_a = 1.25p^*$, $p = 0.25p^*$) of the AUV, but the controller designed using nominal parameter vector p^* of case A2 is retained. The responses are shown in Figure. 3.4. We observe that in spite of the uncertainty in the AUV model, the controller is effective in regulating the AUV to the desired depth and the state vector converges in about 15 seconds. Again, the control fin saturates in the transient phase.

Simulation is also performed with off-nominal lower values of the hydrodynamic parameters ($p = -25\%p^*$, $p_a = 0.75p^*$) of the AUV. Of course the controller designed for the nominal AUV model is retained. The response are shown in Figure. 3.5. We observe that output regulation is accomplished in about 25 seconds. It seems that the controller designed using the underestimated values of the hydrodynamic parameters of the AUV model is more robust compared to controller designed using overestimated values. However, one must note that the weighting parameters in the performance index play an important role in shaping the closed-loop responses.

CASE A4. Control of AUV with saturating control: $U = 1.54 \text{ m/s}$, $z_r = 1 \text{ m}$

Simulation is performed for different velocity $U = 1.54 \text{ (m/s)}$ and $z_r = 1 \text{ (m)}$ using the nominal and off-nominal hydrodynamic parameters ($\pm 25\%$ uncertainties). We observed that in each case, the depth control is accomplished and the state vector converges to an equilibrium state. The control fin saturates only for a brief period in the transient phase. In order to save space, responses only for the worse off-nominal case ($p = -0.25p^*$) are shown in Figure. 3.6. As expected, we observe that controller performs better when the vehicle speed is larger. This is due to the increased control effectiveness of the fins at higher vehicle's speed (See, Figure. 3.5

for comparison).

CASE A5. Control of AUV with saturating control: $U = 2$ m/s, $z_r = 1.5$ m, $W = B_o$

Simulation results of Case A2 to A4 have been obtained for the cases of unbalanced weight (W) and vehicle buoyancy (B_o) ($W \neq B_o$). Now simulation is done for the off-nominal case ($p = -0.25p^*$) for $U = 2$ (m/s) and $z_r = 1.5$ (m), but unlike the previous cases, one has $W = B_o$. The responses are shown in Figure. 3.7. It is observed that compared to Figure. 3.5, the responses are slightly better. The vehicle attains the desired depth, and in this case the state vector converges to the origin. The pitch angle and w tend to zero in the steady-state as expected.

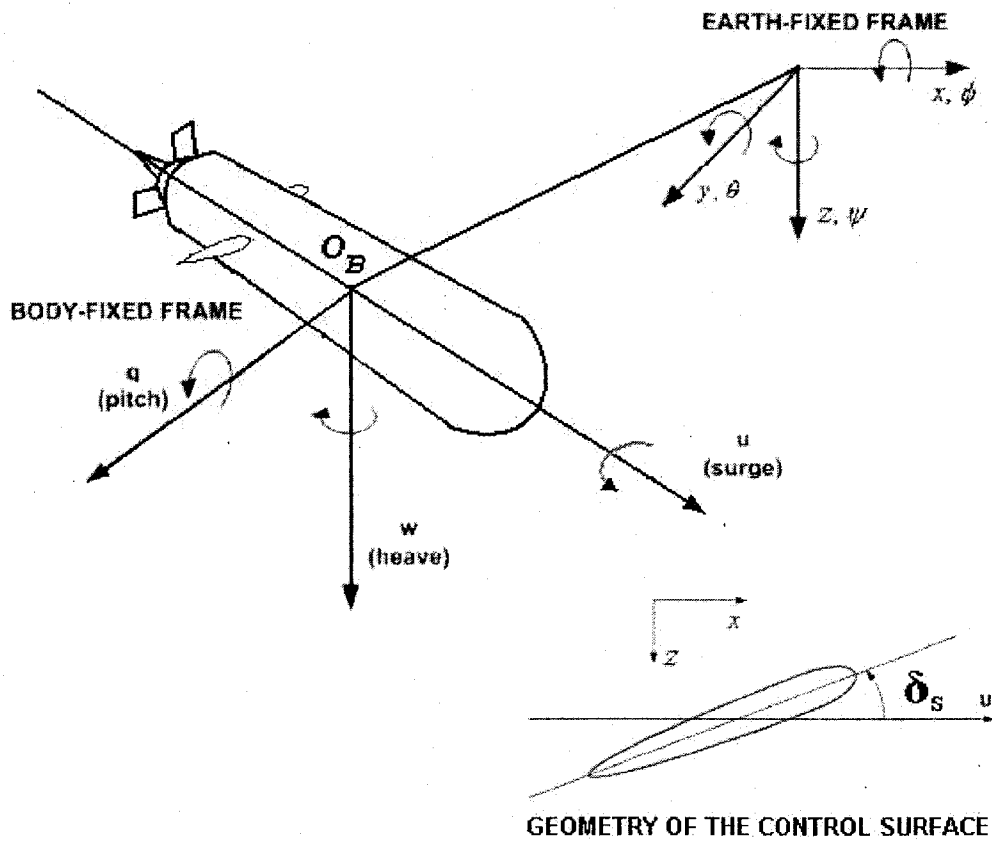


Figure 3.1: The AUV model

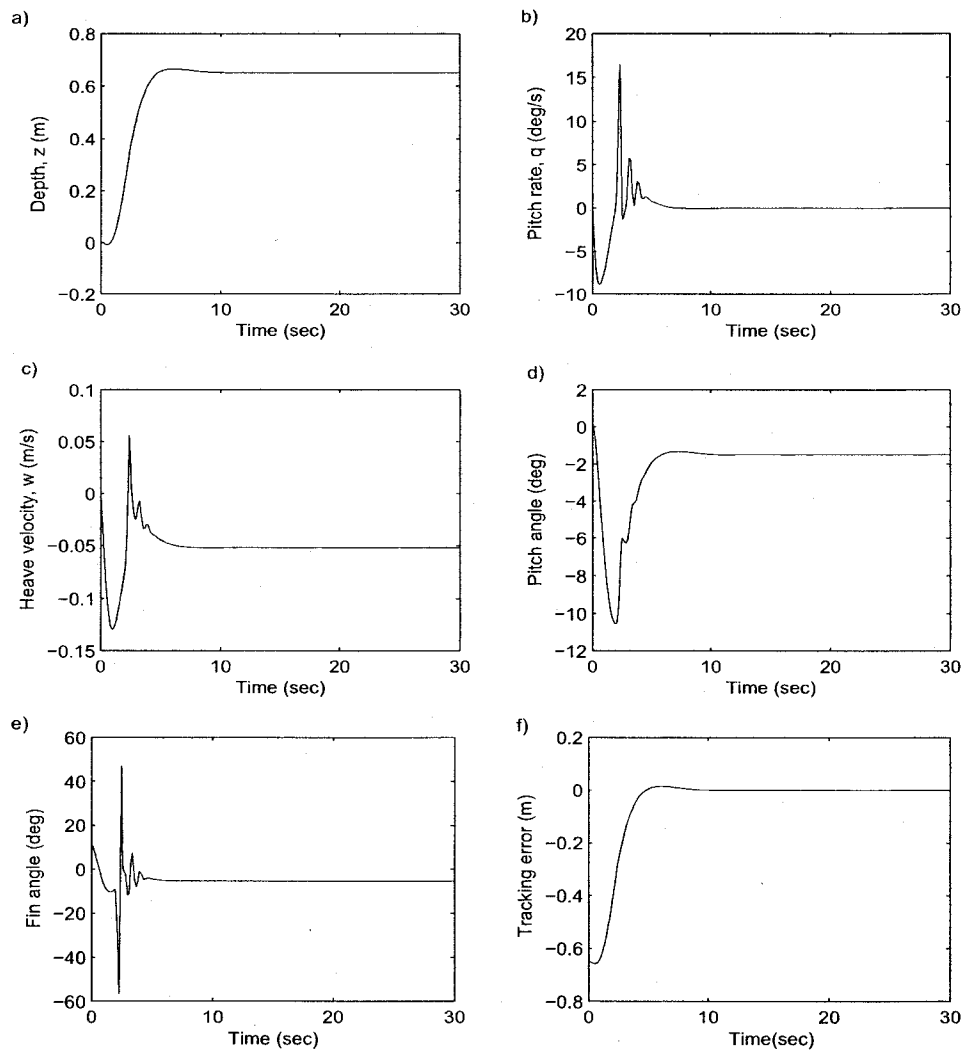


Figure 3.2: Nominal REMUS control with unconstrained input: $U = 2$ m/s, $z_r = 0.65$ m
 (a) Plunge displacement (m) (b) Pitch rate (deg/s) (c) Heave velocity (m/s) (d) Pitch angle (deg) (e) Fin angle (deg) (f) Tracking error (m)

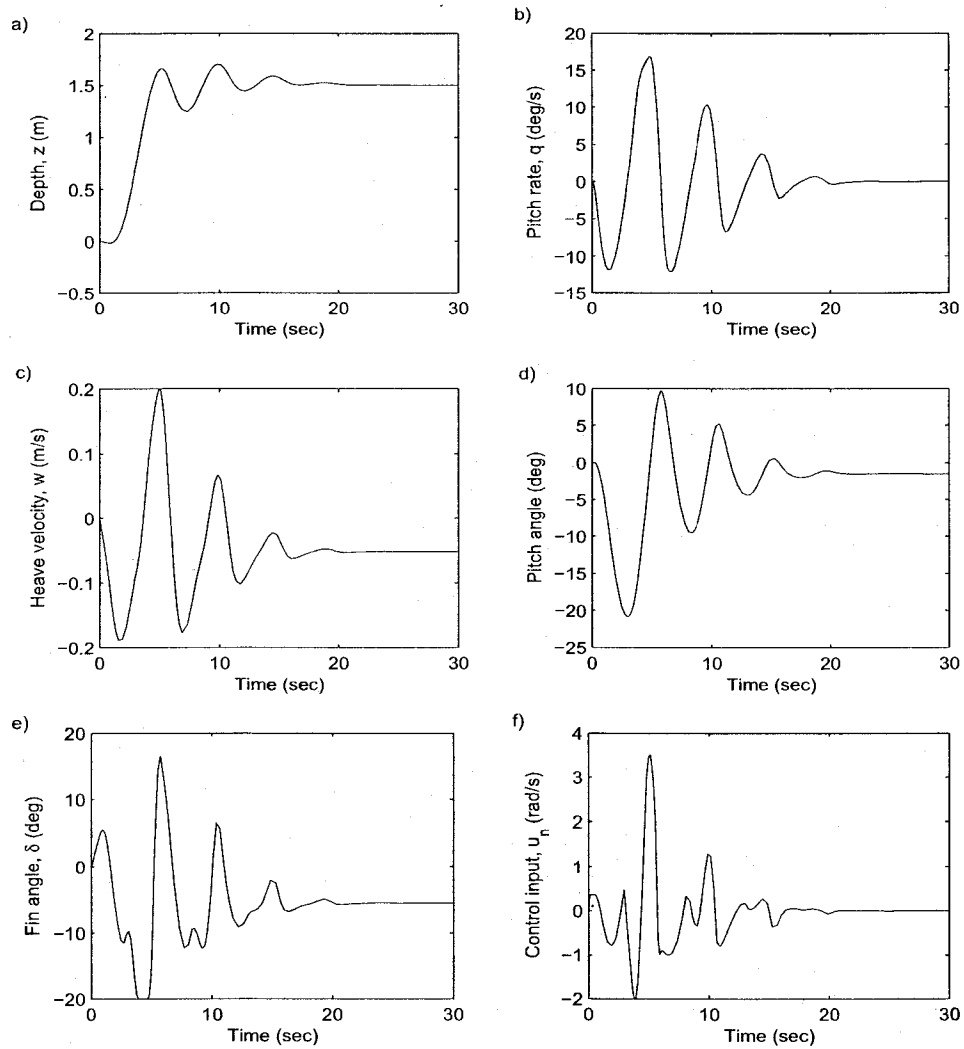


Figure 3.3: Nominal REMUS control with saturating fin: $U = 2$ m/s, $z_r = 1.5$ m
(a) Plunge displacement (m) (b) Pitch rate (deg/s) (c) Heave velocity (m/s) (d) Pitch angle (deg) (e) Fin angle (deg) (f) Control input (rad/s)

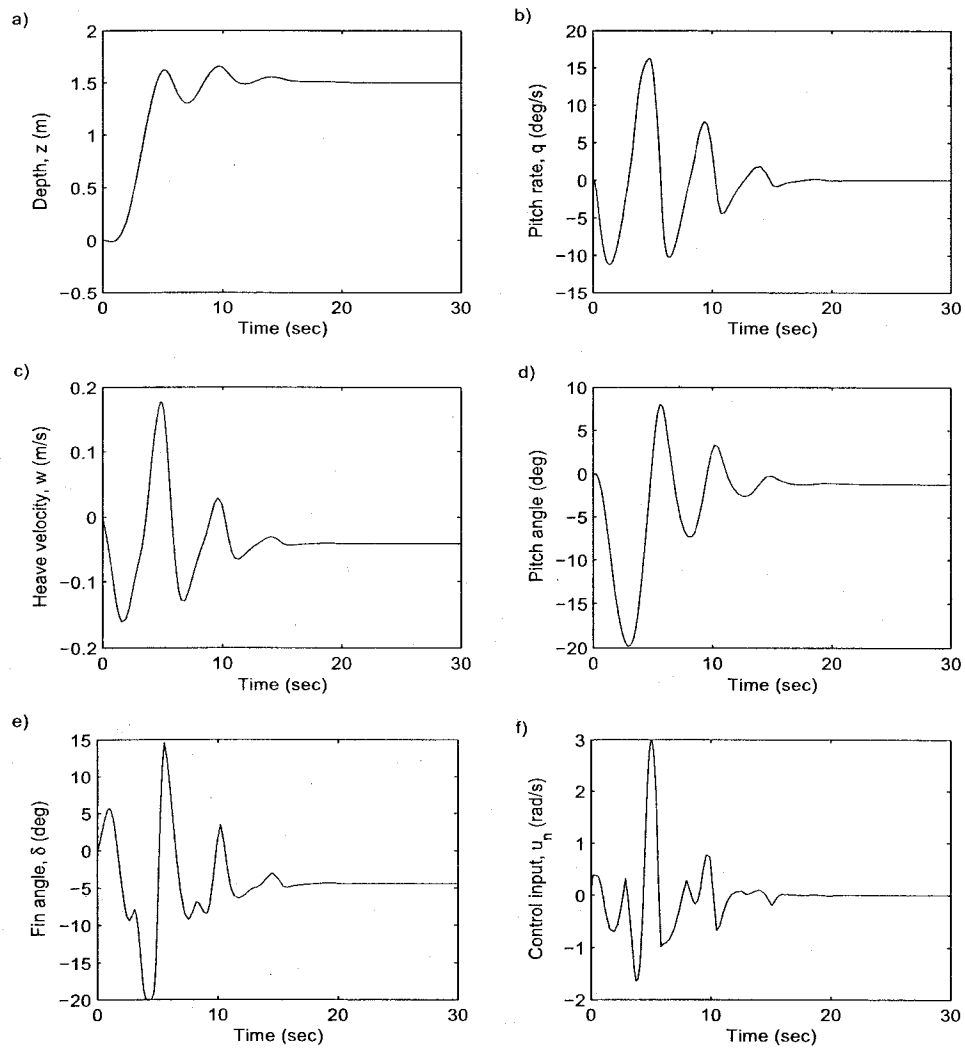


Figure 3.4: Off-nominal ($p = +25p^*$) REMUS control with saturating fin: $U = 2$ m/s, $z_r = 1.5$ m
 (a) Plunge displacement (m) (b) Pitch rate (deg/s) (c) Heave velocity (m/s) (d) Pitch angle (deg) (e) Fin angle (deg) (f) Control input (rad/s)

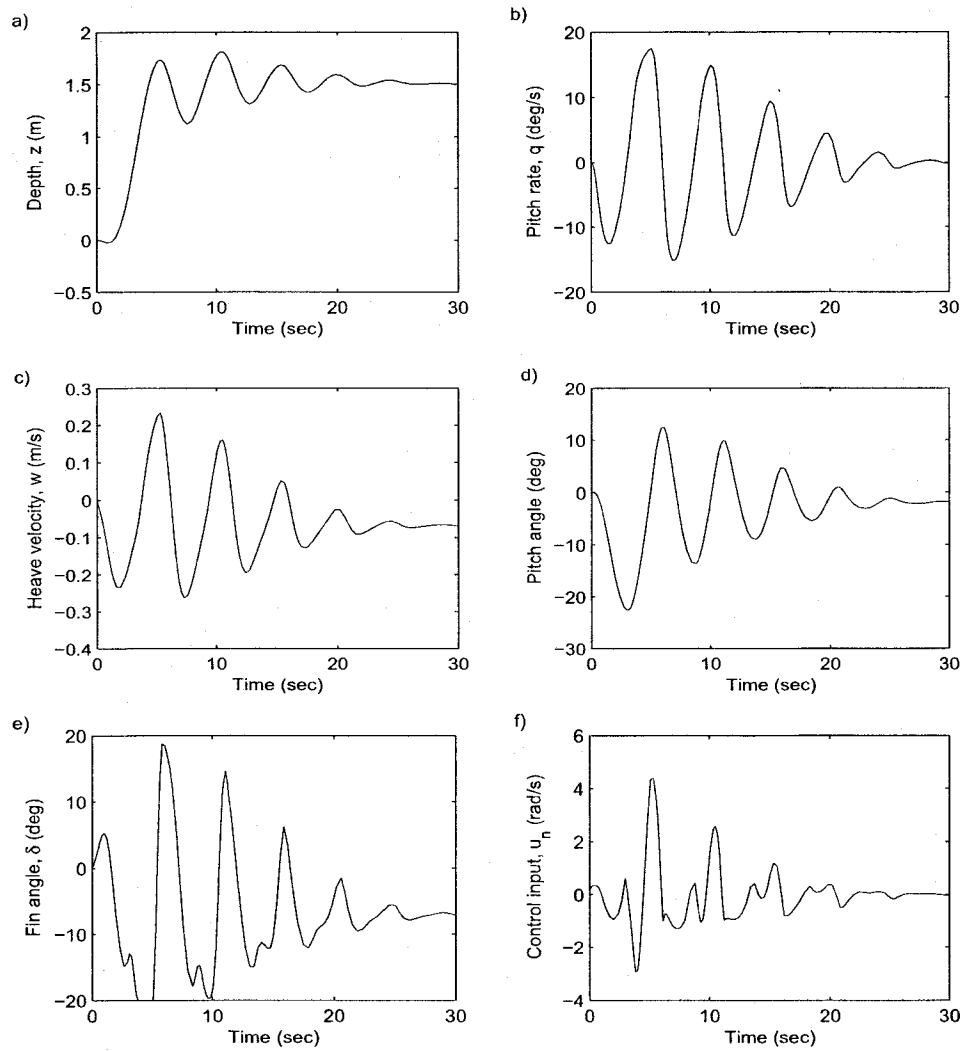


Figure 3.5: Off-nominal ($p = -.25p^*$) REMUS control with saturating fin: $U = 2$ m/s, $z_r = 1.5$ m

(a) Plunge displacement (m) (b) Pitch rate (deg/s) (c) Heave velocity (m/s) (d) Pitch angle (deg) (e) Fin angle (deg) (f) Control input (rad/s)

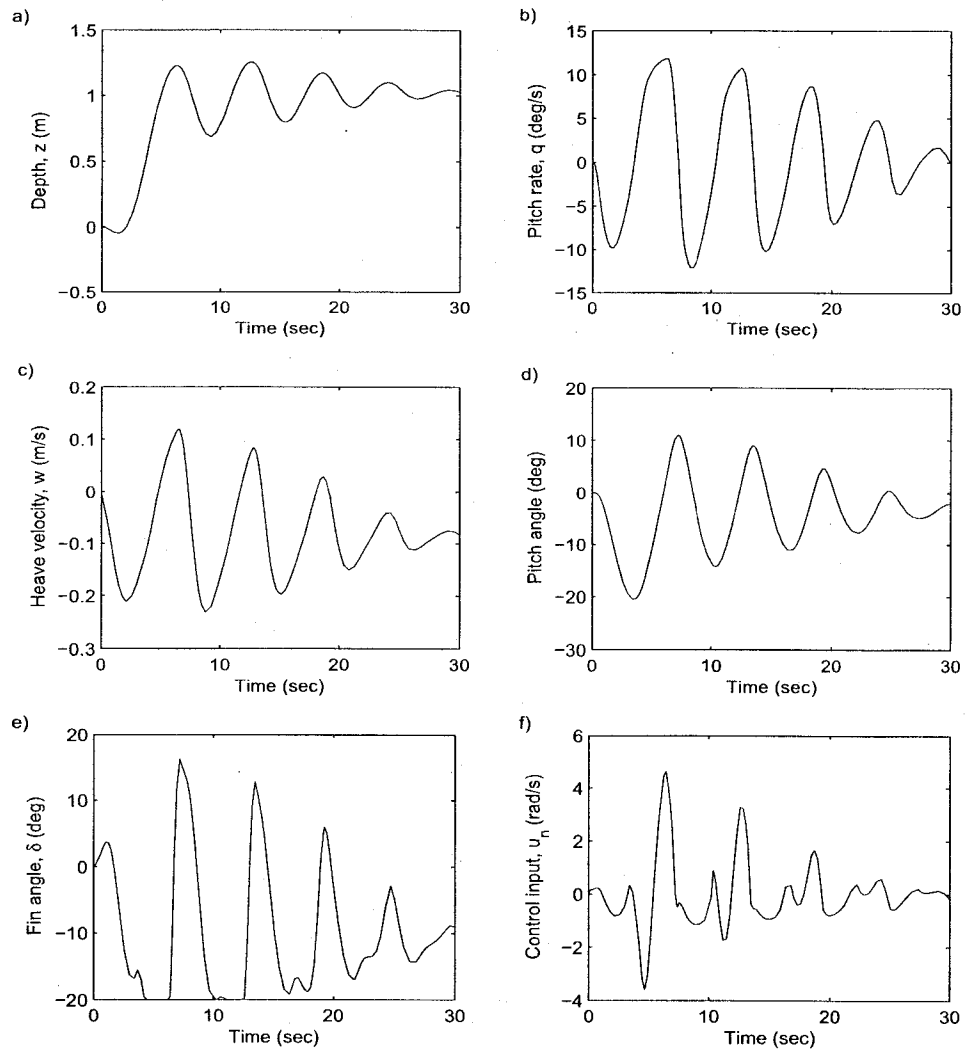


Figure 3.6: Off-nominal ($p = -.25p^*$) REMUS control with saturating: $U = 1.54$ m/s, $z_r = 1$ m
 (a) Plunge displacement (m) (b) Pitch rate (deg/s) (c) Heave velocity (m/s) (d) Pitch angle (deg) (e) Fin angle (deg) (f) Control input (rad/s)

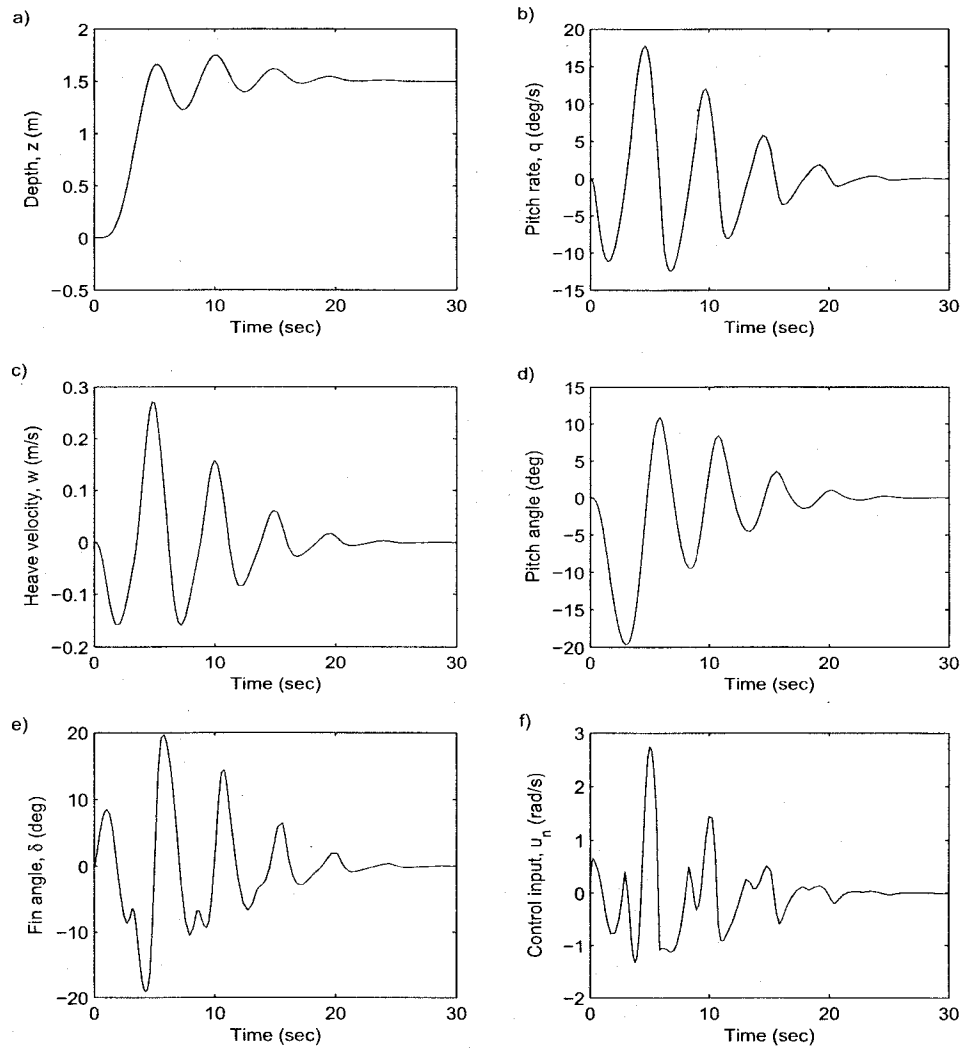


Figure 3.7: Off-nominal ($p = -0.25p^*$) REMUS control with saturating control: $U = 2\text{m/s}$, $z_r = 1.5\text{ m}$, $W = B_o$
 (a) Plunge displacement (m) (b) Pitch rate (deg/s) (c) Heave velocity (m/s) (d) Pitch angle (deg) (e) Fin angle (deg) (f) Control input (rad/s)

CHAPTER 4

STATE FEEDBACK ADAPTIVE PECTORAL-LIKE FIN CONTROL SYSTEM

In the previous chapter, a nonlinear suboptimal control system was designed for dive plane maneuvering of an AUV using traditional control surfaces. Whereas, in this chapter, adaptive control of a biorobotic autonomous underwater vehicle (BAUV) in the yaw plane using biologically-inspired pectoral-like fins is designed. The use of biologically-inspired fins makes the BAUVs energy efficient and is thus a preferred choice over traditional AUVs. The fins are assumed to be oscillating harmonically with a combined linear (sway) and angular (yaw) motion. This control system is presented here in this chapter by using the periodic forces and moments generated by the pectoral fins. The mathematical model used here has been presented in the second chapter.

Using a discrete-time state variable representation of the BAUV, an adaptive sampled data control system for the trajectory control of the yaw angle using state feedback is derived. The bias (mean) angle of the angular motion of the fin is used as a control input. The parameter adaptation law is based on the normalized gradient scheme. In the closed-loop system, time-varying yaw angle reference trajectories are tracked and all the signals in the closed-loop system remain bounded. Simulation results for the set point control, sinusoidal trajectory tracking and turning maneuvers are presented, which show that the control system accomplishes precise trajectory control in spite of the parameter uncertainties, and the inter sample segments of the yaw angle trajectory remain close to the discrete-time reference trajectory.

The organization of the chapter is as follows. The BAUV control problem is presented in section 4.1. It is followed by the adaptive controller in section 4.2 and the simulation results in section 4.3.

4.1 BAUV Control Problem

The continuous-time BAUV model considered for design is

$$\begin{aligned} \dot{x} &= Ax + B\Phi(t)f_c + B\Phi(t)f_v\beta \\ y(t) &= \begin{bmatrix} 0 & 0 & 1 \end{bmatrix} x(t) = Cx(t) \end{aligned} \quad (4.1)$$

(see chapter 2.) We assume that the vehicle's physical parameters, the hydrodynamics coefficients, and the fin forces and moments are not known to the designer. The system (4.1) is time-varying but periodic. The design of control system for a time-varying unknown system is not simple. Moreover, the control law is independent of the number of harmonics retained in the truncated Fourier expansion of the fin force and moment. Further, in order to obtain a meaningful use of the parameterization of the fin force and moment using the CFD analysis, we proceed to design a sampled-data adaptive control system.

We assume that the bias angle changes at a regular interval $T = m_o T_o$, where m_o is an integer and $T_o = 1/f$ is the fundamental period. That is, the bias angle switches after the completion of m_o cycles of the oscillation of the fins, and is kept constant between the switching instants. The solution of (4.1) is given by

$$x(t) = e^{(t-t_o)}x(t_o) + \int_{t_o}^t e^{A(t-\tau)}B\Phi(\tau)[f_c + f_v\beta(\tau)]d\tau \quad (4.2)$$

Taking $t_o = kT$ and $t = (k+1)T$, one has

$$x[(k+1)T] = e^{AT}x(kT) + \int_{kT}^{(k+1)T} e^{A[(k+1)T-\tau]}B\Phi(\tau)[f_c + f_v\beta_k]d\tau \quad (4.3)$$

Let $(k+1)T - \tau = s$. Then, noting that

$$\Phi((k+1)T - s) = \Phi(-s) \quad (4.4)$$

(4.2) gives

$$x[(k+1)T] = e^{AT}x(kT) + \int_0^T e^{As}B\Phi(-s)[f_c + f_v\beta_k]ds \quad (4.5)$$

Thus the discrete dynamic model of the AUV is given by

$$\begin{aligned} x[(k+1)T] &= A_d x(kT) + B_d \beta_k + d_u \\ y(kT) &= Cx(kT) \end{aligned} \quad (4.6)$$

where A_d , B_d and d_u are constant vectors, β_k (a constant) is the bias angle over $t \in [kT, (k+1)T)$, and $k = 0, 1, 2, \dots$. We assume that the matrices A_d , B_d and d_u are unknown to the designer. Here we treat d_u as a constant disturbance input vector.

In the sequel, z denotes the z -transform variable or an advance operator (i.e. $zq(kT) = q[(k+1)T]$). Solving (4.6), the output $y(z)$ can be written as

$$\begin{aligned} y(z) &= C(zI - A_d)^{-1}B_d\beta_k(z) + C(zI - A_d)^{-1}d_u(z) \\ &\triangleq k_p \frac{n(z)}{d(z)}\beta_k(z) + \frac{n_d(z)}{d(z)}d_u(z) \end{aligned} \quad (4.7)$$

where $n(z)$ and $d(z)$ are monic polynomials of degree 2 and 3, respectively, and $n_d(z)$ is a polynomial. For the derivation of the control law, the following assumptions are needed:

Assumption 1:

- (A.1) The discretized system (A_d, B_d, C) is controllable and observable.
- (A.2) The system is minimum phase.
- (A.3) The sign of k_p is known and the upper bound k_p^o of $|k_p|$ is known.

For the vehicle model $n(z)$ is a stable polynomial (i.e. its both the roots are strictly within the unit disk in the complex plane), but the denominator polynomial $d(z)$ is unstable. Furthermore, $n(z)$ and $d(z)$ are coprime, and therefore, the pair (A_d, B_d) is controllable and (C, A_d) is observable. We point out that the stability of the polynomial $n(z)$ depends on the choice of fin location on the vehicle, and it is found that for small d_f (distance from point of attachment of fin to center of buoyancy) the system is minimum phase. The Assumption 1 can be verified by computing $A_d, B_d, k_p, n(z)$ and $d(z)$ for some nominal values of the parameters. Then the assumption remains valid for the perturbations around the nominal condition.

The relative degree of the system is one, therefore we choose a reference model of the form.

$$y_m(kT) = W_m(z)r(kT), \quad k = 0, 1, 2, \dots \quad (4.8)$$

where $r(kT)$ is a discrete-time command input and

$$W_m(z) = \frac{1}{z} \quad (4.9)$$

is the delay operator (i.e., $y_m[(k+1)T] = r[kT]$).

We are interested in the design of an adaptive control law so that the yaw angle $\psi(t)$ asymptotically follows the reference trajectories. For synthesis the state vector is fed back.

4.2 Adaptive Controller

First we consider the existence of the control law assuming that the system parameters are exactly known. Then this control law is modified for the case when the parameters are not known. The design of the control law follows the steps described in [30]. Consider a control law

$$u^*(kT) = \theta_1^{*T} x(kT) + \theta_2^* r(kT) + \theta_3^* \quad (4.10)$$

where $\theta_1^* \in R^3$, and $\theta_2^*, \theta_3^* \in R$ are to be chosen properly. Then in the closed-loop system (4.6) and (4.10), solving for $y(kT)$ gives

$$y(kT) = C(zI - \bar{A}_d)^{-1}B_d\theta_2^*r(kT) + \Delta(z) + CA_d^{-k}x(0) \quad (4.11)$$

where

$$\Delta(z) = [C(zI - \bar{A}_d)^{-1}B_d\theta_3^* + C(zI - \bar{A}_d)^{-1}d_u] \frac{z}{z-1}$$

and θ_1^* is chosen such that $\bar{A}_d = (A_d + B_d\theta_1^{*T})$ has stable eigenvalues.

Now the computation of θ_i^* for the yaw angle trajectory control is done. This is accomplished by model matching. Let us choose the feedback gains θ_i^* ($i = 1, 2$) such that $\theta_2^* = k_p^{-1}$ and

$$C(zI - A_d - B_d\theta_1^{*T})B_d\theta_2^* = W_m = z^{-1} \quad (4.12)$$

This is possible because the system (4.6) is controllable and minimum phase. Then in the closed-loop system, (4.11) takes the form

$$y(kT) = W_m(z)r(kT) + \Delta(z) + C\bar{A}_d^k x(0) \quad (4.13)$$

where $\Delta(z)$ simplifies to

$$\Delta(z) = [\theta_2^{*-1}\theta_3^*W_m(z) + C(zI - \bar{A}_d)^{-1}d_u] \frac{z}{z-1} \quad (4.14)$$

Note that (4.12) has been used to obtain (4.14). Since \bar{A}_d is a stable matrix, as $k \rightarrow \infty$, (4.14) gives

$$\Delta(\infty) = \lim_{z \rightarrow 1} [(z-1) \Delta(z)] = (\theta_2^*)^{-1}\theta_3^* + C(I_{3 \times 3} - \bar{A}_d)^{-1}d_u \quad (4.15)$$

From (4.15), it follows that $\Delta(\infty)$ becomes zero if one chooses

$$\theta_3^* = -\theta_2^*C(I_{3 \times 3} - \bar{A}_d)^{-1}d_u \quad (4.16)$$

Using these values of θ_i^* , and ignoring the exponentially decaying signals, (4.13) gives

$$y(kT) = W_m r(kT) \quad (4.17)$$

This implies that the tracking error $e(kT) = y(kT) - y_m(kT) = W_m[0]$ tends to zero as $k \rightarrow \infty$.

For the system with unknown parameters, the control law is chosen as

$$u(kT) = \theta_1^T(kT)x(kT) + \theta_2(kT)r(kT) + \theta_3(kT) \quad (4.18)$$

where $\theta_1(kT) \in R^3$, $\theta_2(kT) \in R$, and $\theta_3(kT) \in R$ are the time-varying estimates of θ_i^* , $i = 1, 2, 3$.

We are interested in deriving an adaptation law such that the tracking error asymptotically tends to zero. With the control law (4.18), the closed-loop system takes the form

$$\begin{aligned} x[(k+1)T] &= A_d x(kT) + B_d [\theta_1^T(kT)x(kT) + \theta_2(kT)r(kT) + \theta_3(kT)] + d_u \\ &= [A_d + B_d \theta_1^{*T}]x(kT) + B_d \theta_2^* r(kT) + B_d \theta_3^* + B_d \tilde{\theta}^T(kT)w(kT) + d_u \end{aligned} \quad (4.19)$$

where

$$\theta^* = [\theta_1^{*T}, \theta_2^*, \theta_3^*]^T \in R^5,$$

$$w(kT) = [x^T(kT), r(kT), 1]^T \in R^5,$$

$\theta(kT) = (\theta_1^T(kT), \theta_2(kT), \theta_3(kT))^T$, and $\tilde{\theta}(kT) = (\theta(kT) - \theta^*)$ is vector of parameter error. In view of (4.11), (4.12) and (4.14), the output computed from (4.16) takes the form

$$y(kT) = W_m r(kT) + W_m \rho^* \tilde{\theta}(kT)w(kT) + \Delta(z) + C \bar{A}_d^k x(0) \quad (4.20)$$

where $\rho^* = k_p = \theta_2^{*-1}$. Since $\Delta(z)$ tends to zero as $kT \rightarrow \infty$, ignoring the exponential decaying signals, (4.20) yields

$$e(kT) = \rho^* W_m [\tilde{\theta}^T(kT)w(kT)] \quad (4.21)$$

For the derivation of the adaptation law according to [30], one needs to obtain an augmented error beginning from (4.21). Define a signal

$$\xi(kT) = \theta^T(kT)w[(k-1)T] - \theta^T[(k-1)T]w[(k-1)T] \quad (4.22)$$

and the augmented error

$$\epsilon(kT) = e(kT) + \rho(kT)\xi(kT) \quad (4.23)$$

where $\rho(t)$ is an estimate of $\rho^* = k_p$. Then substituting the tracking error (4.21) in (4.23) and using (4.22) gives

$$\begin{aligned} \epsilon(kT) &= \rho^* \{W_m(\theta^T(kT)w(kT)) - \theta^{*T}w[(k-1)T]\} + \rho(kT)\xi(kT) \\ &= \rho^* \{\theta^T(kT)w[(k-1)T] - \xi(kT) - \theta^{*T}w[(k-1)T]\} + \rho(kT)\xi(kT) \\ &= \rho^* \tilde{\theta}^T(kT)w[(k-1)T] + \tilde{\rho}(kT)\xi(kT) \end{aligned} \quad (4.24)$$

where $\tilde{\rho}(kT) = \rho(kT) - \rho^*$ is the parameter error. This linearly parameterized augmented error equation is important for the derivation of the adaptation law.

Now following [30], the normalized gradient based control law is chosen as

$$\begin{aligned} \theta[(k+1)T] &= \theta(kT) - \frac{\text{sign}(\rho^*)\Gamma w[(k-1)T]\epsilon(kT)}{m^2(kT)} \\ \rho[(k+1)T] &= \rho(kT) - \frac{\gamma\xi(kT)\epsilon(kT)}{m^2(kT)} \end{aligned} \quad (4.25)$$

where the symmetric positive definite adaptation gain matrix Γ satisfies $0 < \Gamma = \Gamma^T < \frac{2}{k_p} I_{5 \times 5}$, $0 < \gamma < 2$, and

$$m^2(kT) = 1 + w^T[(k-1)T]w[(k-1)T] + \xi^2(kT)$$

For the stability analysis one chooses the Lyapunov function

$$V(\tilde{\theta}, \tilde{\rho}) = |\rho^*| \tilde{\theta}^T(kT)\Gamma^{-1}\tilde{\theta}(kT) + \gamma^{-1}\tilde{\rho}^2(kT) \quad (4.26)$$

and following [30] shows that

$$V[(k+1)T] - V(kT) \leq -\alpha_1 \frac{\epsilon^2(t)}{m^2(t)} \quad (4.27)$$

where $\alpha_1 > 0$. This implies that $\theta(kT), \rho(kT), \frac{\epsilon(kT)}{m(kT)} \in L^\infty$ (the set of bounded functions), and $\frac{\epsilon(kT)}{m(kT)}, (\theta[(k+1)T] - \theta(kT)), (\rho[(k+1)T] - \rho(kT)) \in L^2$ (the set of square summable functions).

Furthermore, one can show that $e(kT) \rightarrow 0$ and all the signals in the closed-loop system are bounded. This completes the derivation of the adaptive control law for the yaw plane maneuvering. The Figure. 4.1 shows the complete closed-loop system with parameter adaptation law.

4.3 Simulation Results For Yaw Plane Maneuvers

In this section, simulation results using the MATLAB/SIMULINK for yaw angle control are presented. Various time-varying reference trajectories are considered for tracking, and the performance of the adaptive controller in the presence of parameter uncertainties is examined.

The parameters of the model are taken from [33]. The AUV is assumed to be moving with a constant forward velocity of 0.7 (m/sec). The vehicle parameters are $l = 1.391$ (m), mass=18.826 (kg), $I_z = 1.77$ (kgm²), $X_G = -0.012$, $Y_G = 0$. The hydrodynamic parameters for a forward velocity of 0.7 m/sec derived from [33] are $Y_{\dot{r}} = -0.3781$, $Y_{\dot{v}} = -5.6198$, $Y_r = 1.1694$, $Y_v = -12.0868$, $N_{\dot{r}} = -0.3781$, $N_{\dot{v}} = -0.8967$, $N_r = -1.0186$, and $N_v = -4.9587$. It is assumed that $d_f = 0.01$ (m) and the fin oscillation frequency is $f = 8Hz$. The vectors f_a , f_b , m_a , and m_b are found to be [28]

$$f_a = (0, -40.0893, -43.6632, -0.3885, 0.6215, 6.2154, -10.17, -0.1554, 0.6992)$$

$$f_b = (68.9975, 0.4451, -16.4704, 64.1009, -19.5864, -0.8903, -2.2257, 2.2257, 4.8966)$$

$$m_a = (0.0054, 0.6037, 0.4895, 0, -0.0054, 0, -0.0925, 0, -0.0054)$$

$$m_b = (-0.5297, -0.3739, -0.0935, -0.2493, 0.1246, 0.0312, -0.0312, 0.0935, 0)$$

It is pointed out that these parameters are obtained using the Fourier decomposition of the fin force and moment, and are computed by multiplying the Fourier coefficients by $\frac{1}{2}\rho.W_a.U_\infty^2$ and $\frac{1}{2}\rho.W_a.chord.U_\infty^2$, respectively, where W_a is the surface area of the foil. For simulation, the initial conditions of the vehicle are assumed to be $x(0) = 0$.

The closed-loop system (4.6) and (4.18) with the update law (4.25) is simulated. The bias angle is changed to a new value every $T = T_o$ seconds, where $T_o = 1/f$ is the fundamental period of f_p and m_p . For the set point control, the terminal value of the yaw angle is taken as $\psi^* = -5$ deg. Thus one desires to control the BAUV to a heading angle of -5 deg. For the update law, the adaptation gains are selected as $\Gamma = 0.4(2/k_p^o)I_{5 \times 5}$ and $\gamma = 1$, where $k_p^o = 0.08 \geq |k_p|$. Using the values of AUV model, it is found that the actual feedback gains are $\theta_1^* = (1.2139 - 13.0228 - 104.6334)^T$, $\theta_2^* = -104.6334$ and $\theta_3^* = 0.2122$ and $\rho^* = k_p = -0.0096$. The open-loop zeros and poles of the discretized system are (-0.8990, 0.4667) and (1.0000, 1.0864, 0.8715), respectively. Therefore, the transfer function is minimum phase. Simulation results are presented for the parameter uncertainty of 50 %.

Case A1: Adaptive set point control: Parameter uncertainty 50% off-nominal for Yaw angle -5 (deg).

For smooth control, the reference input $r(kT)$ (in rad) is selected as

$$r(kT) = [1 - \exp(-0.35(k-1)T)](-5\pi/180)$$

where the sampling time is $T = 0.125$ (sec). Thus the control law is updated at the completion of each cycle of oscillation. Assuming 50 % uncertainty, the initial estimates $\theta(0)$ and $\rho(0)$ are set to $0.50\theta^*$ and $0.50\rho^*$. This way the control law gains are 50 % lower than the exact θ^* . Figure. 4.2 shows the simulated results. It can be seen that the adaptive controller achieves accurate heading angle control to the target set point in about 15 sec. The control input (bias angle) magnitude required is about 15 deg, which can be provided by the pectoral fins. The plots of the lateral force and moment produced by the fins are also provided in the figure. In the steady-state, the lateral fin force and moment exhibit bounded periodic oscillations. It is found that the control magnitude can be reduced by using slower command $r(kT)$ if desired.

Case A2: Adaptive sinusoidal trajectory control: Parameter uncertainty 50 % off-

nominal

In order to examine, time-varying tracking ability of the controller, a sinusoidal reference trajectory is generated using the command input $r(kT) = 3.5 \times (\pi/180) \sin(kT)$ (*rad*). It is assumed that $\theta(0) = 0.50\theta^*$ and $\rho(0) = 0.50\rho^*$ giving 50% uncertainty. The responses are shown in Figure 4.3. It is seen that, after the initial transients, the heading angle smoothly tracks the sinusoidal command trajectory. The control input (bias angle) magnitude required is about 20 deg.

Case A3: Adaptive turning maneuver

The turning maneuver is an important practical maneuver that BAUVs frequently need to perform. For constant turning rate, a smooth trajectory is generated using the command input $r(kT) = 4kT (\pi/180)$ (*rad*). As seen in Figure 4.4. the trajectory tracked by the system is almost a circle due to the small magnitude of the time-varying lateral velocity. This requires a control input magnitude of 30 deg and less than 100 sec to make a complete circle. It is possible to have a faster turning rate, however, that requires larger control forces.

Simulations for other off-nominal choices of $(\theta(0), \rho(0))$ have been performed. It is found that although, theoretically, asymptotic tracking can be accomplished for any choice of initial estimates of $(\theta(0), \rho(0))$, larger control inputs are required for higher uncertainties. Furthermore, the control system performs relatively well for the choice of under-estimated initial values of the control gains $(\theta(0), \rho(0))$. Of course, the responses also depend on the choice of the command generator and the adaptation gain matrix Γ and γ of the update law.

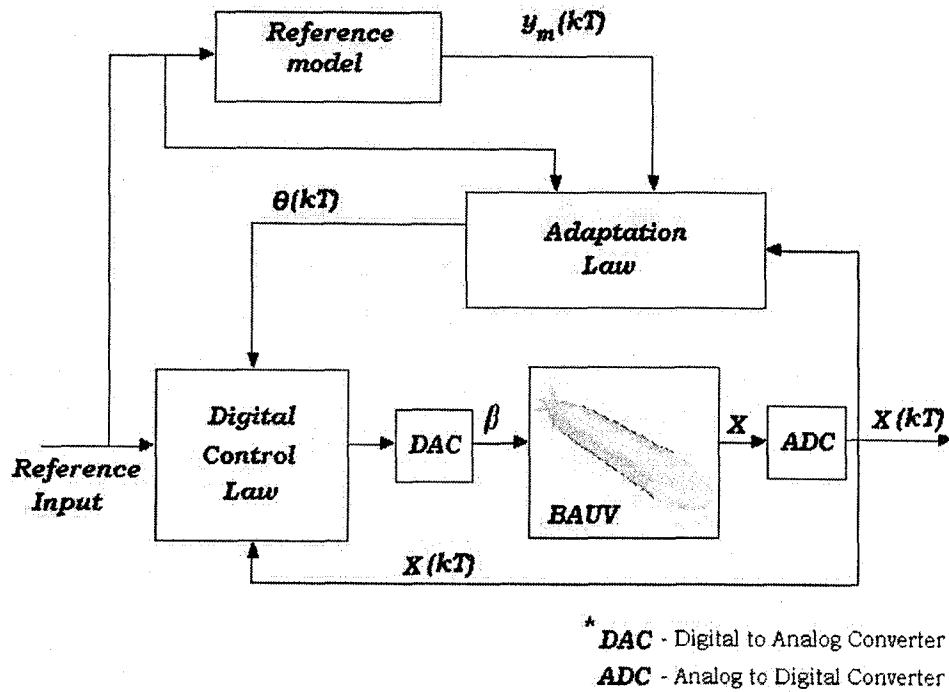


Figure 4.1: The Complete Closed-loop system with State feedback and Parameter Adaptation

Note: For clarity different time scale is used for each plot.

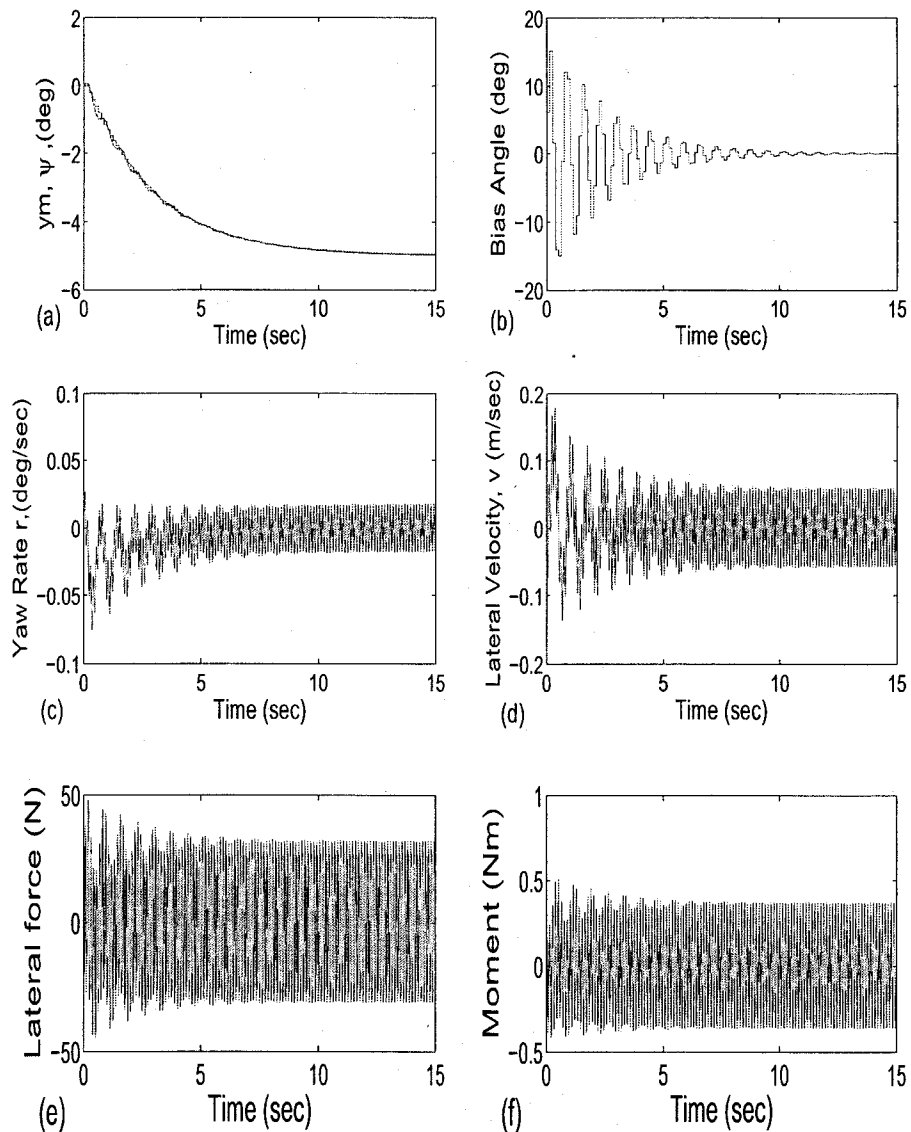


Figure 4.2: Adaptive set point control: Frequency of flapping 8Hz for $\psi^* = -5$ (deg) and parameter uncertainty 50%
 (a) Yaw angle, ψ , (solid) and reference yaw angle (staircase) (deg) (b) Bias angle (deg) (c) Yaw rate (deg/sec) (d) Lateral velocity (m/sec) (e) Lateral force(N) (f) Moment(Nm)

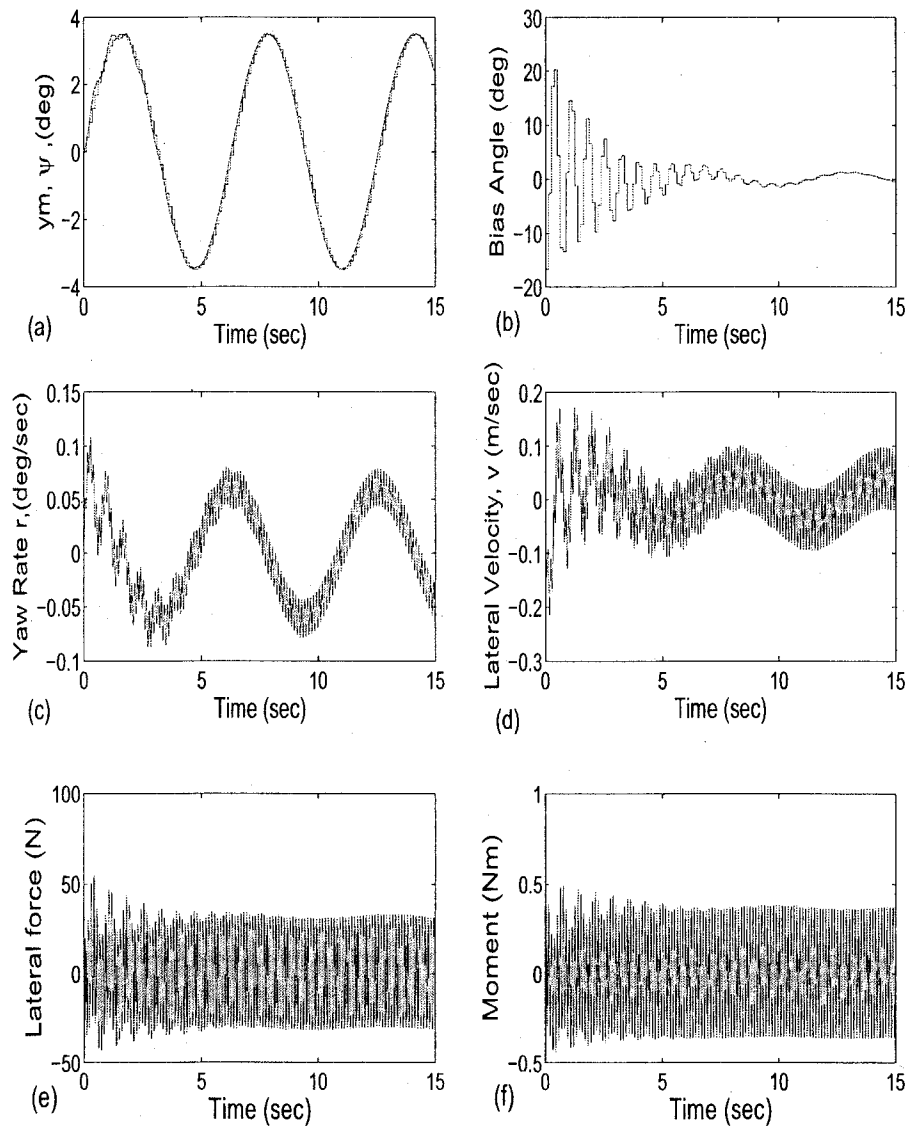


Figure 4.3: Adaptive sinusoidal trajectory control: Frequency of flapping 8Hz for $y_m = 3.5 \sin 2\pi f k T$ (deg) and parameter uncertainty 50%
 (a) Yaw angle, ψ (solid) and reference yaw angle (staircase) (deg) (b) Bias angle (deg) (c) Yaw rate (deg/sec) (d) Lateral velocity (m/sec) (e) Lateral force(N) (f) Moment(Nm)

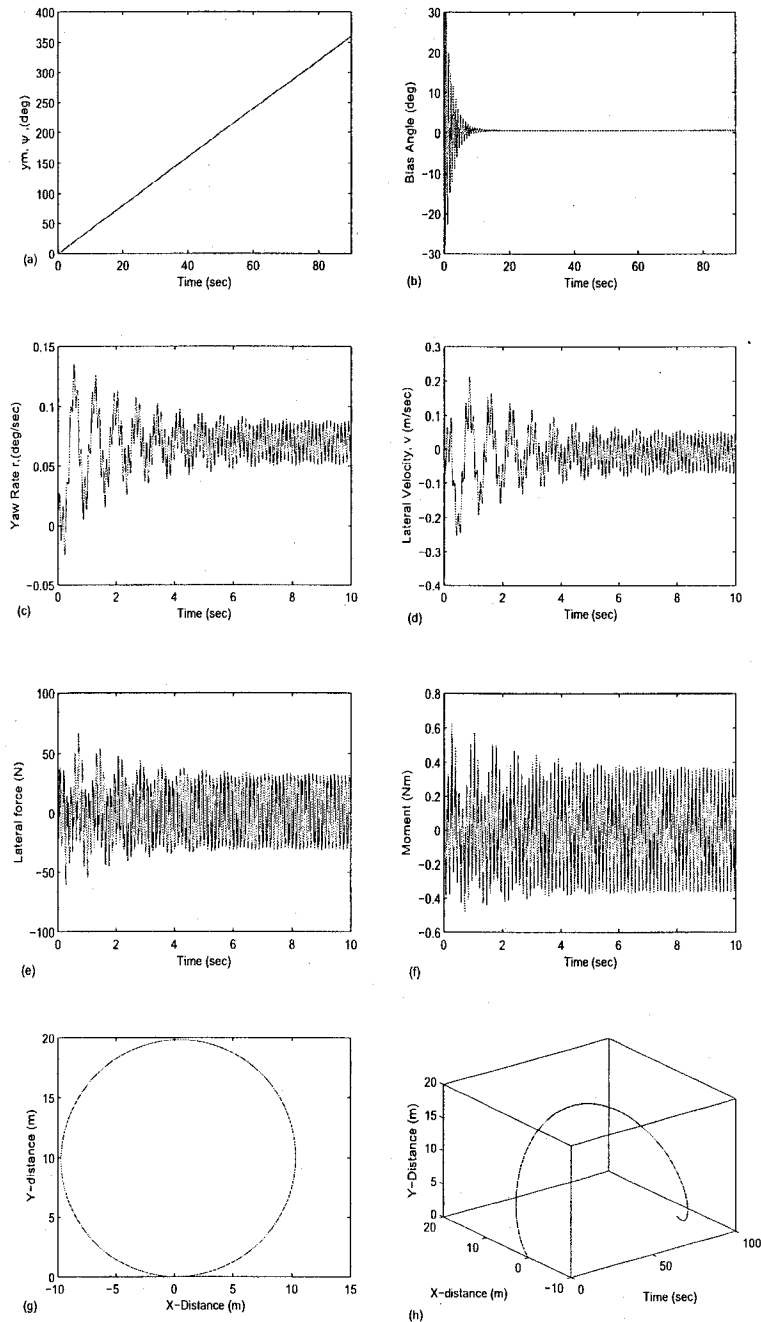


Figure 4.4: Adaptive turning maneuver: Frequency of flapping 8Hz for 360 (deg) turn with turning rate of 4 (deg / sec) and parameter uncertainty 50%
 (a) Yaw angle, ψ (solid) and reference yaw angle (staircase)(deg) (b) Bias angle (deg) (c) Yaw rate (deg/sec) (d) Lateral velocity (m/sec) (e) Lateral force(N) (f) Moment(Nm) (g) Global position of the BAUV (X and Y co-ordinates) (h) Three-dimensional plot of X and Y distances with time

CHAPTER 5

OUTPUT FEEDBACK ADAPTIVE PECTORAL-LIKE FIN CONTROL SYSTEM

In the previous chapter, we considered the design of an adaptive control law. However, for the synthesis, it was assumed that state vector is available for feedback. It was thus essential to measure all the state variables for the synthesis of the control law. But from the practical point of view, the synthesis using state-feedback is not attractive, because one must use sensors to measure each state variable.

In this chapter, an output feedback adaptive control system for the yaw plane maneuvering of a biorobotic AUV using pectoral fin is derived where only the yaw angle is to be measured for feedback. The mathematical model used here has been presented in the second chapter.

A sampled-data adaptive control law is obtained for the trajectory control of the yaw angle. The adaptation law for tuning the controller parameters is derived using the normalized gradient method. In the closed-loop system, the yaw angle asymptotically tracks time-varying reference trajectories, and all the signals in the closed-loop system remain bounded. Simulation results for the set point and sinusoidal trajectory control as well as for turning maneuvers are presented.

The organization of this chapter is as follows. The control problem is posed in section 5.1. The adaptive law for yaw angle control is derived in Section 5.2, and Section 5.3 presents the simulation results.

5.1 Problem Formulation

The discrete-time BAUV model considered for design is

$$\begin{aligned} x[(k+1)T] &= A_d x(kT) + B_d \beta_k + d_u \\ y(kT) &= Cx(kT) \end{aligned} \tag{5.1}$$

where A_d , B_d and d_u are constant vectors, β_k (a constant) is the bias angle over $t \in [kT, (k+1)T)$, and $k = 0, 1, 2, \dots$. We again assume that the matrices A_d , B_d and d_u are unknown to the designer. Here we treat d_u as a constant disturbance input vector.

In the sequel, z denotes the z -transform variable or an advance operator (i.e. $zq(kT) = q[(k+1)T]$). Solving (5.1), the output $y(z)$ can be written as

$$\begin{aligned} y(z) &= C(zI - A_d)^{-1} B_d \beta_k(z) + C(zI - A_d)^{-1} d_u(z) \\ &\triangleq k_p \frac{n(z)}{d(z)} \beta_k(z) + \frac{n_d(z)}{d(z)} d_u(z) \end{aligned} \tag{5.2}$$

where $n(z)$ and $d(z)$ are monic polynomials of degree 2 and 3, respectively, and $n_d(z)$ is a polynomial. For the derivation of the control law, the following assumptions are needed:

Assumptions :

- (A.1) $n(z)$ is stable polynomial.
- (A.2) The degree n of $d(z)$ is known.
- (A.3) The sign of k_p and the upper bound k_p^o of $|k_p|$ is known.
- (A.4) The relative degree $n^* = n - m > 0$ is known.
- (A.5) The disturbance $d(t)$ is bounded.

Of course, these assumptions were also made for the adaptive state feedback design. For the vehicle model, the stability of the polynomial $n(z)$ depends on the choice of fin location on the vehicle. It is seen that for small value of d_f the system is minimum phase. Here $n(z)$ is a stable

polynomial but the denominator polynomial $d(z)$ is unstable.

The relative degree of the system is one, therefore we choose a reference model of the form.

$$y_m(kT) = W_m(z)r(kT), \quad k = 0, 1, 2, \dots \quad (5.3)$$

where $r(kT)$ is a discrete-time command input and

$$W_m(z) = \frac{1}{z} \quad (5.4)$$

is the delay operator (i.e., $y_m[(k+1)T] = r[kT]$).

The objective is to design an adaptive control law for the tracking of reference trajectories. It is assumed that only the yaw angle is needed for feedback.

5.2 Control Law

First we consider the existence of the control law assuming that the system parameters are exactly known. Then this control law is modified for the case when the parameters are not known. The design of the control law follows the steps described in [30]. Consider a control law

$$u^*(kT) = \theta_1^{*T} \omega_1(kT) + \theta_{2a}^{*T} \omega_{2a}(kT) + \theta_{20}^* y(kT) + \theta_3^* r(kT) + \theta_4^* \quad (5.5)$$

where $\omega_1(kT) = a_\lambda(z)[u](t)$ and $\omega_{2a}(kT) = a_\lambda(z)[y](t)$ with $a_\lambda(z) = [z^{-n+1}, \dots, z^{-1}]^T$, $n = 3$ and $\theta_1^*, \theta_{2a}^* \in R^2$, and $\theta_3^*, \theta_4^*, \theta_{20}^* \in R$ are to be chosen properly. We note that unlike state feedback only y is used for feedback. In the control law (5.5) the gain vectors are such that the transfer function from r to y is equal to $W_m(z)$ and θ_4^* asymptotically cancels the contribution of the disturbance d_u in the output. The signals $w_1(kT)$ and $w_{2a}(kT)$ in (5.5) are obtained as the states of the two filters

$$w_1[(k+1)T] = \begin{bmatrix} 0 & 1 \\ 0 & 0 \end{bmatrix} w_1(kT) + \begin{bmatrix} 0 \\ 1 \end{bmatrix} u(kT) \\ \triangleq A_0 w_1(kT) + b_0 u(kT) \quad (5.6)$$

$$w_{2a}[(k+1)T] = A_0 w_{2a}(kT) + b_0 y(kT) \quad (5.7)$$

Then the closed loop system (5.1), using (5.6) and (5.7) is given by

$$\begin{aligned} \begin{bmatrix} x[(k+1)T] \\ w_1[(k+1)T] \\ w_{2a}[(k+1)T] \end{bmatrix} &= \begin{bmatrix} A_d + B_d \theta_{20}^* C & B_d \theta_1^{*T} & B_d \theta_{2a}^{*T} \\ b_0 \theta_{20}^* C & A_0 + b_0 \theta_1^{*T} & b_0 \theta_{2a}^{*T} \\ b_0 C & 0 & A_0 \end{bmatrix} \begin{bmatrix} x(kT) \\ w_1(kT) \\ w_{2a}(kT) \end{bmatrix} \\ &+ \begin{bmatrix} B_d \\ b_0 \\ 0 \end{bmatrix} \theta_3^* r(kT) + \begin{bmatrix} B_d \\ b_0 \\ 0 \end{bmatrix} \theta_4^* + \begin{bmatrix} d_u \\ 0 \\ 0 \end{bmatrix} \\ &\triangleq A_a X_c(kT) + B_a \theta_3^* r(kT) + B_a \theta_4^* + d_a \\ y(kT) &= [C \ 0 \ 0] X_c(kT) = C_a X_c(kT) \end{aligned} \quad (5.8)$$

where

$$X_c(kT) = [x^T(kT), w_1^T(kT), w_{2a}^T(kT)]^T \in R^7$$

Since the system (5.1) is controllable and observable, under assumption (A.1), there exists θ_1^* , θ_{2a}^* , θ_{20}^* and

$$\theta_3^* = (k_p)^{-1} \quad (5.9)$$

satisfying

$$\theta_1^{*T} a_\lambda(z) d(z) + [\theta_{2a}^{*T}, \theta_{20}^*] [a_\lambda^T(z), 1]^T k_p n(z) = d(z) - n(z)z \quad (5.10)$$

such that

$$C_a (zI - A_a)^{-1} B_a \theta_3^* = W_m(z) \quad (5.11)$$

and in the closed-loop system the output is given by

$$y(z) = C_a (zI - A_a)^{-1} B_a \theta_3^* r(z) + C_a (zI - A_a)^{-1} B_a \theta_4^* \left(\frac{z}{z-1} \right) +$$

$$\begin{aligned}
& C_a(zI - A_a)^{-1}d_a\left(\frac{z}{z-1}\right) \\
& \stackrel{\Delta}{=} W_m r(z) + \Delta(z)
\end{aligned} \tag{5.12}$$

where $\rho^* = k_p$ and

$$\Delta(z) = [C_a(zI - A_a)^{-1}B_a\theta_4^* + C_a(zI - A_a)^{-1}d_a]\left(\frac{z}{z-1}\right)$$

Since matrix A_a is Schur and d_a is a constant vector, $\Delta(kT)$ asymptotically tends to a constant value given by

$$\begin{aligned}
\Delta_\infty &= \lim_{k \rightarrow \infty} \Delta(kT) = \lim_{z \rightarrow 1} (z-1)\Delta(z) \\
&= C_a(-A_a)^{-1}[B_a\theta_4^* + d_a]
\end{aligned} \tag{5.13}$$

For canceling the effect of the disturbance vector d_a on the output, there exists θ_4^* in (5.12) such that $\Delta_\infty = 0$.

For the system with unknown parameters, the control law is chosen as

$$u(kT) = \theta_1^T(kT)\omega_1(kT) + \theta_2^T(kT)\omega_2(kT) + \theta_3^T(kT)r(kT) + \theta_4 \tag{5.14}$$

where $\omega_2(kT) = [w_{2a}^T, y]^T$, $\theta_1(kT) \in R^2$, $\theta_2(kT) = [\theta_{2a}^T \ \theta_{20}]^T \in R^3$, and $\theta_3(kT)$, $\theta_4(kT) \in R$ are time varying estimates of θ_i^* , $i = 1, \dots, 4$. Define

$$\begin{aligned}
\omega(kT) &= [\omega_1^T(kT), \omega_2^T(kT), y_m((k+1)T), 1]^T \\
\theta(kT) &= [\theta_1^T(kT), \theta_2^T(kT), \theta_3(kT), \theta_4]^T \\
e(kT) &= y(kT) - y_m(kT), \tilde{\theta}(kT) = \theta(kT) - \theta^*
\end{aligned} \tag{5.15}$$

Using the control (5.15), the closed-loop system takes the form

$$\begin{aligned}
X_a[(k+1)T] &= A_a X_c(kT) + B_a(\theta_3^* r(kT) + \theta_4^*) + d_a + B_a \tilde{\theta}^T(kT) \omega(kT) \\
y &= C_a X_a
\end{aligned} \tag{5.16}$$

and now the output is

$$y(kT) = W_m(z)r(kT) + \Delta(z) + \rho^*W_m(z)\tilde{\theta}^T(kT)w(kT) \quad (5.17)$$

Note that $\Delta(kT)$ is an exponentially decaying signal by the choice of θ_4^* . Therefore, ignoring the decaying signal in (5.17) yields

$$\begin{aligned} e(kT) &= \rho^*W_m(z)\tilde{\theta}^T(kT)w(kT) \\ &= -\rho^*(\theta^{*T}\omega((k-1)T) - \theta^T((k-1)T)w((k-1)T)) \end{aligned} \quad (5.18)$$

We are interested in deriving an adaptation law such that the tracking error asymptotically tends to zero. We define estimation error

$$\epsilon(kT) = e(kT) + \rho(kT)\xi(kT) \quad (5.19)$$

where $\rho(kT)$ is an estimate of $\rho^* = k_p$ and

$$\xi(kT) = \theta^T(kT)w((k-1)T) - \theta^T((k-1)T)w((k-1)T) \quad (5.20)$$

substituting (5.18) and (5.20) into (5.19), we obtain the error equation

$$\epsilon(kT) = \rho^*\tilde{\theta}^T(kT)w((k-1)T) + \tilde{\rho}(kT)\xi(kT) \quad (5.21)$$

where $\tilde{\rho}(kT) = \rho(kT) - \rho^*$. This error equation is linear in the parameter errors $\tilde{\theta}^T(kT)$ and $\tilde{\rho}(kT)$. This equation is important for the derivation of the adaptation law. Now following [30], the normalized gradient based control law is chosen as

$$\begin{aligned} \theta((k+1)T) &= \theta(kT) - \frac{\text{sign}(k_p)\Gamma w((k-1)T)\epsilon(kT)}{m^2(kT)} \\ \rho((k+1)T) &= \rho(kT) - \frac{\gamma\xi(kT)\epsilon(kT)}{m^2(kT)} \end{aligned} \quad (5.22)$$

where the symmetric positive definite adaptation gain matrix Γ satisfies $0 < \Gamma = \Gamma^T < \frac{2}{k_p^0}I_{7 \times 7}$, $0 < \gamma < 2$, and

$$m^2(kT) = 1 + w^T((k-1)T)w((k-1)T) + \xi^2(kT)$$

For the stability analysis one chooses the Lyapunov function

$$V(\tilde{\theta}, \tilde{\rho}) = |\rho^*| \tilde{\theta}^T(kT) \Gamma^{-1} \tilde{\theta}(kT) + \gamma^{-1} \tilde{\rho}^2(kT) \quad (5.23)$$

and following [30] shows that

$$V((k+1)T) - V(kT) \leq -\alpha_1 \frac{\epsilon^2(kT)}{m^2(kT)} \quad (5.24)$$

where $\alpha_1 > 0$. This implies that $\theta(kT), \rho(kT), \frac{\epsilon(kT)}{m(kT)} \in L^\infty$ (the set of bounded functions), and

$$\frac{\epsilon(kT)}{m(kT)}, (\theta((k+i_0)T) - \theta(kT)), (\rho((k+i_0)T) - \rho(kT)) \in L^2$$

(the set of square summable functions) for any integer $i_0 > 0$. Furthermore, one can show that $\epsilon(kT) \rightarrow 0$ and all the signals in the closed-loop system are bounded. This completes the derivation of the adaptive control law for the yaw plane maneuvering.

The Figure. 5.1 shows the complete closed-loop system with parameter adaptation law. It clarifies how the different modules of the control system for BAUV are connected. The command input signal is applied to the reference model. The digital controller provides the discrete bias angle control input according to (5.14). The control output from the controller being discrete is converted to analog before applying to the BAUV. Further the bias angle along with yaw angle and output error is used to tune the parameters of the controller using gradient algorithm (5.22). Thus the combined system works harmoniously to provide efficient control system for the BAUV.

5.3 Simulation Results For Yaw Plane Maneuvers

In this section, simulation results using the MATLAB/SIMULINK for yaw angle control are presented. Various time-varying reference trajectories are considered for tracking, and the performance of the adaptive controller in the presence of parameter uncertainties is examined. The parameters of the model are taken from [33]. The AUV is assumed to be moving with a constant forward velocity of 0.7 (m/sec). The vehicle parameters are $l = 1.391$ (m), mass=18.826

(kg), $I_z = 1.77$ (kgm²), $X_G = -0.012$, $Y_G = 0$. The hydrodynamic parameters for a forward velocity of 0.7 m/sec derived from [33] are $Y_{\dot{r}} = -0.3781$, $Y_{\dot{v}} = -5.6198$, $Y_r = 1.1694$, $Y_v = -12.0868$, $N_{\dot{r}} = -0.3781$, $N_{\dot{v}} = -0.8967$, $N_r = -1.0186$, and $N_v = -4.9587$. It is assumed that $d_f = 0.01$ (m) and the fin oscillation frequency is $f = 8$ Hz. The vectors f_a , f_b , m_a , and m_b are found to be [28]

$$f_a = (0, -40.0893, -43.6632, -0.3885, 0.6215, 6.2154, -10.17, -0.1554, 0.6992)$$

$$f_b = (68.9975, 0.4451, -16.4704, 64.1009, -19.5864, -0.8903, -2.2257, 2.2257, 4.8966)$$

$$m_a = (0.0054, 0.6037, 0.4895, 0, -0.0054, 0, -0.0925, 0, -0.0054)$$

$$m_b = (-0.5297, -0.3739, -0.0935, -0.2493, 0.1246, 0.0312, -0.0312, 0.0935, 0)$$

It is pointed out that these parameters are obtained using the Fourier decomposition of the fin force and moment, and are computed by multiplying the Fourier coefficients by $\frac{1}{2}\rho.W_a.U_\infty^2$ and $\frac{1}{2}\rho.W_a.chord.U_\infty^2$, respectively, where W_a is the surface area of the foil. For simulation, the initial conditions of the vehicle are assumed to be $x(0) = 0$.

The closed-loop system (2.10) and (5.14) with the update law (5.22) is simulated. The bias angle is changed to a new value every $T = T_o$ seconds, where $T_o = 1/f$ is the fundamental period of f_p and m_p . For the set point control, the terminal value of the yaw angle is taken as $\psi^* = 10$ deg.

Thus one desires to control the BAUV to a heading angle of 10 deg. For the update law, the adaptation gains are selected as $\Gamma = 0.0001(2/k_p^o)I_{7 \times 7}$ and $\gamma = 0.002$, where $k_p^o = 0.08 \geq |k_p|$. Using the values of AUV model, it is found that the actual feedback gains are $\theta_1^* = (0.4195 \quad -0.4323)^T$, $\theta_2^* = (99.0671 \quad -303.9286 \quad 309.4949)^T$, $\theta_3^* = -104.6334$ and $\theta_4^* = 0.0001$ and $\rho^* = k_p = -0.0096$. The open-loop zeros and poles of the discretized system are $(-0.8990, 0.4667)$ and $(1.0000, 1.0864, 0.8715)$, respectively. Therefore, the transfer function is minimum phase. Simulation results are

presented for the parameter uncertainty of 50 % and 25%.

Case A1: Adaptive set point control: Parameter uncertainty 25% off-nominal for yaw angle 10 (deg).

For smooth control, the reference input $r(kT)$ (in rad) is selected as

$$r(kT) = [1 - \exp(-0.1(k)T)]10\pi/180$$

where the sampling time is $T = 0.125$ (sec). Thus the control law is updated at the completion of each cycle of oscillation. Assuming 25 % uncertainty, the initial estimates $\theta(0)$ and $\rho(0)$ are set to $0.75\theta^*$ and $0.75\rho^*$. This way the control law gains are 25 % lower than the exact θ^* . Figure. 5.2 shows the simulated results. It can be seen that the adaptive controller achieves accurate heading angle control to the target set point in about 45 sec. The control input (bias angle) magnitude required is around 40 deg, which can be provided by the pectoral fins. The plots of the lateral force and moment produced by the fins are also provided in the figure. In the steady-state, the lateral fin force and moment exhibit bounded periodic oscillations.

Case A2: Adaptive set point control: Parameter uncertainty 50% off-nominal for yaw angle 10 (deg).

Simulation result is also provided for parameter uncertainty as high as 50 %. Figure. 5.3 shows the simulated results for

$$r(kT) = [1 - \exp(-0.2(k)T)]10\pi/180$$

which is little bit faster than the previous command. It can be seen that the controller achieves accurate heading angle control to the target set point in about 25 sec. But as one can expect, that the bias angle required would be high, surprisingly the control input (bias angle) required is around 20 deg. Thus due to the nonlinear nature of adaptive time varying system, the control required for 50 % parameter uncertainty is less than that required for 25% parameter uncertainty even though a faster reference input is applied to the system with 50% parameter uncertainty

than that applied to the system with 25% parameter uncertainty. It is found that the control magnitude can be reduced by using slower command $r(kT)$ if desired.

Case A3: Adaptive set point control: Parameter uncertainty 50% off-nominal for Yaw angle 10 (deg) but for a faster command.

For this case the reference input $r(kT)$ (in rad) is selected as

$$r(kT) = [1 - \exp(-0.3(k)T)]10\pi/180$$

which is little bit faster than the previous command. The simulation are shown in Figure. 5.4. It shows that the control input required to track a faster command is much more. And due to the fin constraints it is better to provide slower command input.

Case A4: Adaptive sinusoidal trajectory control: Parameter uncertainty 25 % off-nominal

In order to examine, time-varying tracking ability of the controller, a sinusoidal reference trajectory is generated using the command input $r(kT) = 10 \times (\pi/180) [1 - \exp(-0.2(k)T)] \sin(kT)$ (rad). It is assumed that $\theta(0) = 0.75\theta^*$ and $\rho(0) = 0.75\rho^*$ giving 25% uncertainty. The responses are shown in Figure. 5.5. It is seen that, after the initial transients, the heading angle smoothly tracks the sinusoidal command trajectory. The control input (bias angle) magnitude required is about 33 deg.

Case A5: Adaptive sinusoidal trajectory control: Parameter uncertainty 50 % off-nominal

Tracking ability of the controller is also examined for 50% parameter uncertainty. The results are shown in Figure. 5.6. It is seen that, after the initial transients, the heading angle smoothly tracks the sinusoidal command trajectory. It is observed that the control input (bias angle) magnitude required is less than 20 deg, which is far less than that required for lower uncertainty.

Case A6: Adaptive sinusoidal trajectory control: Parameter uncertainty 50 % off-

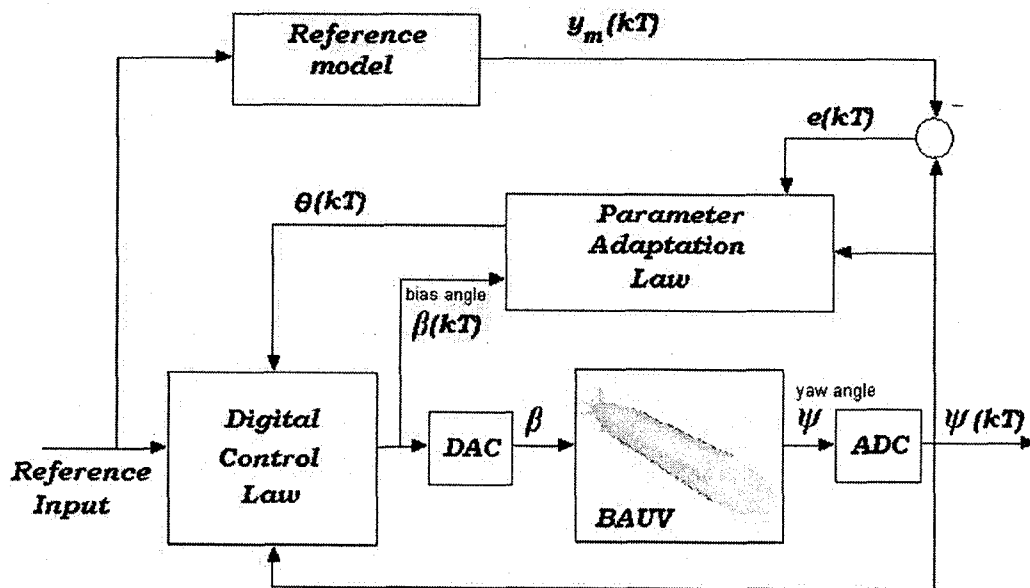
nominal with a faster command input

The controller is also simulated for a faster sinusoidal command input $r(kT) = 10 \times (\pi/180) [1 - \exp(-0.4(k)T)] \sin(kT)$ (*rad*). The simulations are presented in Figure. 5.7. Similar to step input simulations it shows that the control input required for a faster command is little more than the slower one. Thus it is better to use slower commands as the pectoral fins can provide the required bias angle.

Case A7: Adaptive turning maneuver

For constant turning rate, a smooth trajectory is generated using the command input $r(kT) = 2kT (\pi/180)$ (*rad*). As seen in Figure. 5.8. the trajectory tracked by the system is almost a circle, which requires a control input magnitude of 20 deg and less than 200 sec. It is possible to have a faster turning rate, however, that requires larger control forces.

Simulations for other off-nominal choices of $(\theta(0), \rho(0))$ have been performed. It is found that the control system performs relatively well for the choice of under-estimated initial values of the control gains $(\theta(0), \rho(0))$. Of course, the responses also depend on the choice of the command generator and the adaptation gain matrix Γ and γ of the update law.



* **DAC** - Digital to Analog Converter
ADC - Analog to Digital Converter

Figure 5.1: The Complete Closed-loop system with Output feedback and Parameter Adaptation

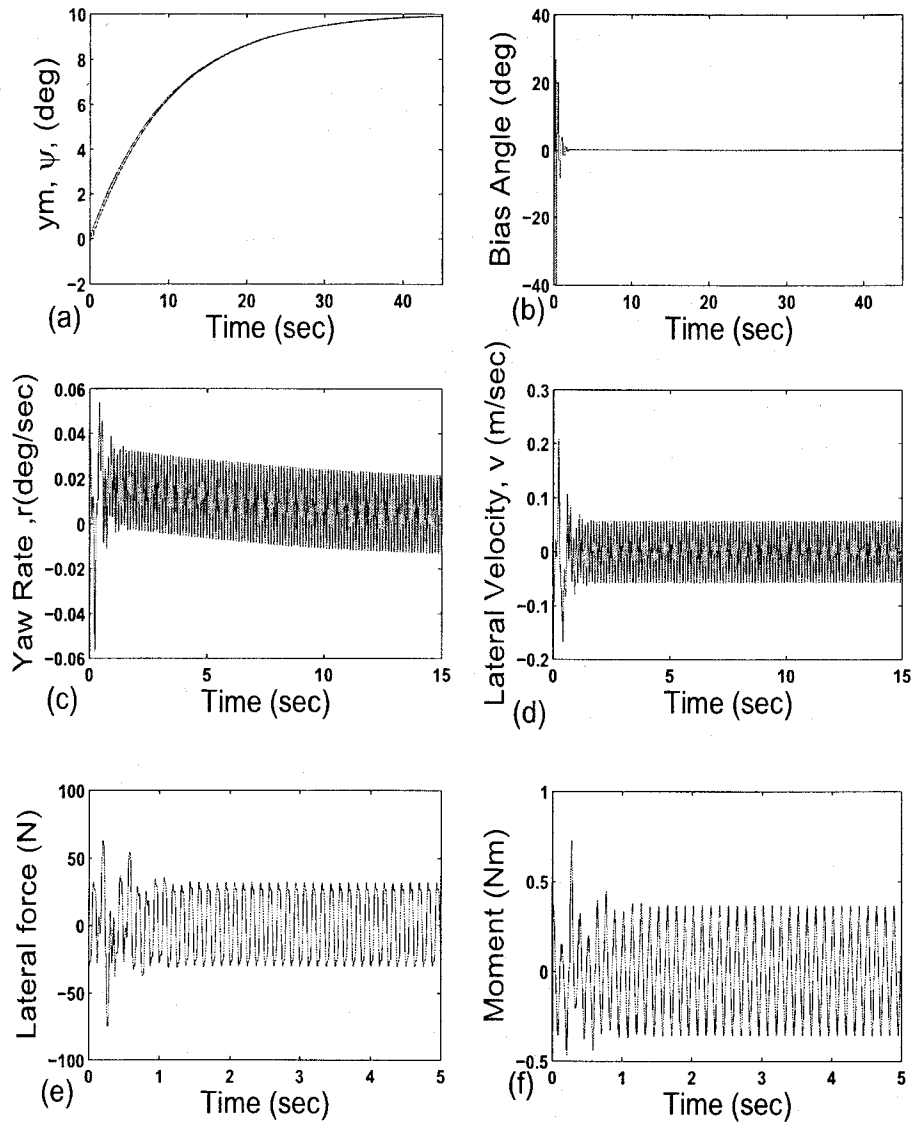


Figure 5.2: Adaptive set point control: Frequency of flapping 8Hz for $\psi^* = 10$ (deg) and parameter uncertainty 25%
 (a) Yaw angle, ψ (solid) and reference yaw angle (staircase)(deg) (b) Bias angle (deg) (c) Yaw rate (deg/sec) (d) Lateral velocity (m/sec) (e) Lateral force(N) (f) Moment(Nm)

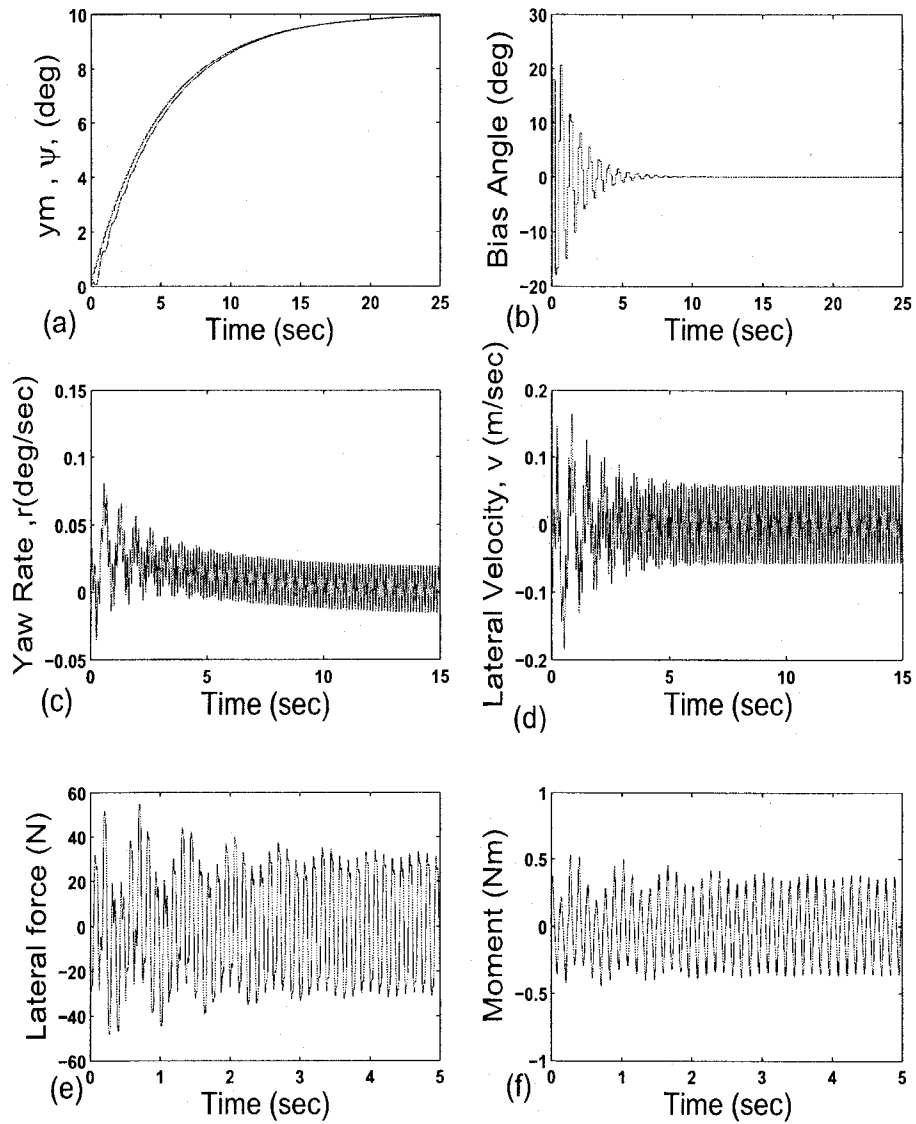


Figure 5.3: Adaptive set point control: Frequency of flapping 8Hz for $\psi^* = 10$ (deg) and parameter uncertainty 50%
 (a) Yaw angle, ψ (solid) and reference yaw angle (staircase)(deg) (b) Bias angle (deg) (c) Yaw rate (deg/sec) (d) Lateral velocity (m/sec) (e) Lateral force(N) (f) Moment(Nm)

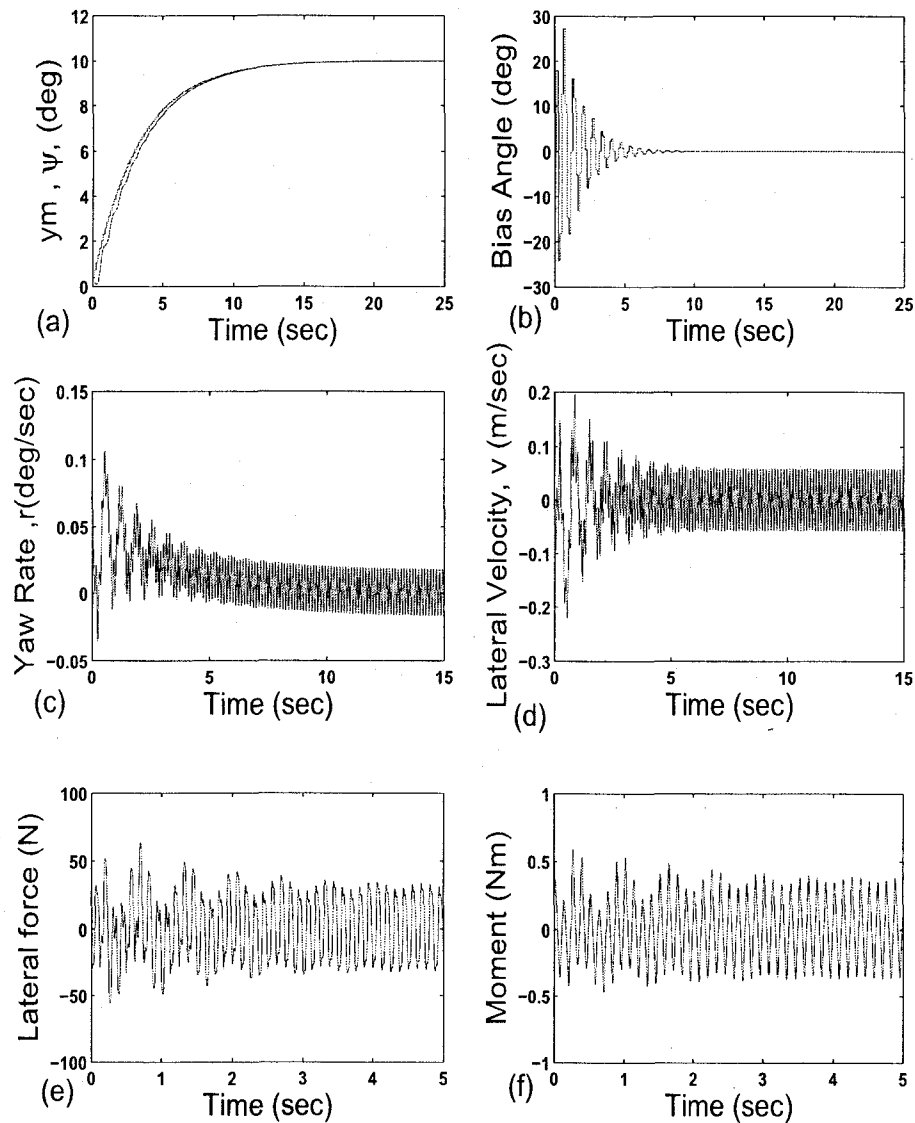


Figure 5.4: Adaptive set point control: Frequency of flapping 8Hz for $\psi^* = 10$ (deg) and parameter uncertainty 50% but the command is faster
 (a) Yaw angle, ψ (solid) and reference yaw angle (staircase)(deg) (b) Bias angle (deg) (c) Yaw rate (deg/sec) (d) Lateral velocity (m/sec) (e) Lateral force(N) (f) Moment(Nm)

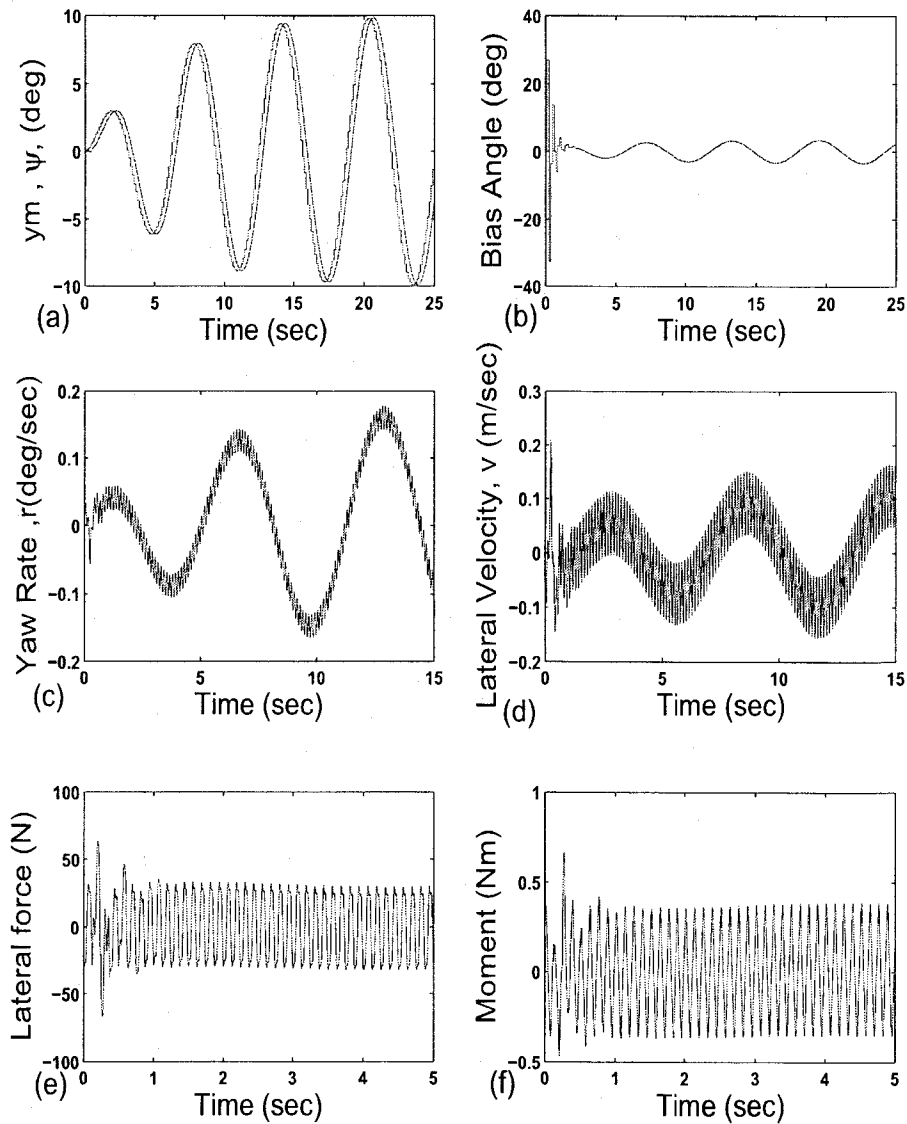


Figure 5.5: Adaptive sinusoidal trajectory control: Frequency of flapping 8Hz for $y_m = 10 \sin 2\pi f k T$ (deg) and parameter uncertainty 25%
 (a) Yaw angle, ψ (solid) and reference yaw angle (staircase)(deg) (b) Bias angle (deg) (c) Yaw rate (deg/sec) (d) Lateral velocity (m/sec) (e) Lateral force(N) (f) Moment(Nm)

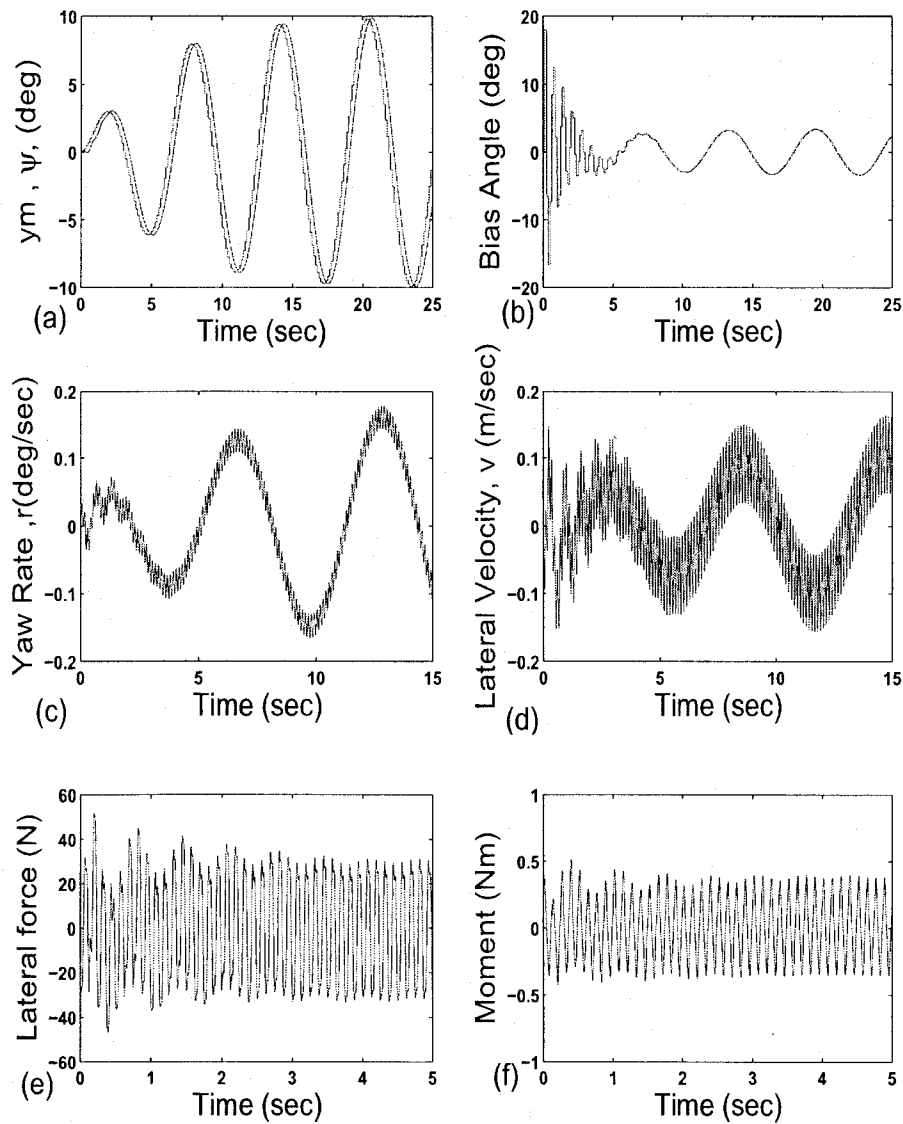


Figure 5.6: Adaptive sinusoidal trajectory control: Frequency of flapping 8Hz for $y_m = 10 \sin 2\pi f k T$ (deg) and parameter uncertainty 50%
 (a) Yaw angle, ψ (solid) and reference yaw angle (staircase)(deg) (b) Bias angle (deg) (c) Yaw rate (deg/sec) (d) Lateral velocity (m/sec) (e) Lateral force(N) (f) Moment(Nm)

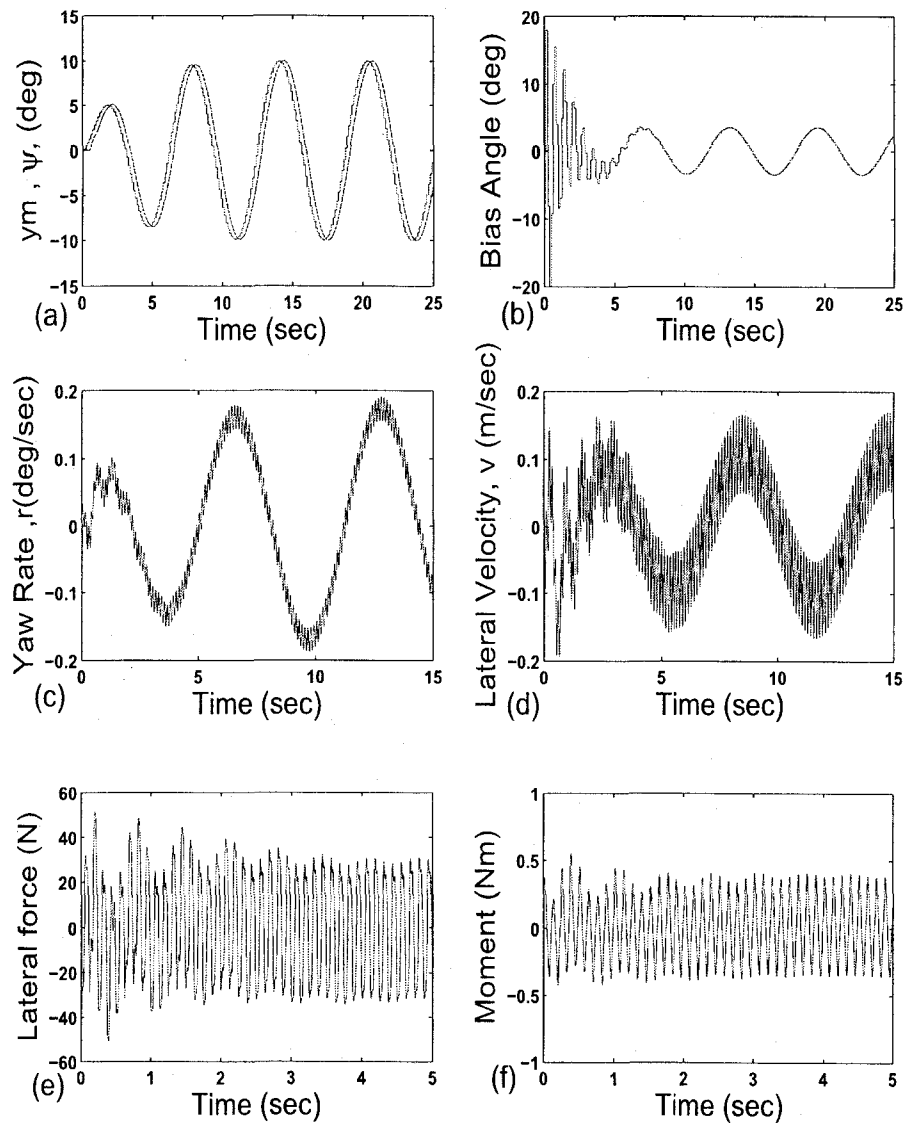


Figure 5.7: Adaptive sinusoidal trajectory control: Frequency of flapping 8Hz for $y_m = 10 \sin 2\pi f k T$ (deg) and parameter uncertainty 50% but for faster command
 (a) Yaw angle, ψ (solid) and reference yaw angle (staircase)(deg) (b) Bias angle (deg) (c) Yaw rate (deg/sec) (d) Lateral velocity (m/sec) (e) Lateral force(N) (f) Moment(Nm)

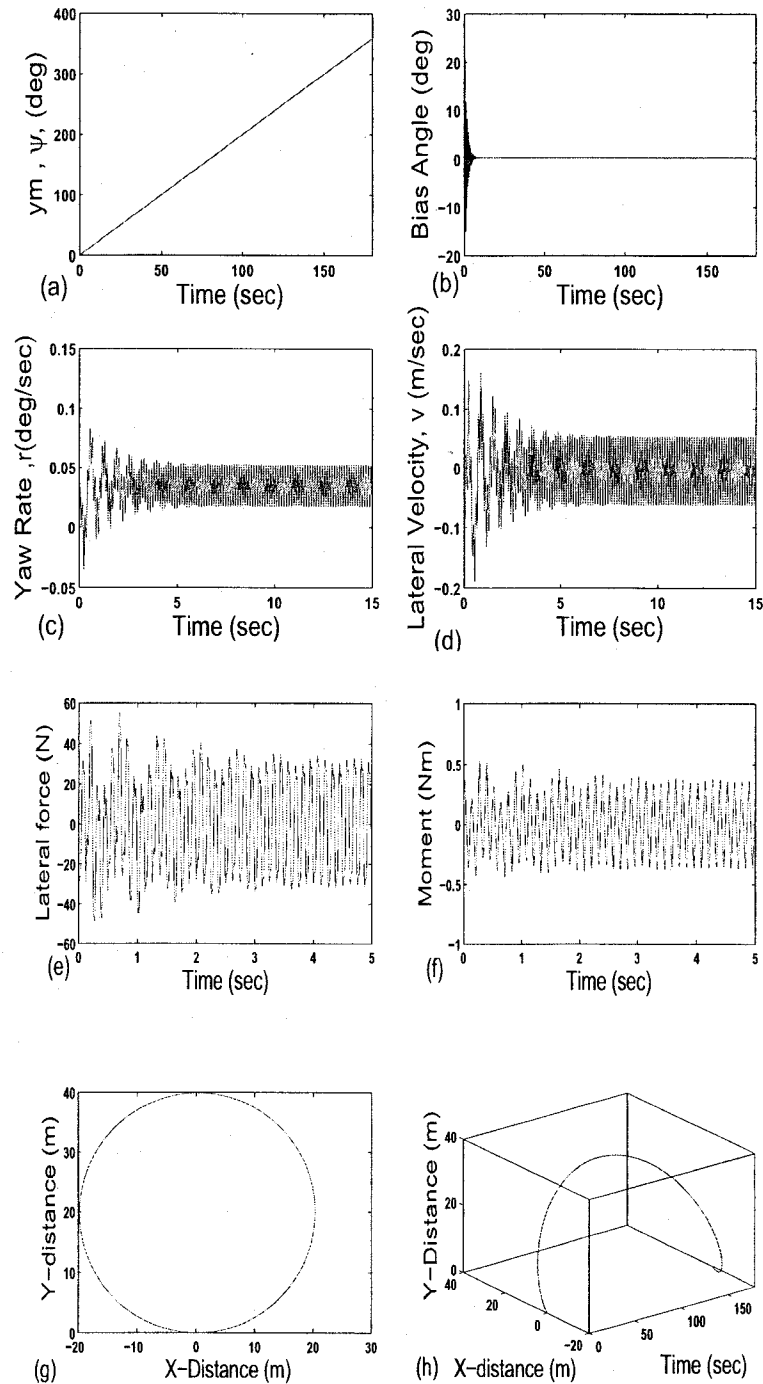


Figure 5.8: Adaptive turning maneuver: Turn rate of 2 deg/sec and parameter uncertainty 50% (a) Yaw angle, ψ (solid) and reference yaw angle (staircase)(deg) (b) Bias angle (deg) (c) Yaw rate (deg/sec) (d) Lateral velocity (m/sec) (e) Lateral force(N) (f) Moment(Nm) (g) Global position of the BAUV (X and Y co-ordinates) (h) Three-dimensional plot of X and Y distances with time

CHAPTER 6

INDIRECT ADAPTIVE OUTPUT FEEDBACK SERVOREGULATION

In chapter 4 and 5, adaptive control systems have been designed for the control of BAUVs. For designing these control laws, the vehicle is required to be minimum phase. Apparently it is an interesting problem to develop a control law, which can be used for minimum and nonminimum phase vehicles. This chapter treats the question of servoregulation of autonomous underwater vehicles (AUVs) in the yaw plane using pectoral-like fins where the system is not necessarily minimum phase.

For the trajectory control of the yaw angle, a sampled-data indirect adaptive control system using output (yaw angle) feedback is derived. The control system has a modular structure, which includes a parameter identifier and a stabilizer. For the control law derivation, an internal model of the exosignals (reference signal (constant or ramp) and constant disturbance) is included. Unlike the direct adaptive control scheme derived in the previous two chapters, the control law derived here is applicable to minimum as well as nonminimum phase biorobotic AUVs (BAUVs). This is important, because for most of the fin locations on the vehicle, the model is nonminimum phase. In the closed-loop system, the yaw angle trajectory tracking error converges to zero and the remaining state variables remain bounded. Simulation results are presented for set point yaw angle control and turning maneuvers in presence of the uncertainties in the system parameters.

The organization of this chapter is as follows. The problem statement is specified in section 6.1. An identifier is designed in Section 6.2. This is followed by the derivation of a stabilizer in

Section 6.3, and finally, Section 6.4 presents numerical results.

6.1 Problem Statement

The BAUV model is

$$\begin{aligned} x[(k+1)T] &= A_d x(kT) + B_d \beta_k + d_u \\ y(kT) &= Cx(kT) \end{aligned} \quad (6.1)$$

where A_d and B_d are constant matrices and d_u is a constant disturbance input vector. It is assumed that the matrices A_d , B_d and the vector d_u are not known.

It will be convenient to obtain a realization of the system (6.1) in the observable canonical form. Since the system (6.1) is observable, one can find a state transformation $q = Mx$ such that the new representation of the system takes the form [32]

$$\begin{aligned} q[(k+1)T] &= \begin{bmatrix} -a_2 & 1 & 0 \\ -a_1 & 0 & 1 \\ -a_0 & 0 & 0 \end{bmatrix} q(kT) + \begin{bmatrix} b_2 \\ b_1 \\ b_0 \end{bmatrix} \beta_k + \begin{bmatrix} d_{u2} \\ d_{u1} \\ d_{u0} \end{bmatrix} \\ &\triangleq A_0 q(kT) + B_0 \beta_k + D_0 \\ y(kT) &= \begin{bmatrix} 1 & 0 & 0 \end{bmatrix} x(kT) = Cq(kT) \end{aligned} \quad (6.2)$$

where M is a nonsingular matrix, $A_0 = MA_d M^{-1}$, $B_0 = MB_d$, $C = C_p M^{-1}$, and $D_0 = Md_u$.

We are interested in the design of an indirect control system for the tracking of yaw angle. The indirect adaptive control system has modular structure which includes an identifier and stabilizer.

6.2 Parameter Identifier

First we consider the design of identifier. From (6.2), it easily follows that the transfer function of the BAUV, when $D_0 = 0$, is given by

$$\frac{y(z)}{\beta(z)} = g(z) = \frac{b_2 z^2 + b_1 z + b_0}{z^3 + a_2 z^2 + a_1 z + a_0} = \frac{Z(n_z)}{P(n_p)} \quad (6.3)$$

where z is the z-transform variable, $n_z = (b_0, b_1, b_2)^T \in R^3$, and $n_p = (a_0, a_1, a_2)^T \in R^3$ are formed by the coefficients of the numerator and denominator polynomials of the transfer function $g(z)$. (Note that symbols (y, β) have been used for denoting $(y(kT), \beta(kT))$ as well as their z-transforms for simplicity in notation.) The system has two zeros and three poles, and its relative degree is one. The poles and zeros of the transfer function as well as the vector D_0 are assumed to be unknown. Of course, these depend on the parameters of the BAUV model.

For the purpose of parameter identification, first a linearly parameterized output equation is derived. Using (6.2), one has

$$\begin{aligned} y[(k+1)T] &= -a_2 y(kT) + q_2(kT) + b_2 \beta_k + d_{u2} \\ y[(k+2)T] &= -a_2 y[(k+1)T] - a_1 y(kT) + q_3(kT) + b_2 \beta_{k+1} + b_1 \beta_k + d_{u2} + d_{u1} \\ y[(k+3)T] &= -a_2 y[(k+2)T] - a_1 y[(k+1)T] - a_0 y(kT) \\ &\quad + b_2 \beta_{k+2} + b_1 \beta_{k+1} + b_0 \beta_k + d_{u2} + d_{u1} + d_{u0} \end{aligned} \quad (6.4)$$

Treating z as the advance operator (i.e. for any signal $l(kT)$, $zl(kT) = l[(k+1)T]$), one can write the last equation of (6.4) in the form

$$z^3 y(kT) = (b_2 z^2 + b_1 z + b_0) \beta(kT) - (a_2 z^2 + a_1 z + a_0) y(kT) + d^* \quad (6.5)$$

where $d^* = d_{u1} + d_{u2} + d_{u0}$, is a constant. The parameters b_i , a_i and d^* are unknown.

Let

$$\Lambda(z) = z^3 + \lambda_2 z^2 + \lambda_1 z + \lambda_0 \quad (6.6)$$

be a stable polynomial such that its zeros are in $|z| < 1$ (strictly within the unit disk in the complex plane). Then operating (6.5) by $\Lambda^{-1}(z)$ gives

$$\frac{z^3}{\Lambda(z)}y(kT) = \frac{b_2z^2 + b_1z + b_0}{\Lambda(z)}\beta(kT) - \frac{a_2z^2 + a_1z + a_0}{\Lambda(z)}y(kT) + \frac{d^*}{\Lambda(z)} \quad (6.7)$$

Noting that

$$z^3\Lambda^{-1}(z) = 1 - (\lambda_2z^2 + \lambda_1z + \lambda_0)\Lambda^{-1}(z)$$

(16) gives

$$y(kT) = \frac{b_2z^2 + b_1z + b_0}{\Lambda(z)}\beta(kT) + \frac{[(\lambda_2 - a_2)z^2 + (\lambda_1 - a_1)z + (\lambda_0 - a_0)]}{\Lambda(z)}y(kT) + \frac{d^*}{\Lambda(z)} \quad (6.8)$$

Defining the parameter vector

$$\theta^* = [b_0, b_1, b_2, (\lambda_0 - a_0), (\lambda_1 - a_1), (\lambda_2 - a_2), d^*]^T \in R^7$$

and the regressor vector

$$\phi_p(kT) = \left[\frac{1}{\Lambda(z)}\beta(kT), \frac{z}{\Lambda(z)}\beta(kT), \frac{z^2}{\Lambda(z)}\beta(kT), \frac{1}{\Lambda(z)}y(kT), \frac{z}{\Lambda(z)}y(kT), \frac{z^2}{\Lambda(z)}y(kT), \Lambda^{-1}(z)1 \right]^T \in R^7 \quad (6.9)$$

(6.8) can be written as

$$y(kT) = \theta^{*T} \phi_p(kT) \quad (6.10)$$

The regressor vector $\phi_p(kT)$ is obtained by filtering the input $\beta(kT)$, output $y(kT)$ and the unit step sequence. There exist many parameter identification schemes to obtain an estimate of the parameter vector θ^* . For simplicity, here a normalized gradient algorithm is considered for the identification of these parameters.

Let the $\theta(kT)$ be an estimate of θ^* . Define the estimation error

$$\epsilon(kT) = \theta^T(kT)\phi_p(kT) - y(kT), \quad k \in 0, 1, 2, \dots \quad (6.11)$$

Using (6.10) in (6.11) gives

$$\epsilon(kT) = \tilde{\theta}^T(kT)\phi_p(kT)$$

where

$$\tilde{\theta}(kT) = \theta(kT) - \theta^* \quad (6.12)$$

is the parameter error vector. For the derivation of the identifier [30, 31], a normalized quadratic cost function

$$J(\theta) = \frac{\epsilon^2}{2m^2} = \frac{\tilde{\theta}^T(kT)\phi_p(kT)\phi_p^T(kT)\tilde{\theta}(kT)}{m^2} \quad (6.13)$$

is minimized, where m is the normalizing signal. The steepest descent direction of $J(\theta)$ is $-(\frac{\partial J}{\partial \theta}) = -(\frac{\epsilon}{m^2}\phi_p(kT))$, which suggests the adaptive update law for $\theta(kT)$ given by

$$\begin{aligned} \theta[(k+1)T] &= \theta(kT) - \frac{\Gamma\phi_p(kT)\epsilon(kT)}{k_0 + \phi_p^T(kT)\phi_p(kT)} \\ \theta(0) &= \theta_0, k \in 0, 1, 2, \dots \end{aligned} \quad (6.14)$$

where Γ is a positive definite symmetric matrix (denoted as $\Gamma > 0$) satisfying $0 < \Gamma < 2I$ (I denotes an identity matrix), the normalizing signal $m = [k_0 + \phi_p^T(kT)\phi_p(kT)]^{\frac{1}{2}}$, and $k_0 > 0$ being a design parameter.

The stability analysis of this identifier can be done using a Lyapunov function

$$V(\tilde{\theta}) = \tilde{\theta}^T\Gamma^{-1}\tilde{\theta} \quad (6.15)$$

and then showing that

$$V(\tilde{\theta}(k+1)T) - V(\tilde{\theta}(kT)) \leq -\alpha_1 \frac{\epsilon^2(kT)}{m^2(kT)} \quad (6.16)$$

for $\alpha_1 = (2 - \lambda_{\max}(\Gamma)) > 0$ where $\lambda_{\max}(\cdot)$ denotes the maximum eigenvalue of Γ . Using (6.16), one can show that the algorithm (6.13) guarantees that $\theta(kT), \frac{\epsilon(kT)}{m(kT)} \in L^\infty$ (the set of bounded sequences) and $\frac{\epsilon(kT)}{m(kT)}, (\theta[(k+1)T] - \theta(kT)) \in L^2$ (the set of square summable sequences). (See [30, 31] for the details.)

The elements of the regressor vector $\phi_p(kT)$ can be obtained using two filters having state variable forms given by

$$\begin{aligned} w_1[(k+1)T] &= A_\lambda w_1(kT) + b_\lambda u(kT), \\ w_2[(k+1)T] &= A_\lambda w_2(kT) + b_\lambda y(kT) \end{aligned} \quad (6.17)$$

where $w_i \in R^3$,

$$A_\lambda = \begin{bmatrix} 0 & 1 & 0 \\ 0 & 0 & 1 \\ -\lambda_0 & -\lambda_1 & -\lambda_2 \end{bmatrix}, \quad b_\lambda = \begin{bmatrix} 0 \\ 0 \\ 1 \end{bmatrix}$$

Then it easily follows that $\phi_p(kT) = [w_1^T(kT), w_2^T(kT), \Lambda^{-1}(z)1]^T$. A simplification in the regressor is possible if one ignores the exponentially decaying signal of $\Lambda^{-1}(z)1$. Since $\Lambda^{-1}(z)1$ tends to the constant sequence $\lambda_f = (1 + \lambda_0 + \lambda_1 + \lambda_2)^{-1}$, one can replace $\phi_{p\tau}$ by λ_f^{-1} , where ϕ_{pi} denotes the i th elements of ϕ_p .

6.3 Adaptive Control Law

In the previous section, an adaptation law for the estimation of the parameters a_i , b_i and d^* has been developed. In this section, the indirect adaptive control approach described in [30] is taken for the design of a servoregulator for the output regulation of the BAUV to follow step and ramp yaw angle reference trajectories, despite the presence of the constant disturbance input D_0 . Apparently, this is a problem of command tracking and disturbance rejection.

For the purpose of design, first it is essential to obtain an internal model of the exosignals (the disturbance and the reference signals). Note that the z-transforms of constant and ramp signals are $y_{ms}(z) = l_1 \frac{z}{z-1}$ and $y_{mr}(z) = l_2 \frac{Tz}{(z-1)^2}$ ($l_i \in R$), respectively; and the least common denominator of y_{ms} and y_{mr} is $Q_m(z) = (z-1)^2$. As such the reference and disturbance inputs

satisfy

$$\begin{aligned}(z-1)^2 y_m(kT) &= 0 \\ (z-1)^2 D_0 &= 0\end{aligned}\tag{6.18}$$

and according to the internal model principle, the transfer function $Q_m^{-1}(z)$ must be inserted in tandem with the transfer function $(g(z))$ of the BAUV for solving the output regulation problem [32].

We first consider the design when the parameters of the BAUV (6.2) are known, but the disturbance signal D_0 is not known. Then this control law is modified to obtain the adaptive law using the estimates of the parameters of the model (6.2). Figure. 6.1 shows the unity feedback closed-loop system including the controller. In the forward path, the controller includes the internal model $Q_m^{-1}(z)$ of the exosignals. For the solution of the output regulation problem, one finds appropriate polynomials C and D such that the closed-loop system is asymptotically stable [32]. Thus the output regulation problem essentially reduces to a stabilization problem. The control law is given by

$$\beta(kT) = \left[\frac{D(z, n_d)}{C(z, n_c) Q_m(z)} \right] (y_m(kT) - y(kT))\tag{6.19}$$

where the polynomials D and C are chosen as

$$\begin{aligned}C(z, n_c) &= z^2 + c_1 z + c_0 \\ D(z, n_d) &= d_4 z^4 + d_3 z^3 + d_2 z^2 + d_1 z + d_0\end{aligned}\tag{6.20}$$

and controller parameter vectors n_c and n_d are

$$\begin{aligned}n_c &= (c_0, c_1)^T \in R^{n-1} = R^2 \\ n_d &= (d_0, d_1, \dots, d_4) \in R^{n+n_q} = R^5\end{aligned}\tag{6.21}$$

Note that the degree of the monic polynomial C is

$$\delta(C) = (n - 1)$$

where $n = 3$ is the dimension of the state vector x (δ denotes the degree of a polynomial); and $\delta(D) = n + n_q - 1 = 4$, where $n_q = \delta(Q_m)$.

Suppose that a stable monic polynomial $F^*(z)$ with $\delta(F^*) = 2n + n_q - 1 = 7$ of the form

$$F^*(z) = z^7 + f_6z^6 + \dots + f_1z + f_0 \quad (6.22)$$

is given; that is, all its zeros are in $|z| < 1$. The characteristic polynomial of the closed-loop system shown in Figure. 6.1 is

$$\Pi(z) = C(z, n_c)Q_m(z)P(z, n_p) + D(z, n_d)Z(z, n_z) \quad (6.23)$$

The stabilization of the closed-loop system (6.2) (with $D_0 = 0$) and the control law (6.19) is accomplished if for some choice of C and D , one has $\Pi(z) = F^*(z)$, that is

$$C(z, n_c)Q_m(z)P(z, n_p) + D(z, n_d)Z(z, n_z) = F^*(z) \quad (6.24)$$

For the given polynomials $Q_m(z)$, $P(z, n_p)$ and $Z(z, n_z)$, there exist polynomials $C(z, n_c)$ and $D(z, n_d)$ for any $F^*(z)$ if and only if $Z(z, n_z)$ and $(Q_m(z)P(z, n_p))$ are coprime. For the BAUV model, this condition is satisfied, because the polynomials $Z(z, n_z)$ and $P(z, n_p)$ are coprime, and the zeros of $g(z)$ do not coincide with the zeros of $Q_m(z)$. (An explicit solution for the stabilizer parameters (c_i, d_i) of C and D are given in the appendix.)

It is easily seen that the transfer function relating the tracking error $(y_m(z) - y(z))$ and the input $y_m(z)$ has the polynomial $Q_m(z)$ as a factor in its numerator, which cancels the unstable poles of $y_m(z)$. This is also true for the transfer function relating the output $y(z)$ and disturbance input d^* in (6.4). This has been possible due to the inclusion of the internal model of

the exosignals in the forward path, and the stability of the closed-loop system guarantees the convergence of the tracking error to zero, despite the presence of the disturbance signal D_0 .

Now a linearly parameterized form of the control law (6.19) for synthesis is obtained [28]. Let $\Pi_\mu(z)$ ($\delta(\Pi_\mu(z)) = n + n_q - 1 = 4$) be a monic stable polynomial of the form

$$\Pi_\mu(z) = z^4 + \mu_3 z^3 + \mu_2 z^2 + \mu_1 z + \mu_0 \quad (6.25)$$

Manipulating the control law (6.19) and operating by $\Pi_\mu^{-1}(z)$ gives

$$\beta(kT) = (\Pi_\mu(z) - C(z, n_c)Q_m(z)) \frac{1}{\Pi_\mu(z)} \beta(kT) + D(z, n_d) \frac{1}{\Pi_\mu(z)} [y_m(kT) - y(kT)] \quad (6.26)$$

Since Π_μ and CQ_m are monic polynomials $\delta(\Pi_\mu - CQ_m) < \delta(\Pi_\mu)$. Define

$$\Pi_\mu(z) - C(z, n_c)Q_m(z) = [l_0, l_1, l_2, l_3] \nu(z) \triangleq l^T \nu(z)$$

$$D(z, n_d) \Pi_\mu^{-1}(z) = d_4 + [d_{a0}, d_{a1}, d_{a2}, d_{a3}] \nu(z) \triangleq d_4 + d_a^T \nu(z) \quad (6.27)$$

where $\nu(z) = [1, z, z^2, z^3]^T \in R^4$. (The vectors l and d_a are given in the appendix II.) Then control law (6.26) takes the form

$$\beta(kT) = l^T w_\beta(kT) + d_a^T w_e(kT) + d_4 [y_m(kT) - y(kT)] \quad (6.28)$$

where $w_\beta(kT)$ and $w_e(kT)$ satisfy the state equations

$$w_\beta[(k+1)T] = A_\mu w_\beta(kT) + B_\mu \beta(kT)$$

$$w_e[(k+1)T] = A_\mu w_e(kT) + B_\mu (y_m(kT) - y(kT)) \quad (6.29)$$

where

$$A_\mu = \begin{bmatrix} 0 & 1 & 0 & 0 \\ 0 & 0 & 1 & 0 \\ 0 & 0 & 0 & 1 \\ -\mu_0 & -\mu_1 & -\mu_2 & -\mu_3 \end{bmatrix} \quad B_\mu = \begin{bmatrix} 0 \\ 0 \\ 0 \\ 1 \end{bmatrix} \quad (6.30)$$

The control law is linearly dependent on the parameter vectors l , d_a and d_4 which are functions of the compensator parameters. Of course, the compensator parameters c_i , d_i are functions of the BAUV model parameters.

Now a modification of the control law is considered, when the parameters of the model are unknown. The compensator design is performed, assuming that the parameter estimate θ of θ^* is the true parameter vector of the BAUV (certainty equivalence principle). It is assumed that there exists a unique solution of the compensator equation for every value of the parameter estimate. Thus the compensator equation

$$C(z, n_c)Q_m(z)P(z, \hat{n}_p) + D(z, n_d)Z(z, \hat{n}_z) = \Pi(z) \quad (6.31)$$

using the estimated coefficients of the numerator and denominator polynomials of $g(z)$ is solved to obtain the controller gains n_c and n_d , where $\hat{n}_z = (\hat{b}_0, \hat{b}_1, \hat{b}_2)^T$, $\hat{n}_p = (\hat{a}_0, \hat{a}_1, \hat{a}_2) \in R^3$ are formed by the estimates of the parameters a_i and b_i . Using these values of n_c and n_d , the vectors l , d_a and d_4 are computed to obtain the control law (6.28) at each sampling instant. It can be shown according to [30] that in the closed-loop system, the tracking error $y(kT) - y_m(kT)$ converges to zero and all the signals are bounded. This completes the servoregulator design. The complete closed-loop system including the identifier and the stabilizer is shown in Figure. 6.2.

For the solvability of the compensator equation (6.31), it is essential that the polynomials $Z(z, \hat{n}_z)$ and $Q_m(z)P(z, \hat{n}_p)$ remain coprime as the parameter adaptation continues. Of course, one can use parameter projection to keep the estimated parameters \hat{n}_z and \hat{n}_p within a suitable set in which the coprimeness condition holds.

Remark 1: For simplicity, the polynomials $\Lambda(z)$, $F^*(z)$ and $\Pi_\mu(z)$ can be taken as $\Lambda(z) = z^3$, $F^*(z) = z^7$ and $\Pi_\mu(z) = z^4$. For these choices of polynomials, only delayed values of $y(kT)$, $y_m(kT)$ and $\beta(kT)$ are used for the estimator and the stabilizer.

Remark 2: The derived servoregulator rejects any constant disturbance input D_0 . It is inter-

esting to note that in the closed-loop system, the adaptive law can accomplish output regulation despite the action of arbitrary periodic wave forces on the BAUV, if its period coincides with the period of the oscillation of the fins. This is due to the fact that in the discretized model of the BAUV, including the wave forces, a constant disturbance vector appears in (6.1). In other words, it is possible to cancel the effect of any periodic wave forces at the sampling instants by the selection of oscillation frequency of the fins. Of course, for this it is necessary to know the frequency of the wave forces.

6.4 Simulation Results For Yaw Plane Maneuvers

In this section, simulation results using the MATLAB/SIMULINK for yaw angle control are presented. Various time-varying reference trajectories are considered for tracking, and the performance of the adaptive controller in the presence of parameter uncertainties is examined. The parameters of the model are taken from [33]. The AUV is assumed to be moving with a constant forward velocity of 0.7 (m/sec). The vehicle parameters are $l = 1.391$ (m), mass=18.826 (kg), $I_z = 1.77$ (kgm²), $X_G = -0.012$, $Y_G = 0$. The hydrodynamic parameters for a forward velocity of 0.7 m/sec are $Y_{\dot{r}} = -0.3781$, $Y_{\dot{v}} = -5.6198$, $Y_r = 1.1694$, $Y_v = -12.0868$, $N_{\dot{r}} = -0.3781$, $N_{\dot{v}} = -0.8967$, $N_r = -1.0186$, and $N_v = -4.9587$. It is assumed that the fin oscillation frequency is $f = 8Hz$. Using CFD analysis, the fin forces and the moments coefficients have been obtained in [28]. The parameter vectors f_a , f_b , m_a , and m_b used for simulations are

$$f_a = (0, -40.0893, -43.6632, -0.3885, 0.6215, 6.2154, -10.17, -0.1554, 0.6992)$$

$$f_b = (68.9975, 0.4451, -16.4704, 64.1009, -19.5864, -0.8903, -2.2257, 2.2257, 4.8966)$$

$$m_a = (0.0054, 0.6037, 0.4895, 0, -0.0054, 0, -0.0925, 0, -0.0054)$$

$$m_b = (-0.5297, -0.3739, -0.0935, -0.2493, 0.1246, 0.0312, -0.0312, 0.0935, 0)$$

(Readers may refer to [28] for the details.) It is pointed out that these parameters are obtained using the Fourier decomposition of the fin force and moment, and are computed by multiplying the Fourier coefficients by $\frac{1}{2}\rho.W_a.U_\infty^2$ and $\frac{1}{2}\rho.W_a.chord.U_\infty^2$, respectively, where W_a is the surface area of the foil. For simulation, the initial conditions of the vehicle are assumed to be $x(0) = 0$.

The closed-loop system (2.10) and (6.28) with the update law (6.14) is simulated. The bias angle is changed to a new value every $T = T_o$ seconds, where $T_o = 1/f$ is the fundamental period of f_p and m_p . For the set point control, the terminal value of the yaw angle is taken as $\psi^* = 10$ or 50 deg. Thus one desires to control the BAUV to a heading angle of 10 or 50 deg. For the update law, the adaptation gains are selected as $\Gamma = 0.01I_{7 \times 7}$ and k_o is set to 1. The parameter d_f is assumed to be 0.03944 (m). The open-loop zeros and poles of the system for the frequency of fin oscillation 8 Hz are (6295.5, -0.4) and (1.0000, 1.0864, 0.8715), respectively. The transfer function, $g(z)$ is nonminimum phase, since one of the zeros (at $z = 6295.5$) lies far away in the unstable region. We point out that the adaptive design approach of [29] cannot be applied to this nonminimum BAUV model.

For simplicity, the filter parameters of the identifier ($\lambda_i, i = 0, 1, 2$) and the stabilizer ($\mu_i, i = 0, 1, \dots, 3$) have been set to zero. We point out that response characteristics of the closed-loop system are critically dependent on the zeros of polynomial $F^*(z)$ used for pole placement. But unfortunately, there does not exist any systematic procedure for its selection. A practical approach is to try different choices of zeros of $F^*(z)$, and select an appropriate $F^*(z)$ by observing the simulated responses. Here we have chosen

$$F^*(z) = (z^3)(z^2 - 0.5^2)(z - 0.6)(z - 0.7)$$

Certainly, there can be another choice of $F^*(z)$ giving better performance.

Case A1: Adaptive set point control: Parameter uncertainty 20% off-nominal with frequency of fin oscillation 8 Hz for yaw angle command of 10 (deg)

Although theoretically, the derived control law can accomplish set point control of the yaw angle to any target value, it turns out that this may require extremely large bias angles. This is especially true for nonminimum phase systems. We observed that by appropriate command shaping, one can accomplish output regulation using smaller bias angles. For this reason, for smooth set point control, we have chosen command input of the form

$$r(kT) = [1 - \exp(-0.04 \times \tau \times (k)T)]\psi^*$$

where the terminal value of the yaw angle is $\psi^* = 10(\pi/180)$ radians, the sampling time is $T = 0.125$ (sec) and τ is incremented in steps of 0.01 from 0 to 1. It is pointed out that although the controller has been designed to track step and ramp commands, exponentially decaying signals of the reference inputs $r(kT)$ cannot cause instability in the closed-loop system. Assuming 20% uncertainty, the initial estimates $\theta(0)$ is set to $0.80\theta^*$. This way the control law gains are 20% lower than the exact vector θ^* . The frequency of fin oscillations is 8 Hz. Fig. 6.3 shows the simulated results. It can be seen that the adaptive controller achieves accurate heading angle control to the target value in about 35 sec. The control input (bias angle) magnitude required is less than 30 deg, which can be provided by the pectoral fins. Of course, multiple fins can be utilized if faster maneuvers and smaller control inputs (bias angles) are desired. The plots of the lateral force and moment produced by the fins are also provided in the figure. In the steady-state, the lateral fin force and moment exhibit bounded periodic oscillations. As expected, the bias angle tends to zero. We observe that the heading angle closely follows the discrete reference trajectory, and its intersample oscillations are of tiny amplitudes.

Case A2: Adaptive set point control: Parameter uncertainty 20% off-nominal with frequency of fin oscillation 8 Hz for yaw angle command of 50 (deg)

In order to examine large angle regulation capability of the controller, a reference trajectory is generated using $\psi^* = 50(\pi/180)$ (rad). Thus it is desired to change the heading angle to 50 deg.

Figure. 6.4 shows the simulated results. We observe smooth output regulation. The response time remains of the same order (35 sec) as for case A1. Surprisingly the control required is less than 30 (deg), which is same as that required for a smaller command of 10 (deg). This unexpected behavior of the designed control system is attributed to the nonlinear time-varying nature of the adaptive system. Again the steady-state value of β is zero.

Case A3: Adaptive turning maneuver

For constant turning rate, a smooth trajectory is generated using the command input $r(kT) = 1.3kT (\pi/180) (rad)$. It is desired to maneuver the BAUV for a 180 (deg) turn. We observe that the vehicle performs turning maneuver smoothly as seen in Figure. 6.5. The peak bias angle for this maneuver is around 30 deg. The vehicle takes less than 140 sec to make a turn of 180 (deg). After the initial transients, only a small nonzero bias angle (less than 0.25 (deg)) (not apparent from the figure for the chosen scale) is required to complete the turning maneuver. It is possible to have a faster turning rate, however, it requires larger control forces.

Simulations for other off-nominal choices of $\theta(0)$ have been performed. It is found that the control system performs relatively well for the choice of under-estimated initial values of the control gains $\theta(0)$. The response of the system largely depends on the choice of $F^*(z)$. Of course, the responses also depend on the choice of the command generator and the adaptation gain matrix Γ of the update law. Simulations show that the controller accomplishes regulation for other fin locations as well.

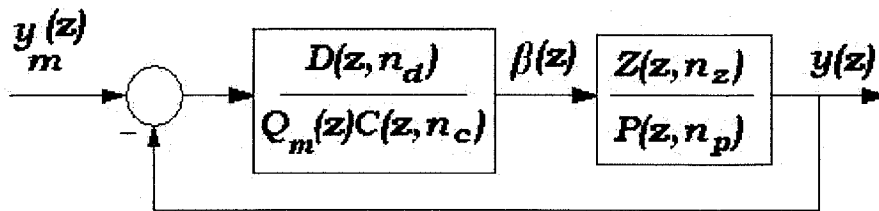


Figure 6.1: The Closed-loop system including the internal model

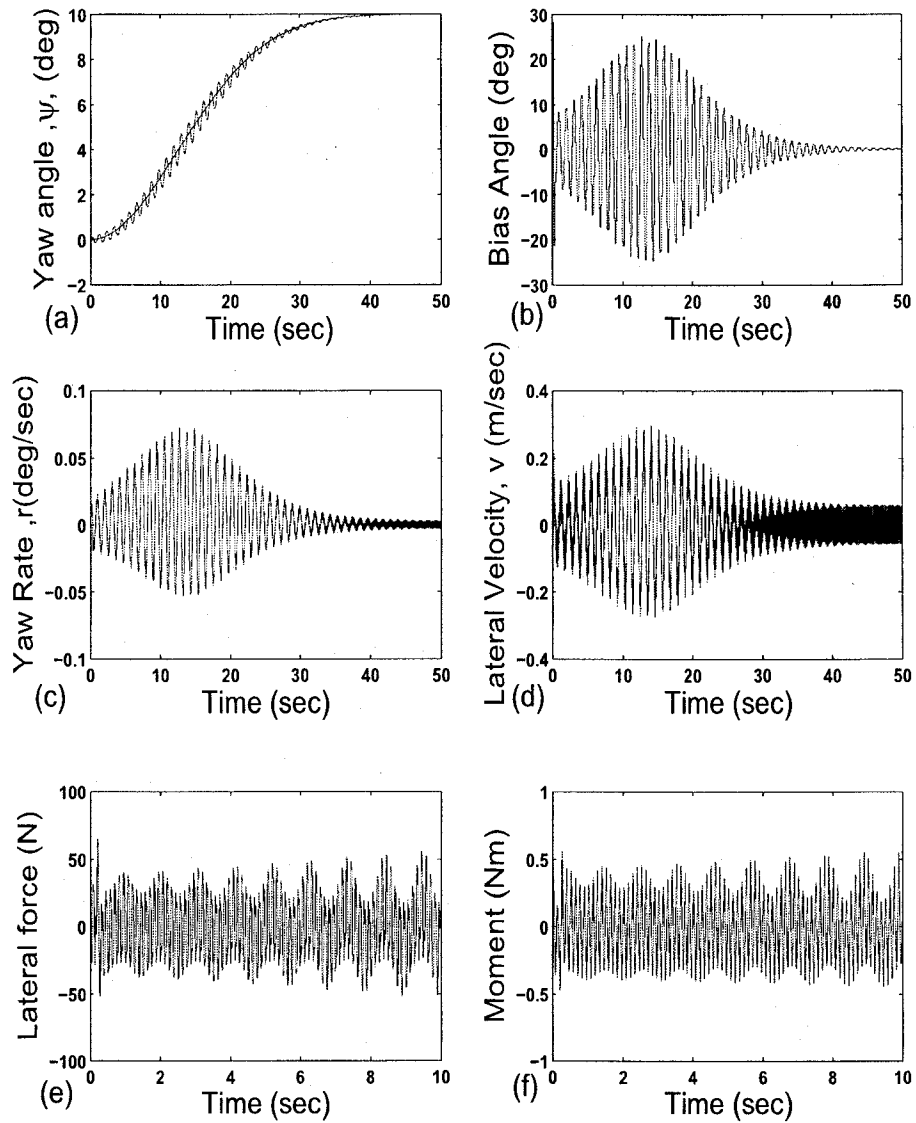


Figure 6.3: Adaptive set point control: Frequency of flapping 8Hz for $\psi^* = 10$ (deg) and parameter uncertainty 20%

(a) Yaw angle, ψ , (solid) and reference yaw angle (staircase) (deg) (b) Bias angle (deg) (c) Yaw rate (deg/sec) (d) Lateral velocity (m/sec) (e) Lateral force (N) (f) Moment (Nm)

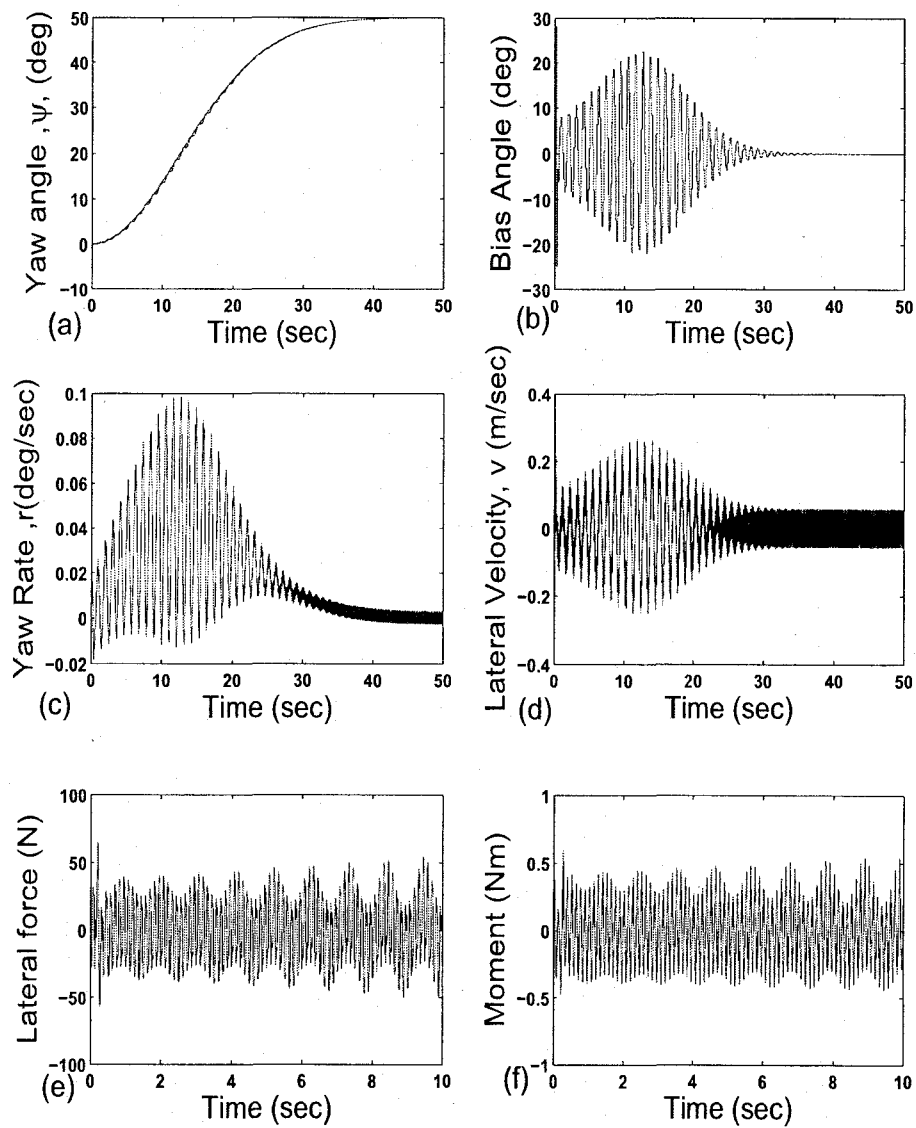


Figure 6.4: Adaptive set point control: Frequency of flapping 8Hz for $\psi^* = 50$ (deg) and parameter uncertainty 20%
 (a) Yaw angle, ψ , (solid) and reference yaw angle (staircase) (deg) (b) Bias angle (deg) (c) Yaw rate (deg/sec) (d) Lateral velocity (m/sec) (e) Lateral force (N) (f) Moment (Nm)

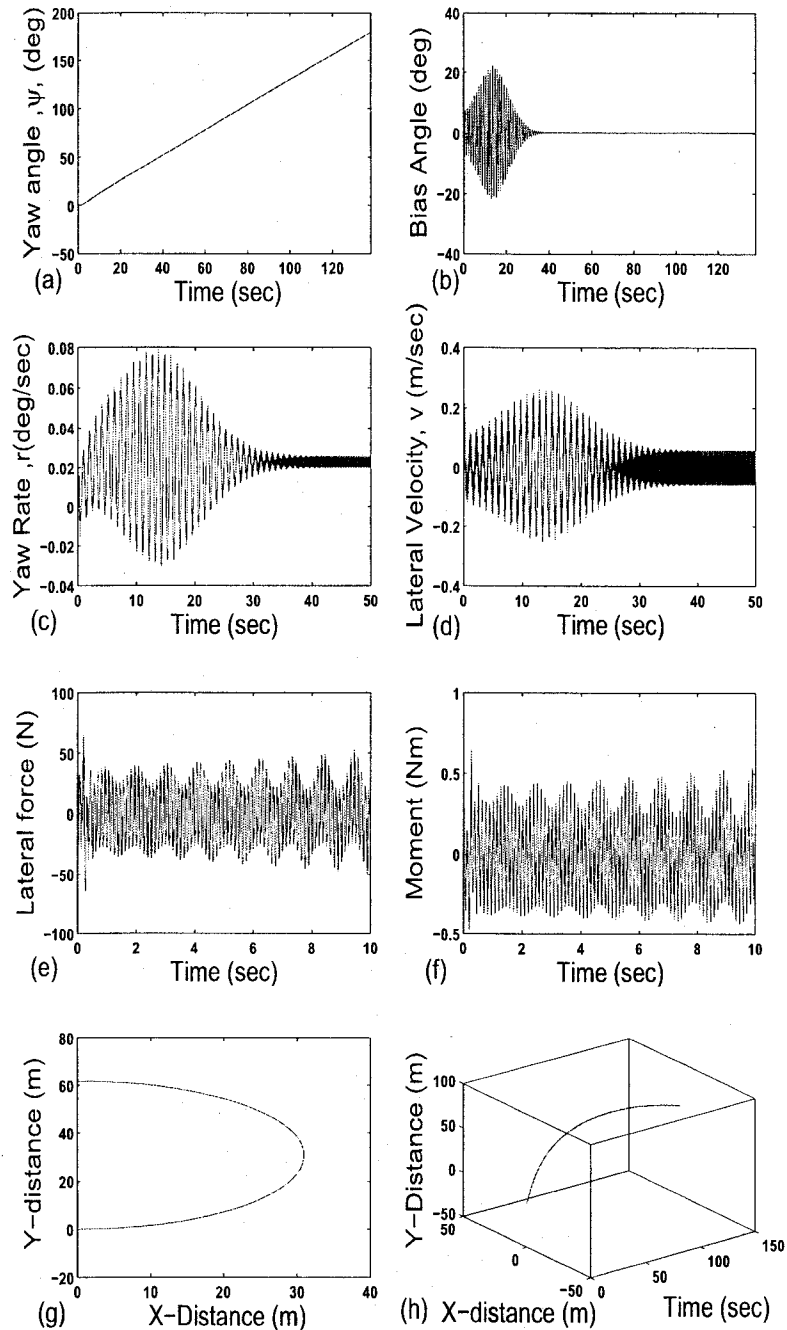


Figure 6.5: Adaptive turning maneuver: Frequency of flapping 8Hz for 180 (deg) turn with turning rate of 1.3 (deg / sec) and parameter uncertainty 20%

(a) Yaw angle, ψ , (solid) and reference yaw angle (staircase) (deg) (b) Bias angle (deg) (c) Yaw rate (deg/sec) (d) Lateral velocity (m/sec) (e) Lateral force (N) (f) Moment (Nm) (g) Global position of the BAUV (X and Y co-ordinates) (h) Three-dimensional plot of X and Y distances with time

CHAPTER 7

CONCLUSION

The design of control systems for the dive plane and yaw plane maneuvering of autonomous underwater vehicles (AUVs) was considered. In chapter 3, the dive plane control of AUVs using the state-dependent Riccati equation method was considered. For the design, nonlinearities in the AUV model were retained and it was assumed that the parameters of the vehicle were not known precisely. Furthermore, hard constraints on the control fin angle were imposed for a practical design. Using the SDRE method, control systems were designed with the constrained as well as unconstrained input (control fin angle). Simulation results were presented which showed that the SDRE-based control system accomplishes depth control in spite of the control saturation and the presence of parameter uncertainties.

In chapter 4, the design of a state feedback adaptive control system for the yaw plane control of a BAUV using pectoral-like fins was considered. These fins were assumed to undergo a combined oscillatory swaying and yawing motion for generating control forces. The periodic fin force and moment were parameterized using CFD analysis, and a discrete-time AUV dynamic model was used for control system design. The bias angle was treated as the control input. The systems parameters were assumed to be unknown. A sampled-data adaptive control law was derived for the control of the yaw angle using the state variable feedback. In the closed-loop system, it was shown that the yaw angle asymptotically follows prescribed time-varying yaw angle trajectories in the presence of model uncertainties. Further, in chapter 5, the design of an output feedback

adaptive control system for the yaw plane control of a BAUV using biologically -inspired pectoral-like fins was considered. A sampled-data adaptive control law was derived for the control of the yaw angle using only the yaw angle feedback. In the closed-loop system, it was shown that the yaw angle asymptotically follows prescribed time-varying yaw angle trajectories. The designed output feedback adaptive control system was simulated for various types of yaw-plane maneuvers. The simulations also showed that using pectoral fins, one can perform precise and rapid maneuvers in the presence of model uncertainties using a single sensor. Moreover, the designed controller is preferable from the view point of simplicity and cost of implementation compared to control systems using full state measurement.

In chapter 6, an indirect adaptive control of AUVs in the yaw plane using pectoral-like fins was considered. The system parameters were assumed to be unknown, and only the yaw angle was measured for feedback. In this study, the parametrization of the periodic fin forces by CFD analysis was used. For output regulation, an internal model of the reference yaw angle (constant and ramp) and constant disturbance trajectories was introduced in the control loop. The designed adaptive control system has a modular structure and consists of a normalized gradient based parameter identifier and a stabilizer designed using pole placement method. It was shown that in the closed-loop system, asymptotic regulation of the yaw angle is accomplished and all the signals in the system remain bounded. Interestingly, the designed control is capable of rejecting any constant as well as periodic wave forces acting on the vehicle provided that the oscillation frequency of the fins coincides with the fundamental frequency of the wave forces. Furthermore, unlike the published work, derived control system is applicable to minimum as well as nonminimum phase BAUVs.

Even though this thesis provides various ways to control BAUVs, the maneuverability of the BAUV is limited. Better maneuverability can be achieved by employing control system for

simultaneously using variety of fins attached to a flexible main body. Thus future development in the above mentioned areas will provide a new approach for designing control systems for BAUVs. Designing nonlinear control laws to control BAUVs using multiple control surfaces for maneuverability in various planes simultaneously is an interesting problem for future research.

APPENDIX I

SYSTEM PARAMETERS

1. The Hydrodynamic parameters for the REMUS for simulation are [55]

$$M_{\dot{q}} = -4.88 \text{ kg. m}^2/\text{rad. } M_{\dot{w}} = -1.93 \text{ kg. m.}$$

$$M_{w|w|} = 3.18 \text{ kg. } M_{q|q|} = -188 \text{ kg.m}^2/\text{rad}^2. M_{uu\delta} = -6.15 \text{ kg./rad}$$

$$M_{uq} = -2 \text{ kg. m/rad. } M_{uw} = 24 \text{ kg. } Z_{\dot{w}} = -35.5 \text{ kg.}$$

$$Z_{\dot{q}} = -1.93 \text{ kg. m/rad. } Z_{ww} = -131 \text{ kg/m. } Z_{q|q|} = -0.632 \text{ kg. m/rad}^2.$$

$$Z_{uw} = -28.6 \text{ kg./m. } Z_{uq} = -5.22 \text{ kg/rad. } Z_{uu\delta} = -6.15 \text{ kg./m. rad}.$$

2. The Vehicle physical parameters are

$$x_{cg} = 0. \ y_{cg} = 0. \ z_{cg} = 0.0196 \text{ m.}$$

$$x_B = 0. \ y_B = 0. \ z_B = 0.$$

$$W = 299 \text{ N. } B_o = 306 \text{ N. } m = 30.48 \text{ kg.}$$

$$I_{yy} = 3.45 \text{ kg. m}^2.$$

APPENDIX II

1. Stabilizer parameters (c_i, d_i)

The compensator equation (6.24) can be further expanded as

$$\begin{aligned} (z^2 + c_1z + c_0)(z^2 - 2z + 1)(z^3 + a_2z^2 + a_1z + a_0) + (d_4z^4 + d_3z^3 + d_2z^2 + d_1z + d_0)(b_2z^2 + b_1z + b_0) \\ = z^7 + f_6z^6 + f_5z^5 + f_4z^4 + f_3z^3 + f_2z^2 + f_1z + f_0 \end{aligned} \quad (7.1)$$

and then converted into matrix form as follows

$$\begin{bmatrix} c_0 & d_0 & c_1 & d_1 & d_2 & d_3 & d_4 \end{bmatrix} \times S = \begin{bmatrix} f_0 \\ f_1 \\ (f_2 - a_0) \\ (f_3 - a_1 + 2a_0) \\ (f_4 - a_2 + 2a_1 - a_0) \\ (f_5 - 1 + 2a_2 - a_1) \\ (f_6 + 2 - a_2) \end{bmatrix}^T \quad (7.2)$$

where

$$S = \begin{bmatrix} a_0 & (a_1 - 2a_0) & (a_2 - 2a_1 + a_0) & (1 - 2a_2 + a_1) & (a_2 - 2) & 1 & 0 \\ b_0 & b_1 & b_2 & 0 & 0 & 0 & 0 \\ 0 & a_0 & (a_1 - 2a_0) & (a_2 - 2a_1 + a_0) & (1 - 2a_2 + a_1) & (a_2 - 2) & 1 \\ 0 & b_0 & b_1 & b_2 & 0 & 0 & 0 \\ 0 & 0 & b_0 & b_1 & b_2 & 0 & 0 \\ 0 & 0 & 0 & b_0 & b_1 & b_2 & 0 \\ 0 & 0 & 0 & 0 & b_0 & b_1 & b_2 \end{bmatrix}$$

Post multiplying (7.2) by S^{-1} gives the controller parameters (c_i, d_i) .

2. The vectors l and d_a of control law

$$d_a = \begin{bmatrix} (d_0 - d_4\mu_0) & (d_1 - d_4\mu_1) & (d_2 - d_4\mu_2) & (d_3 - d_4\mu_3) \end{bmatrix}^T$$
$$l = \begin{bmatrix} (\mu_0 - c_0) & (\mu_1 + 2c_0 - c_1) & (\mu_2 - c_0 + 2c_1 - 1) & (\mu_3 - c_1 + 2) \end{bmatrix}^T$$

REFERENCES

1. A. Azuma, *The Bio-Kinetics of Flying and Swimming*. Springer-Verlag, New York, 1992.
2. M. Sfakiotakis, D. M. Lane, and J. B. C. Davies, "Review of Fish Swimming Modes for Aquatic Locomotion," *IEEE J. Oceanic Engg.*, Vol. 24, No. 2, pp 237-253, April 1999.
3. F. E. Fish, "Structure and Mechanics of Nonpiscine Control Surfaces," *IEEE Journal of Oceanic Engineering*, 29, pp. 605-621, 2004.
4. J. A. Walker, "Kinematics and Performance of Maneuvering Control Surfaces in Teleost Fishes," *IEEE Journal of Oceanic Engineering*, 29, pp. 572-584, 2004.
5. G. V. Lauder, and E. G. Drucker, "Morphology and Experimental Hydrodynamics of Fish Fin Control Surfaces," *IEEE Journal of Oceanic Engineering*, 29, pp. 556-571, 2004.
6. P. R. Bandyopadhyay, J. M. Castano, J. Q. Rice, R. B. Philips, W. H. Nedderman, and W. K. Macy, "Low-Speed Maneuvering Hydrodynamics of Fish and Small Underwater Vehicles," *ASME J. Fluids Eng.*, 119, pp. 136-144, 1997.
7. P. W. Webb, "Maneuverability - general issues," *IEEE Journal of Oceanic Engineering*, 29, pp. 547-555, July 2004.
8. M. W. Westneat, D. H. Thorsen, J. A. Walker, M. E. Hale, "Structure, Function, and Neural Control of Pectoral Fins in Fishes," *IEEE Journal of Oceanic Engineering*, 29, pp. 674-683, July 2004.

9. N. Kato, T. Inaba, "Guidance and control of fish robot with apparatus of pectoral fin motion," IEEE International Conference on Robotics and Automation, Belgium., pp. 446-451, 1998.
10. P. R. Bandyopadhyay, "Maneuvering Hydrodynamics of Fish and Small Underwater Vehicles," Integrative and Comparative Biology., 42(1), pp. 102-117, February 2002.
11. G. S. Triantafyllou, and M. S. Triantafyllou, "An Efficient Swimming Machine," Scientific American., pp. 64-70, 1995.
12. S. Guo, K. Sugimoto, S. Hata, J. Su, K. Oguro, "A new type of underwater fish-like microrobot," IEEE ICIRS2000., pp. 867-872, 2000.
13. Nakashimal, "Dynamics of two-joint dolphin-like propulsion mechanism," Nippon Kikai Gakkai Ronbunshu, B Hen/Transactions of the Japan Society of Mechanical Engineers., 62(602)., pp. 3607-3613.
14. T. Ichikizaki, I. Yamamoto, "Development of Robotic Fish with Various Swimming Functions," Symposium on Underwater technology, Japan, April 2007.
15. P. R. Bandyopadhyay, "Trends in biorobotic autonomous undersea vehicles," IEEE Journal of Oceanic Engineering, 30, pp. 109-139, 2005.
16. J. D. W. Madden, N. A. Vandesteeg, P. A. Anquetil, P. G. A. Madden, A. Takshi, R. Z. Pytel, S. R. Lafontaine, P. A. Wieringa, and I. W. Hunter, "Artificial Muscle Technology: Physical Principles and Naval prospects," IEEE Journal of Oceanic Engineering, 29, pp. 706-728, July 2004.
17. R. R. Llinas, E. Leznik, and V. I. Makarenko, "The Olivo - Cerebellar Circuit as a Universal Motor Control System," IEEE Journal of Oceanic Engineering, 29, pp. 631-639, July 2004.

18. M. S. Triantafyllou, A. H. Techet, and F. S. Hover, "Review of Experimental Work in Biomimetic Foils," *IEEE Journal of Oceanic Engineering*, 29, pp. 585-594, 2004.
19. N. Kato, "Control Performance in the Horizontal Plane of a Fish Robot with Mechanical Pectoral Fins," *IEEE J. Oceanic Engg.*, 25 (1), pp. 121-129, 2000.
20. R. Mittal, "Computational Modeling in Biohydrodynamics: Trends, Challenges, and Recent Advances," *IEEE Journal of Oceanic Engineering*, 29, pp. 595-604, 2004.
21. H. S. Udaykumar, R. Mittal, P. Rampungoon, and A. Khanna, "A Sharp Interface Cartesian Grid Method for Simulating Flows with Complex Moving Boundaries," *J. Comput. Phys.*, 174, 345-380, 2001.
22. R. Ramamurti, R. Lohner, and W. Sandberg, "Computation of the unsteady-flow past a tuna with caudal fin oscillation," *Adv. Fluid Mech. Series*, vol 9, pp. 169-178, 1996.
23. H. Suzuki, N. Kato, T. Katayama, Y. Fukui, "Motion Simulation of an Underwater Vehicle with Mechanical Pectoral Fins Using a CFD-based Motion Simulator," *Symposium on Underwater technology, Japan.*, pp. 384 - 390, April 2007.
24. T. I. Fossen, *Guidance and Control of Ocean Vehicles*. John Wiley and Sons, New York, 1999.
25. L. Schenato, "Analysis and Control of Flapping Flight: from Biologically to Robotic Insects," *Ph. D. Dissertation*, University of California, Berkeley, 2003.
26. I. Yamamoto, Y. Terada, T. Nagamatu, and Y. Imaizumi, "Propulsion System with Flexible/Rigid Oscillating Fin," *IEEE J. Oceanic Engg.*, 20 (1), pp. 23-30, 1995.
27. S. N. Singh, A. Simha, and R. Mittal, "Biorobotic AUV Maneuvering by Pectoral Fins:

- Inverse Control Design based on CFD Parameterization," *IEEE Journal of Oceanic Engineering*, 29 (3), pp. 777-785, 2004.
28. M. Narasimhan, H. Dong, R. Mittal, S. N. Singh, "Optimal yaw regulation and trajectory control of a Biorobotic AUV using Mechanical fins based on CFD Parametrization," *Journal of Fluids Engineering*, 128 (4), pp. 687-698, 2006.
 29. M. S. Naik, S. N. Singh, R. Mittal, "Biologically-inspired adaptive pectoral-like fin control system for CFD parameterized AUV," *International Symposium on Underwater Technology*, Tokyo, Japan. 17th – 20th, April 2007.
 30. G. Tao, *Adaptive Control Design and Analysis*. John Wiley and Sons, New Jersey, 2003.
 31. P. A. Ioannou, J. Sun, *Robust Adaptive Control*. Prentice-Hall Inc, New Jersey.
 32. C. T. Chen, *Linear System Theory and Design*. Oxford University Press, 1999.
 33. P. Ridley, J. Fontan, P. Corke, "Submarine Dynamic Modeling," *Australian Conference on Robotics and Automation*, Brisbane, Australia, 2003.
 34. P. R. Bandyopadhyay, S. N. Singh, F. Chockalingam, "Biologically-inspired Bodies under Surface Waves - Part 2: theoretical control of maneuvering". *ASME Journal of Fluids Engineering*, 121, pp. 479-487, 1999.
 35. K. A. Harper, M. D. Berkemeier, S. Grace, "Modeling the dynamics of spring-driven oscillating foil propulsion". *IEEE Journal of Oceanic Engineering*, 23, pp. 285-296, 1998.
 36. A. J. Healey, D. Lienard, "Multi-variable sliding mode control for autonomous diving and steering of unmanned underwater vehicles". *IEEE Journal of Oceanic Engineering* 18 (3), 327-338, 1993.

37. N. Kato, "Pectoral Fin Controllers. Neurotechnology for Biometric Robots". Cambridge, MA: MIT Press, pp. 325-350, 2002.
38. M. Narasimhan, S. N. Singh, "Adaptive input-output feedback linearizing yaw plane control of BAUV using dorsal fins". *Ocean Engineering*, 33, pp. 1413-1430, 2006.
39. M. S. Triantafyllou, A. Techet, F. Hover, "Review of Experimental Work in Biomimetic Foils". 13th International Symposium on Unmanned Untethered Submersible Technology (UUST), New England Center, Durham, New Hampshire, USA, 2003.
40. D. R. Yoerger, J. E. Slotine, "Robust trajectory control of underwater vehicles". *IEEE Journal of Oceanic Engineering* 29 (3), 572-584, 1985.
41. J. R. Cloutier, C. P. Mracek, D. B. Ridgely, K. D. Hammett, "State dependent Riccati equation techniques: theory and applications". Notes from the SDRE Workshop Conducted at the American Control Conf., Philadelphia, 1998.
42. J. R. Cloutier, D. T. Stansbery, "Nonlinear hybrid bank-to-turn/skid-to-turn autopilot design". AIAA Paper 2001-5929, 2001.
43. U. Demirci, F. Kerestecioglu, "A re-configuring sliding-mode controller with adjustable robustness". *Ocean Engineering* 31, 1669-1682, 2003.
44. K. Do, J. Pan, Z. Jiang, "Robust and adaptive path following for underactuated autonomous underwater vehicles". *Ocean Engineering* 31(2004), 1967-1997, 2004.
45. O. Fjellstad, T. Fossen, "Position and attitude tracking of AUVs : a quaternion feedback approach". *IEEE Journal of Oceanic Engineering* 19(4), 512-518, 1994.
46. J. Guo, F. Chiu, C. Huang, "Design of a sliding mode fuzzy controller for the guidance and control of an autonomous underwater vehicle". *Ocean Engineering* 30, 2137-2155, 2003.

47. J. Huang, *Nonlinear Output Regulation Theory and Application*. Philadelphia: SIAM, 2004.
48. K. Ishii, T. Fujii, T. Ura, "An on-line adaptation method in a neural network based control system for AUVs". *IEEE Journal of Oceanic Engineering* 20(3), 221-228, 1995.
49. A. Isidori, *Nonlinear control systems*. NY:Springer-Verlag, 1989.
50. B. Jalving, "The NDRE-AUV flight control system". *IEEE Journal of Oceanic Engineering* 19(4), 497-501, 1994.
51. J. Li, P. Lee, "Design of an adaptive nonlinear controller for depth control of an autonomous underwater vehicle". *Ocean Engineering* 32, 2165-2181, 2005.
52. C. P. Mracek, J. R. Cloutier, "Full Envelope missile longitudinal autopilot design using the state-dependent Riccati equation method", AIAA Paper 97-3767, 1997.
53. C. P. Mracek, J. R. Cloutier, "Control designs for the nonlinear bench-mark problem via the state-dependent Riccati equation method". *International Journal of Robust Nonlinear Control*, Vol. 8, 401-433, 1998.
54. M. Narasimhan, S. N. Singh, "Adaptive optimal control of an autonomous underwater vehicle in the dive plane using dorsal fins". *Ocean Engineering* 33 (3-4), 404-416, 2006.
55. T. Prester, Verification of a six-degree of freedom simulation model for the REMUS autonomous underwater vehicles. Masters Thesis, Department of Ocean Engineering and Mechanical Engineering, MIT, USA, 2001.
56. J. Yuh, "Modeling and control of underwater robotic vehicles". *IEEE Transactions on Systems, Man, and Cybernetics* 20(6), 1475-1483, 1990.

57. M. S. Naik, S. N. Singh, "State-dependent Riccati equation-based robust dive plane control of AUV with control constraints". *Ocean Engineering* 34(11-12), 1711-1723, August 2007.
58. M. S. Naik, "Output feedback sampled-data adaptive control of Biorobotic AUV using pectoral fins". 15th International symposium on unmanned untethered submersible technology, University of New Hampshire, Durham. 19th - 22nd August 2007

VITA
Graduate College
University of Nevada, Las Vegas

Mugdha S. Naik

Local Address:

4224 Cottage Circle, Apt 4
Las Vegas, Nevada 89119

Home Address:

Flat 5, 57-58 Vedang Apts
Lane 5, Dahanukar Colony, Kothrud
Pune, Maharashtra
India 411038

Degrees:

Bachelors of Engineering, Electronics Engineering, 2004
All India Shri Shivaji Memorial Society's College of Engineering, (Pune)
University of Pune, Maharashtra, India

Publications:

M.S.Naik, S.N.Singh, State-dependent Riccati equation-based robust dive plane control of AUV with control constraints.
Ocean Engineering, Vol. 34, Issues 11-12, August 2007.

M.S.Naik, S.N.Singh, R.Mittal, Biologically-Inspired Adaptive Pectoral-Like Fin Control System For CFD Parameterized AUV.
The International Symposium on Underwater Technology.
(UT07), Tokyo, Japan, 2007.

M. S. Naik, Output feedback sampled-data adaptive control of Biorobotic AUV using pectoral fins.
15th International symposium on unmanned untethered submersible technology.
(UUST07), Durham, New Hampshire, USA, 19th - 22nd August 2007.

Thesis Title:

Nonlinear Suboptimal and Adaptive Pectoral Fin Control of Autonomous Underwater Vehicle

Thesis Examination Committee:

Chairperson, Dr. Sahjendra Singh, Ph.D.

Committee Member, Dr. Venkatesan Muthukumar , Ph.D.

Committee Member Dr. Emma Regentova, Ph.D.

Graduate Faculty Representative, Dr. Woosoon Yim, Ph.D.